Summer 7-1-2014

Pharmacokinetic Characterization of Procoagulation Proteins

Nicholas C. Vanderslice
University of Nebraska-Lincoln, vanderslice.nicholas@gmail.com

Pharmacokinetic Characterization of Procoagulation Proteins

by

Nicholas Cary Vanderslice

A DISSERTATION

Presented to the Faculty of

The Graduate College at the University of Nebraska

In Partial Fulfillment of Requirements

For the Degree of Doctor of Philosophy

Major: Chemical and Biomolecular Engineering

Under the Supervision of Professor William H Velander

Lincoln, Nebraska

August, 2014

Pharmacokinetic Characterization of Procoagulation Proteins

Nicholas C. Vanderslice, Ph.D.

University of Nebraska, 2014

Adviser: William H. Velander

The cessation of bleeding in mammals occurs due to a well-conserved sequence of protein activation known as the coagulation cascade. However, people who have a deficiency in one or more proteins in this cascade, whether due to genetics or blood loss, struggle to maintain hemostasis. In order to aid patients in the restoration of hemostasis, exogenous proteins are often administered in response to bleeding events. However, these proteins are limited and costly due to limited supply of donor blood available for the production of plasma-derived proteins and the high cost of mammalian cell bio-reactors required for the production of recombinant proteins. As an alternative to the two previously aforementioned methods, human recombinant coagulation proteins have also been produced in the mammary gland of mice, swine, and bovine. This technique offers high production of active coagulation protein at low scaled-up cost. The research in this dissertation details the preclinical trials and characterization of two such proteins, factor IX produced in swine (FIX) and fibrinogen produced in bovine (FI), as well as one traditional recombinant protein, factor XIII produced in *Pichia pastoris* (FXIII). FXIII and FI, in addition to thrombin, are the main components of fibrin sealant, which is

typically used to seal a wound in the case of a catastrophic bleeding event. FIX is used in a completely different context: the treatment of hemophilia B, a disease where the body produces no active FIX. Pharmacokinetic analysis and characterization of FIX were performed both intravenously and buccally in mice and dogs. The analysis revealed that FIX produced in the mammary gland of swine exhibited enhanced endothelial binding while maintaining normal whole blood clotting times despite the reduced plasma retention times. FIX stored in the extravascular reservoir was shown to influence FIX retention times for samples infused over 24 hours after plasma levels had been depleted. FXIII produced in yeast was shown to be monomeric and containing an artificial activation peptide that enhanced the crosslinking of fibrinogen with a reduced activation time lag.

Author's Acknowledgements

I would like to thank Dr. Velander for his guidance and this opportunity to research a truly interesting problem. I would also like to thank my undergraduate adviser, Dr. Marrero, for his continued guidance and for opening my eyes to the possibilities of graduate school. In addition, I would like to thank Ayman Ismail, Jennifer Calcaterra, Mostafa Fatemi, and Weijie Xu for all of their training and guidance. Finally, I would like to thank Lauren Geppi and Brad Kossel for their time and patience in reading this document and finding all the pieces that weren't quite ready to be published yet.

Table of Contents

List of Tables

List of Figures

Chapter 1:

Introduction

1.1 Background

The coagulation cascade [1, 2], as seen in Figure 1.1, is the primary method for maintaining hemostasis in most mammalian organisms. This delicate cycle reacts to the presence of tissue factor, which comes into contact with the coagulation proteins after vascular injury, in order to trigger a chain reaction of serine proteases, transglutaminases, tenase complexes, and glycoproteins [1]. This reaction terminates with the formation of a cross-linked fibrin mesh which holds together a thrombus containing platelets, collagen, red blood cells, and fibroblast [2]. However, even after the thrombus is formed, degradation steps for many of the coagulation proteins must occur in order to prevent the creation or buildup of thrombi in the circulatory system. Proteins such as protein C [3], antithrombin [4], and plasmin [5] are responsible for preventing runaway coagulation reactions by degrading activated coagulation factors in the bloodstream in addition to the removal of fibrin scaffolds as wound healing progresses.

Unfortunately, this cycle of activation, inactivation, and degradation can be disrupted in many ways. The most direct and common method for coagulation factor depletion is in the case of catastrophic blood loss. In this case, the loss of platelets which contain key elements of the coagulation cascade and coagulation factors contained in the plasma preclude the restoration of hemostasis by native thrombus formation. Hospitals

combat scenarios such as these by administering coagulation factors and artificial scaffolds both topically and intravenously.

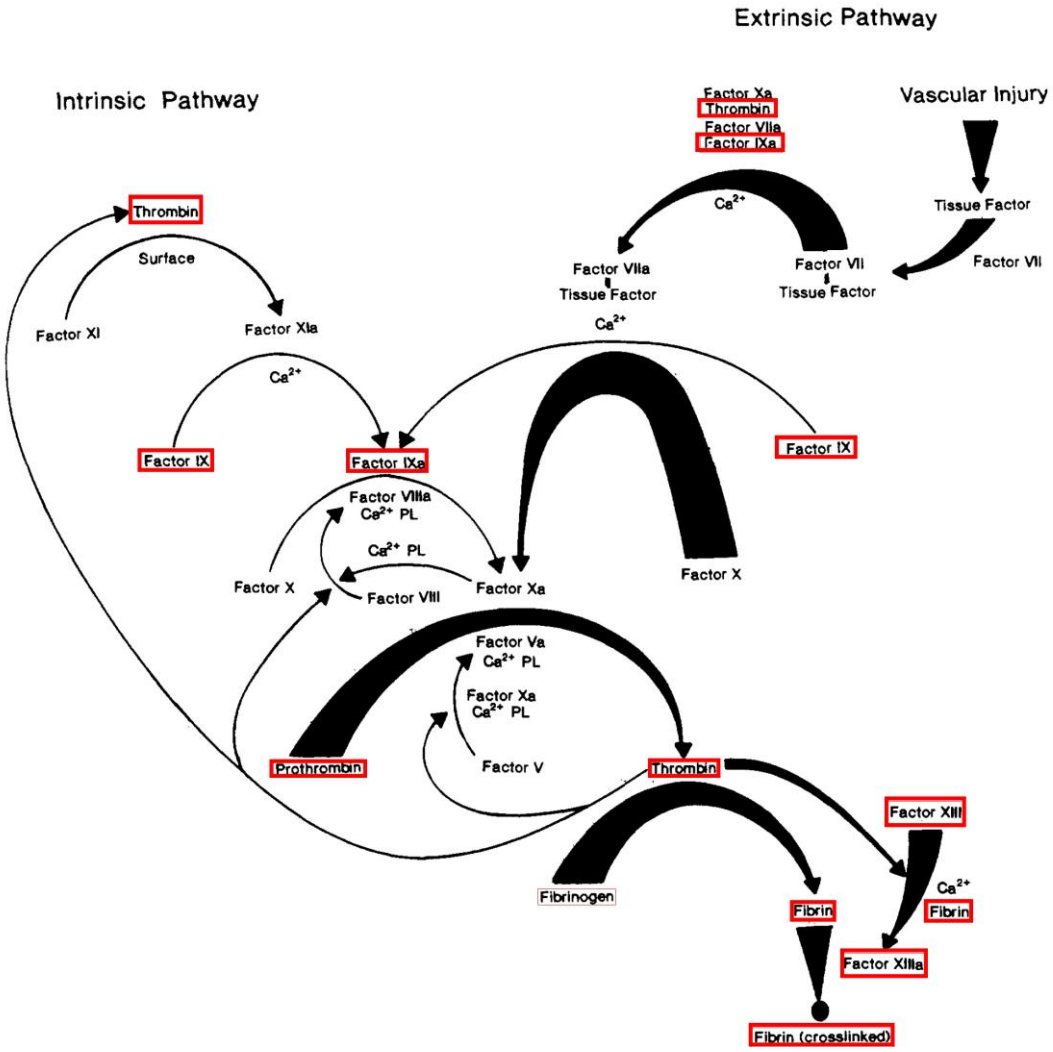

Figure 1.1. Intrinsic and Extrinsic Pathways of the Coagulation Cascade. Recombinant versions of the proteins with boundaries are the focus of this dissertation. Adapted from Davie et al. [1]

Genetics and immune malfunctions can also play a role in the depletion of one or more coagulation factor. Diseases such as Hemophilia A [6], Hemophilia B [6], and von Willebrand [7] disease manifest when levels of a specific protein are either not produced by the body due to a genetic abnormality, which is often hereditary, or are removed from

the body by the development of autoantibodies. Treatment of these diseases, depending on the severity, can currently be a lifelong and costly procedure. In addition, patients who do not produce one of these proteins natively and rely on the prophylactic infusions have an increased risk of autoantibody development, which can exponentially increase the cost of an already costly treatment [8]. Traditionally, prophylactic treatment of these diseases had been delivered using purified proteins from donor plasma. However, with the limited supply of donor plasma available for pharmaceutical use and the increased awareness of the risk of blood-born viral infection, efforts were made in the 1970s and 1980s to develop recombinant techniques for producing pharmaceutical proteins. It was quickly established that basic bacterial bioreactors did not provide proper post translational modifications (PTM) for many proteins, and as a result, higher order organisms such as yeast and bovine have been modified to produce high yields of proteins with PTM similar to their respective endogenous human protein [9-11].

1.2 Fibrinogen

Fibrinogen (FI), through its activated form fibrin, forms the foundation of the mesh that holds a thrombus together in the event of an injury [12, 13]. This foundation is formed by both the crosslinking of fibrin fibers and the attachment of fibrin to key components such as platelets (Figure 1.2). These fibrin fibers are formed when FI encounter thrombin (FIIa), the activated form of prothrombin, and they are crosslinked by the transglutaminase factor XIII (FXIII) to form a fibrin scaffold [12]. During wound healing, this scaffold serves as a pathway for the migration of macrophages, fibroblasts, and neutrophils in addition to aiding in native cell migration and proliferation [14]. As wound healing nears completion, exposed fibrin sites activate plasminogen into plasmin,

which breaks down the fibrin scaffold allowing for the complete restoration of native cells [13].

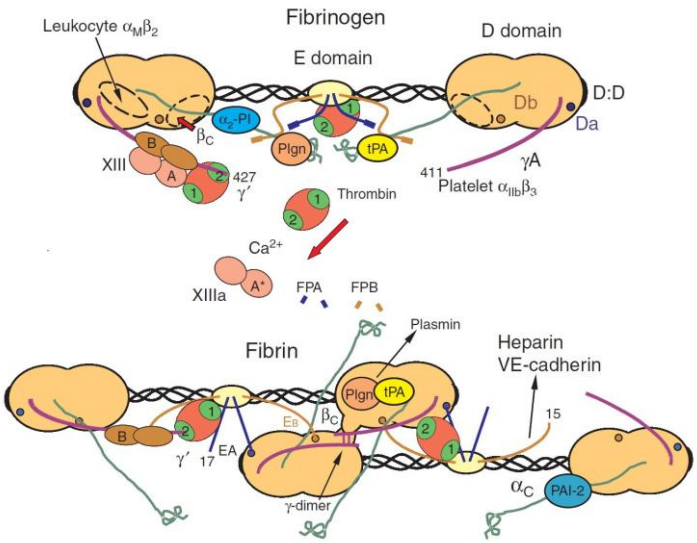

Figure 1.2. Schematic of fibrinogen activation into fibrin by thrombin in the presence of factor XIII. FI forms double-stranded fibrin protofibrils when exposed to both FXIII and FIIa. These protofibrils are capable of crosslinking laterally to form a fibrin mesh. Adapted from Mosesson [13].

On a molecular level, FI is a 340 kDa glycoprotein produced by hepatocytes and assembled in the endoplasmic reticulum (ER). The assembled structure contains two α-chains, two β-chains, and two γ-chains. Two major variants of FI exist, each containing either one or two altered γ-chains (γγ' or γ'γ'). The γ'-chain contains a substitution of 20 amino acids in place of γ-chain 408-412 [13]. This change in the γ-chain induces binding of activated FI to FXIII and FIIa, sequestering them into the hemostatic plug[15]. These variants form a minor subpopulation of the total FI concentration with approximately 8% of γ-chains population being γ'-chains [13]. The γγ' variant is more common than the γ'γ' variant, the former corresponding to 15% of the total FI population while the latter accounts for less than 1% of the total FI population [13].

Fibrinogen deficiency is a rare disease (1:1,000,000 people have been diagnosed with the most severe form of the disease) wherein the body does not produce functional FI [16]. Prophylactic measures similar to hemophilia are used to treat the disease. FI has also be found to be useful as secondary form of treatment in patients with a high risk of bleeding and in patients who are currently or have recently suffered from severe blood loss [17]. As a result of these factors, there are several commercial ways to obtain FI. Fresh-frozen plasma is occasionally administered despite its low concentration of FI, but modern targeted treatments for FI deficiency typical rely on cryoprecipitates and FI concentrates [17]. At the time of writing this dissertation, there are four commercial FI concentrates from plasma sources currently available; however, only one is available for medical use in the USA [18]. In contrast, cryoprecipitate is widely available in the USA and UK, but not available in most EU countries [17].

1.3 Factor XIII

FXIII is also activated by FIIa in the presence of calcium to form the activated species FXIIIa. FXIIIa is the last enzymatic step in the coagulation cascade and is responsible for covalently crosslinking the α-chains and γ-chains of FI in an antiparallel fashion, resulting in a stronger, insoluble fibrin clot that is resistant to fibrinolysis [19, 20]. The γ-γ chain crosslinking is kinetically favored and is completed within 10 minutes of interaction, while α-γ crosslinking is a slower process, taking up to one day, that solidifies and stabilizes the fibrin mesh [21-23]. Fully-formed plasma FXIII has a molecular weight (MW) of approximately 326 kDa and contains two α-chains (75 kDa) and two β-chains (88 kDa) [24]. However, FXIII that is stored on platelets loses the two

β-chains while maintaining all catalytic activity [24]. This has led to the conclusion that the β-chains acts primarily as a stabilizing agent in plasma, preventing non-specific activation and transporting the α-chains after expression from monocytes, megakaryocytes, and hepatocytes [25-28].

1.4 Factor IX

Factor IX (FIX) is a vitamin-dependent protein traditionally thought of as a key component in the intrinsic pathway of the coagulation cascade; however, recent research has revealed that FIX also has a key role in extrinsic pathway [1, 29]. The intrinsic pathway of FIX activation into FIXa involves activated factor XI (factor XI) in the presence of calcium. The extrinsic pathway of FIX was found when systems containing no factor XI or factor XII [30] were found to coagulate much faster than systems containing no factor IX. Further research determined that factor IX was also able to be activated by factor Xa (FXa) and played a key role in both the intrinsic and extrinsic pathways by the formation of a FIXa/factor VIIIa (FVIIIa) tenase complex [31].

Molecularly, FIX is a 56 kDa serine protease made up of one vitamin K-dependent γ-carboxyglutamic (Gla) domain, two epidermal growth factor (EGF)-like, and one catalytic domain [32, 33]. The catalytic domain contains the active site responsible for cleavage of FXa and acts in parallel to the second EGF-like domain to form the tenase complex with FVIIIa [34, 35]. The Gla domain is responsible for binding FIX to the extracellular matrix (ECM) in a sequestration phenomenon which is currently being researched [36]. It is known that the Gla domain of fully carboxylated FIX contains 12 potential Gla residues which play a large role in the tertiary structure of the Gla domain

and consequently the binding of FIX to the ECM [37]. Also playing a role in tertiary structure are magnesium and calcium concentrations. FIX contains a total of 10 divalent metal sites, which at physiological conditions contain six calcium-dependent sites, three magnesium-dependent sites, and one non-specific site [38, 39].

1.5 Fibrin Sealants

Fibrin sealants (FS) have been researched by the medical community for use in wound healing since the early 1900s, but the first mass-produced commercial FS only became available the 1970s [5, 40]. While FI is considered the most prominent component contained in FS, almost all FS contain additional proteins from the coagulation cycle. Additionally, calcium is included in all fibrin sealants as a necessary component for timely coagulation. FIIa is included in all major FS as an activation step; however, the inclusion of FIIa necessitates a dual-syringe or similar dual-storage container delivery device. This is due to the decrease in solubility of FI as it activates into fibrin monomer. The fibrin monomer created by this activation is capable of jamming medical application devices due to the high activity FIIa, and it is therefore essential that FIIa and FI be delivered separately to the wound site, with disposable equipment, or mixed in transport to the wound site [40]. FXIII and aprotinin are also commonly included in FS formulations for their clot strengthening and antifibrinolytic properties respectively [41].

FS provides a native hemostatic agent capable of both sealing wounds and encouraging the proliferation of native wound healing. The Food and Drug Administration (FDA) has approved commercially available FS for use as a hemostat, for

all surgeries; a sealant, for surgeries such as colostomy closure; and as an adhesive, for attaching skin grafts to burns [42]. There are records of additional off-label uses of FS such as tissue engineering and drug delivery that have been documented in literature [42]. Unfortunately, most FS are currently produced using plasma-derived material, which inherently contain a risk for virus transmission and due to limitations on supply remain economically unfeasible for most commercial purposes [43].

1.6 Hemophilia

Hemophilia is a hereditary genetic disorder wherein a patient is unable to produce active FVIII (hemophilia A) or FIX (hemophilia B), and treatment for the disorder can cost over 100,000 USD per annum in severe cases [44]. This cost can increase drastically if a patient develops inhibitors to replacement protein after receiving treatment [45]. Treatment of hemophilia is prescribed in two regimes: on-demand and prophylaxis. On-demand treatment requires immediate infusions of coagulation proteins when a bleeding episode occurs, while prophylaxis requires infusions of coagulation protein 2-3 times per week [46]. For severe hemophiliacs over a life-long basis, it has been found that prophylaxis provides better health outcomes for a cost equal to on-demand; however, the up-front cost nature of prophylaxis makes this option unaffordable for many patients [46]. The equivalence in cost for the two treatment regimens is partially due to undetected internal bleeding which can damage many types of tissue. Patients using both regimes still often suffer from having inadequate supply of coagulation proteins to completely stop internal bleeding, and this can be clearly demonstrated by the large

amount of knee, elbow, ankle, and hip replacements required by hemophilic patients [47, 48].

Hemophilia is a relatively rare disease, 1 in 5,000 and 1 in 30,000 male children who survive childbirth are affected by hemophilia A and hemophilia B respectively [49]. Despite the rarity of the disease, hemophilia has a large economic impact on countries that can afford to treat it. Hemophilia is different than most common diseases, as the coagulation factors used to treat the disease make up, on average, at least 75% of the healthcare cost of a patient [50]. The global market demand in 2002 for recombinant and plasma-derived coagulation factors was estimated to be 2 billion USD [50], and 2011 market research estimates the global demand for hemophilia treatment products to be 8.5 billion USD [51]. Considering that 70% of the world's hemophiliacs are underdiagnosed or untreated according World Federation of Hemophilia [52], the market for hemophilia treatment products has the potential to greatly expand.

1.7 Recombinant Proteins

In order to circumvent the supply issues and risk factors of plasma-derived products, recombinant proteins have been manufactured as an alternative since the 1980s. Since 1982 when the FDA approved production of recombinant insulin in *Escherichia coli* [53], recombinant proteins have also been produced in other types of bacteria, yeast, plants, mammalian cell bioreactors, and most recently in transgenically modified animals. Each production system provides its own unique advantages, from human-like PTM to efficient high yields to minimized risk factors.

Human coagulation proteins are a target for development of recombinant versions due to the limitations on plasma supply. There are currently many varieties of commercially-available, FDA approved recombinant coagulation factors including two FIX drugs [54, 55], one FXIII drug [56], and one thrombin drug [57]. All four of these drugs were produced in either yeast or a mammalian cell bioreactor. There has been no commercially-available, FDA approved recombinant FI approved to date.

Recombinant human proteins produced by transgenic animals were first approved by the FDA in 2009 [58, 59]. This product, antithrombin, was produced in the milk of transgenic goats and exemplifies the typical approach for production of recombinant proteins in transgenic animals. The labs of Dr. William H. Velander have begun preclinical trials and characterization of two such proteins: transgenic FIX (tg-FIX) produced in swine milk [9, 60] and transgenic FI (tg-FI) produced in bovine milk [61]. In addition, a recombinant FXIII subunit A (r-FXIIIA1a has been produced in *Pichia pastoris* to be used alongside tg-FI and commercially available recombinant FIIa [62].

1.8 Dissertation Objectives

Recombinant coagulation factors provide a treatment approach that does not deplete the supply of available plasma, and this dissertation focuses on the characterization and preclinical trials of tg-FIX, tg-FI, and r-FXIIIA1a. The objectives for these coagulation factors were as follows:

1. *Pharmacokinetics of tg-FIX delivered intravenously to mice*: A preliminary study on the efficacy of intravenous tg-FIX was carried out in normal, knock-out, and R333Q cross-reactive material positive mice.

2. *Pharmacokinetics of tg-FIX delivered intravenously to dogs*: tg-FIX was evaluated in hemophilia B dogs, the penultimate model before clinical trials, for safety and efficacy. A molecular basis for the pharmacokinetics presented was also sought.
3. *Pharmacokinetics of tg-FIX delivered buccally and orally to mice and dogs*: tg-FIX was administered to both mice and dogs as untreated tg-FIX milk and formulated as calcium-phosphate encapsulated FIX in order to evaluate the pharmacokinetics of both buccal and oral delivery of FIX.
4. *Characterize the compaction of FIX by divalent metals*: FIX was characterized for the first time as a zymogen for divalent metal compaction using orthogonal methods.
5. *Characterization of r-FXIIIA1*: r-FXIIIA1 was produced in *Pichia pastoris* and characterized for structure and function. The FXIII produced had normal activity while presenting with several novel properties not found in human FXIII or previously documented FXII produced in yeast.
6. *Characterization of the clot strengthening properties of FXIIIA1*: FXIII was evaluated *ex vivo* for clot strengthening properties in FS, human whole blood, platelet-poor plasma, and platelet-rich plasma. FXIII was also evaluated as a factor in efficacy of traditional measurements for clot strength measurements.
7. *In vivo application of liquid fibrin sealant in the presence of carrier foam*: Liquid fibrin sealant containing FI, FIIa, and FXIII has been optimized for wound sealing in swine hepatic resection models.

Each objective has been written as a self-contained chapter for this dissertation.

1.9 References

1 Davie EW, Fujikawa K, Kisiel W. The coagulation cascade: initiation, maintenance, and regulation. *Biochemistry*. 1991; 30: 10363-70.

2 Furie B, Furie BC. Mechanisms of thrombus formation. *New England Journal of Medicine*. 2008; 359: 938-49.

3 Esmon CT. The roles of protein C and thrombomodulin in the regulation of blood coagulation. *Journal of Biological Chemistry*. 1989; 264: 4743-6.

4 Quinsey NS, Greedy AL, Bottomley SP, Whisstock JC, Pike RN. Antithrombin: in control of coagulation. *The international journal of biochemistry & cell biology*. 2004; 36: 386-9.

5 Jackson CM, Nemerson Y. Blood coagulation. *Annual review of biochemistry*. 1980; 49: 765-811.

6 Coppola A, Di Capua M, Di Minno M, Di Palo M, Marrone E, Ieranò P, Arturo C, Tufano A, Cerbone AM. Treatment of hemophilia: a review of current advances and ongoing issues. *Journal of blood medicine*. 2009; 1: 183-95.

7 Ruggeri Z, Zimmerman T. von Willebrand factor and von Willebrand disease [published erratum appears in Blood 1988 Mar; 71 (3): 830]. *Blood*. 1987; 70: 895-904.

8 Sharathkumar A, Lillicrap D, Blanchette V, Kern M, Leggo J, Stain A, Brooker L, Carcao M. Intensive exposure to factor VIII is a risk factor for inhibitor development in mild hemophilia A. *Journal of Thrombosis and Haemostasis*. 2003; 1: 1228-36.

9 Van Cott KE, Velander WH. Transgenic animals as drug factories: a new source of recombinant protein therapeutics. *Expert opinion on investigational drugs*. 1998; 7: 1683-90.

10 Butler S, Van Cott K, Subrumanian A, Gwazduaskas F, Velander W. Current progress in the production of recombinant human fibrinogen in the milk of transgenic animals. *Thrombosis and haemostasis*. 1997; 78: 537-42.

11 Walsh G, Jefferis R. Post-translational modifications in the context of therapeutic proteins. *Nature biotechnology*. 2006; 24: 1241-52.

12 Furie B, Furie BC. The molecular basis of blood coagulation. *Cell*. 1988; 53: 505-18.

13 Mosesson M. Fibrinogen and fibrin structure and functions. *Journal of Thrombosis and Haemostasis*. 2005; 3: 1894-904.

14 Epstein FH, Singer AJ, Clark RA. Cutaneous wound healing. *New England Journal of Medicine*. 1999; 341: 738-46.

15 Doolittle RF. Fibrinogen and fibrin. *eLS*. 2001.

16 Acharya S, Dimichele D. Rare inherited disorders of fibrinogen. *Haemophilia*. 2008; 14: 1151-8.

17 Franchini M, Lippi G. Fibrinogen replacement therapy: a critical review of the literature. *Blood Transfusion*. 2012; 10: 23.

18 Francis CW, Marder VJ, Barlow GH. Plasmic degradation of crosslinked fibrin. Characterization of new macromolecular soluble complexes and a model of their structure. *J Clin Invest*. 1980; 66: 1033-43. 10.1172/JCI109931 [doi].

19 Lorand L. Factor XIII: structure, activation, and interactions with fibrinogen and fibrin. *Ann N Y Acad Sci*. 2001; 936: 291-311.

20 Yee VC, Pedersen LC, Le Trong I, Bishop PD, Stenkamp RE, Teller DC. Three-dimensional structure of a transglutaminase: human blood coagulation factor XIII. *Proc Natl Acad Sci U S A*. 1994; 91: 7296-300.

21 Purves L, Purves M, Brandt W. Cleavage of fibrin-derived D-dimer into monomers by endopeptidase from puff adder venom (Bitis arietans) acting at cross-linked sites of the gamma-chain. Sequence of carboxy-terminal cyanogen bromide gamma-chain fragments. *Biochemistry*. 1987; 26: 4640-6.

22 Spraggon G, Everse SJ, Doolittle RF. Crystal structures of fragment D from human fibrinogen and its crosslinked counterpart from fibrin. *Nature*. 1997; 389: 455-62. 10.1038/38947 [doi].

23 Gaffney PJ, Whitaker AN. Fibrin crosslinks and lysis rates. *Thromb Res*. 1979; 14: 85-94. 0049-3848(79)90027-6 [pii].

24 Schwartz ML, Pizzo SV, Hill RL, McKee PA. Human Factor XIII from plasma and platelets. Molecular weights, subunit structures, proteolytic activation, and cross-linking of fibrinogen and fibrin. *J Biol Chem*. 1973; 248: 1395-407.

25 Nagy JA, Kradin RL, McDonagh J. Biosynthesis of factor XIII A and B subunits. *Adv Exp Med Biol*. 1988; 231: 29-49.

26 Kradin RL, Lynch GW, Kurnick JT, Erikson M, Colvin RB, McDonagh J. Factor XIII A is synthesized and expressed on the surface of U937 cells and alveolar macrophages. *Blood*. 1987; 69: 778-85.

27 Muszbek L, Adany R, Kavai M, Boda Z, Lopaciuk S. Monocytes of patients congenitally deficient in plasma factor XIII lack factor XIII subunit a antigen and transglutaminase activity. *Thromb Haemost*. 1988; 59: 231-5.

28 Adány R, Glukhova MA, Kabakov A, Muszbek L. Characterisation of connective tissue cells containing factor XIII subunit a. *Journal of clinical pathology*. 1988; 41: 49-56.

29 Gui T, Reheman A, Funkhouser WK, Bellinger DA, Hagaman JR, Stafford DW, Monahan PE, Ni H. In vivo response to vascular injury in the absence of factor IX: examination in factor IX knockout mice. *Thrombosis Research*. 2007; 121: 225-34.

30 Oliver JA, Monroe DM, Roberts HR, Hoffman M. Thrombin activates factor XI on activated platelets in the absence of factor XII. *Arteriosclerosis, thrombosis, and vascular biology*. 1999; 19: 170-7.

31 Zur M, Nemerson Y. Kinetics of factor IX activation via the extrinsic pathway. Dependence of Km on tissue factor. *Journal of Biological Chemistry*. 1980; 255: 5703-7.

32 Freedman SJ, Furie BC, Furie B, Baleja JD. Structure of the Calcium Ion-Bound. gamma.-Carboxyglutamic Acid-Rich Domain of Factor IX. *Biochemistry*. 1995; 34: 12126-37.

33 Brandstetter H, Bauer M, Huber R, Lollar P, Bode W. X-ray structure of clotting factor IXa: active site and module structure related to Xase activity and hemophilia B. *Proceedings of the National Academy of Sciences*. 1995; 92: 9796-800.
34 Kolkman J, Lenting P, Mertens K. Regions 301–303 and 333–339 in the catalytic domain of blood coagulation factor IX are factor VIII-interactive sites involved in stimulation of enzyme activity. *Biochem J*. 1999; 339: 217-21.
35 Wilkinson FH, Ahmad SS, Walsh PN. The factor IXa second epidermal growth factor (EGF2) domain mediates platelet binding and assembly of the factor X activating complex. *Journal of Biological Chemistry*. 2002; 277: 5734-41.
36 Feng D, Stafford KA, Broze GJ, Stafford DW. Evidence of clinically significant extravascular stores of factor IX. *Journal of Thrombosis and Haemostasis*. 2013; 11: 2176-8.
37 Gui T, Reheman A, Ni H, Gross P, Yin F, Monroe D, Monahan P, Stafford D. Abnormal hemostasis in a knock-in mouse carrying a variant of factor IX with impaired binding to collagen type IV. *Journal of Thrombosis and Haemostasis*. 2009; 7: 1843-51.
38 Handford P, Baron M, Mayhew M, Willis A, Beesley T, Brownlee G, Campbell I. The first EGF-like domain from human factor IX contains a high-affinity calcium binding site. *The EMBO journal*. 1990; 9: 475.
39 Agah S, Sutton A, Velander WH, Bajaj SP. Role of Mg2+ in Extrinsic and Intrinsic Coagulation Under Physiologic Conditions. *Blood*: American Society of Hematology, 2008, 705-6.
40 Sierra DH. Fibrin sealant adhesive systems: a review of their chemistry, material properties and clinical applications. *Journal of Biomaterials Applications*. 1993; 7: 309-52.
41 Jackson MR. Fibrin sealants in surgical practice: an overview. *The American journal of surgery*. 2001; 182: S1-S7.
42 Spotnitz WD. Fibrin sealant: past, present, and future: a brief review. *World journal of surgery*. 2010; 34: 632-4.
43 Radosevich M, Goubran H, Burnouf T. Fibrin sealant: scientific rationale, production methods, properties, and current clinical use. *Vox sanguinis*. 1997; 72: 133-43.
44 Johnson KA, Zhou Z-Y. Costs of care in hemophilia and possible implications of health care reform. *ASH Education Program Book*. 2011; 2011: 413-8.
45 Kempton CL, White GC. How we treat a hemophilia A patient with a factor VIII inhibitor. *Blood*. 2009; 113: 11-7.
46 Fischer K, Van Der Bom J, Molho P, Negrier C, Mauser-Bunschoten E, Roosendaal G, De Kleijn P, Grobbee D, Van Den Berg H. Prophylactic versus on-demand treatment strategies for severe haemophilia: a comparison of costs and long-term outcome. *Haemophilia*. 2002; 8: 745-52.
47 Cohen I, Heim M, Martinowitz U, Chechick A. Orthopaedic outcome of total knee replacement in haemophilia A. *Haemophilia*. 2000; 6: 104-9.
48 Heeg M, Meyer K, Smid W, Van Horn J, Meer J. Total knee and hip arthroplasty in haemophilic patients. *Haemophilia*. 1998; 4: 747-51.

49 Franchini M, Mannucci PM. Past, present and future of hemophilia: a narrative review. *Orphanet J Rare Dis*. 2012; 7: 24.
50 Kelley K, Verma I, Pierce G. Gene therapy: reality or myth for the global bleeding disorders community? *Haemophilia*. 2002; 8: 261-7.
51 Conover D, Morozov A, Andersen K, Coffina M, Miller C, Waterhouse M, Krempa D, Stralow J, Migilore L, Wang D. Healthcare Observer *Morningstar*. 2013.
52 O'Mahony B, Black C. Expanding hemophilia care in developing countries. *Seminars in thrombosis and hemostasis*: New York: Stratton Intercontinental Medical Book Corporation, c1974-, 2005, 561-8.
53 Swartz JR. Advances in< i> Escherichia coli</i> production of therapeutic proteins. *Current Opinion in Biotechnology*. 2001; 12: 195-201.
54 Lambert T, Recht M, Valentino L, Powell J, Udata C, Sullivan S, Roth D. Reformulated BeneFix®: efficacy and safety in previously treated patients with moderately severe to severe haemophilia B. *Haemophilia*. 2007; 13: 233-43.
55 Shapiro AD, Ragni MV, Valentino LA, Key NS, Josephson NC, Powell JS, Cheng G, Thompson AR, Goyal J, Tubridy KL. Recombinant factor IX-Fc fusion protein (rFIXFc) demonstrates safety and prolonged activity in a phase 1/2a study in hemophilia B patients. *Blood*. 2012; 119: 666-72.
56 Dorey E. First recombinant Factor XIII approved. *Nature Biotechnology*. 2014; 32: 210-.
57 Ratner M. Recombinant thrombin approved. *Nature Biotechnology*. 2008; 26: 250-.
58 Kling J. First US approval for a transgenic animal drug. *Nature Biotechnology*. 2009; 27: 302-4.
59 Echelard Y, Meade H, Ziomek C. The first biopharmaceutical from transgenic animals: ATryn. *Modern Biopharmaceuticals*. 2005; 4: 995-1016.
60 Lindsay M, Gil G-C, Cadiz A, Velander WH, Zhang C, Van Cott KE. Purification of recombinant DNA-derived factor IX produced in transgenic pig milk and fractionation of active and inactive subpopulations. *Journal of Chromatography A*. 2004; 1026: 149-57.
61 Calcaterra J, Van Cott KE, Butler SP, Gil GC, Germano M, van Veen HA, Nelson K, Forsberg EJ, Carlson MA, Velander WH. Recombinant human fibrinogen that produces thick fibrin fibers with increased wound adhesion and clot density. *Biomacromolecules*. 2012; 14: 169-78.
62 Carlson MA, Calcaterra J, Johanning JM, Pipinos II, Cordes CM, Velander WH. A totally recombinant human fibrin Sealant. *Journal of Surgical Research*. 2013.

Chapter 2:

Preliminary Preclinical Pharmacokinetics of Transgenic Human Factor IX in Factor IX Knockout Mice

Nicholas C. Vanderslice*, Weijiu Xu*, Mostafa Fatemi*, Tong Gui†, Genlin Hu†, Nick Masiello‡, Paul E. Monahan†, William H. Velander*

*Department of Chemical and Biomolecular Engineering, University of Nebraska-Lincoln, Lincoln, Nebraska; † Department of Pediatrics, University of North Carolina at Chapel Hill, Chapel Hill, North Carolina; ‡Revobiologics, Framingham MA

2.1 Abstract

Hemophilia B is an x-linked disorder caused by a deficiency of coagulation factor IX (FIX). Current replacement therapy for hemophilia B patients comes from two sources: factor IX derived from human plasma (pd-FIX) or human recombinant factor IX (r-FIX) produced in CHO cell culture bioreactors. The post-translational complexity of FIX governs both its coagulation activity and pharmacokinetic behavior. The use of recombinant human factor IX expressed in the milk of transgenic pigs (tg-FIX) is a promising alternative because of the high level of expression that can be realized by the mammary gland. Here we investigate the relative pharmacokinetic behaviors pd-, r-, and tg-FIX in hemophilia B knockout mice. The time course of FIX protein, coagulation activity, and specific activity levels were followed for recovery and terminal clearance phases. The specific activity of both r-FIX and tg-FIX detected in circulation were maintained constant for the first 16 hours of the terminal clearance phase, indicating that

the detected circulating FIX was not degraded. Additionally, tail-cut studies were performed on FIX knockout mice infused with r-FIX and tg-FIX. Mice infused with r-FIX and tg-FIX had significantly reduced bleeding times compared to untreated mice. These preclinical trials hint at the complexity of FIX infusion therapy while establishing the safety and efficacy of the tg-FIX.

2.2 Introduction

Hemophilia B is a bleeding disorder characterized by a deficiency of biologically active coagulation factor IX (FIX) [1, 2]. The severity of this condition varies between individuals ranging from mild to severe, where severe cases present with coagulation activity level of FIX of less than 1% of the normal activity [3]. In order to maintain normal levels of FIX and decrease the occurrence of bleeding episodes, intravenous periodic replacement therapy is the recommended treatment for most patients [4]. There are currently two commercially available versions factor IX approved for clinical use: plasma derived pools (pd-FIX) and human recombinant cell culture bioreactors (r-FIX) [4-6]. Despite the creation of r-FIX, the price of treatment for Hemophilia B still remains unaffordable or unavailable for many people [7, 8].

FIX is a vitamin K-dependent plasma glycoprotein that in its zymogen form is found, under normal physiological conditions, at concentration levels of 5 μg/mL (M_r = 57,000) [9]. The mammary gland has been looked to as a vehicle to manufacture complex biomolecules, such as FIX, because of its well-recognized capacity to perform multiple post-translational modifications (PTMs) and high levels of expression [10, 11]. Factor IX

is a prime example of the application of transgenic animals to produce protein due to its biological activity being intimately linked to its PTMs [12].

We have previously demonstrated the production and purification of recombinant human factor IX expressed in the milk of transgenic pigs (tg-FIX) [13, 14]. This tg-FIX is comprised of multiple subpopulations of factor IX varying on the degree of γ-carboxylation in the Vitamin K-dependent γ-carboxyglutamic (Gla) domain [15]. This paper aims to demonstrate the safety and efficacy of tg-FIX in cross-reactive material negative (CRM-) FIX knockout (FIXKO) mice [16].

2.3 Materials and Methods

Unless otherwise indicated, all reagents were analytical or biological grade and were obtained from VWR International LLC (Radnor, PA, USA), Thermo Fisher Scientific (Waltham, MA, USA) or Sigma (St. Louis, MO, USA). Reference proteins pd-FIX (Mononine, CSL Behring, USA) and r-FIX (BeneFIX, Wyeth, USA) were outdated for clinical use but displayed full procoagulant activity on reconstitution as per manufacturer instructions.

Purification of tg-FIX

Whole milk of transgenic pigs containing tg-FIX was mixed with a 100 mM solution of ε-aminocaproic acid, 430 mM sodium citrate, and 40 mM benzamidine. The mixture was subjected to ultrafiltration-diafiltration to separate caseins and fat globules [13]. The filtrate was loaded into an affinity column (FIXSelect, GTC Biotherapeutics) and eluted with 2M $MgCl_2$. The elute was dialyzed against a 10 mM sodium citrate solution pH 6.8 and loaded into a Q-Sepharose Fast Flow column that was equilibrated

with a 2 mM imidazole buffer solution pH 7.5. The column was washed with 525 mM ammonium acetate and the protein eluted with an 800 mM ammonium acetate solution. The eluted mixture was dialyzed against a 20 mM imidazole, 50mM NaCl buffer solution pH 7.5.

The dialyzed solution was further purified using a ceramic hydroxyapatite column (CHT) equilibrated with a 20 mM imidazole, 50mM NaCl buffer solution pH 7.5. Then it was washed with 1M NaCl, re-equilibrated with a 20 mM imidazole, 50mM NaCl buffer solution pH 7.5 and washed with 80 mM potassium phosphate solution. The purified tg-FIX was eluted with a 200 mM potassium phosphate solution.

The integrity of the purified tg-FIX was verified by standard 12% sodium dodecyl sulfate-polyacrylamide gel electrophoresis (SDS-PAGE) under non-reduced and reduced conditions; and Western blot detection using an anti-human factor IX rabbit polyclonal (Sigma, St Louis, MO, US) paired with a goat anti-rabbit IgG H&L peroxidase conjugate (Sigma, St Louis, MO, US). The procoagulant activity of the stock protein solutions was measured with an activated partial thromboplastin time (aPTT) assay as previously described [14].

Clearance studies

In vivo experiments were performed following institutional guidelines. CRM-FIXKO were previously described by Lin et al. [17]. We assumed a plasma concentration of 0.9 mL per 20 g of body weight in mice and calculated a target dose concentration of 35 μg/mL-plasma and 75 μg/mL-plasma for recovery and terminal clearance phase studies, respectively. FIXKO mice with an average weight of 20 g were

injected with a solution containing the target concentration of protein via the tail vein for each type of pd-, r-, and tg- factor IX.

Blood samples were collected from the retro-orbital plexus at time intervals of 1, 5, 10, 15, and 30 minutes post injection (recovery phase) and 0.5, 6, 9, 12, 16, and 24 hours post injection (terminal clearance phase). Plasma was separated from blood cells by microcentrifugation [18] and stored at -80°C until assayed for protein concentration and procoagulant activity at each time point as described before[19].

Clearance curves corresponding to the recovery and elimination phase studies were constructed for each pd-, r-, and tg- factor IX injected by plotting the mean average value of procoagulant activity and its corresponding protein concentration against time. Each experimental data set was fitted using two-parameter exponential decay models with and without data weighting[20]. The fitting models were compared and the best fitting curve selected based on an F-test ($P<0.05$) of the extra sum-of-squares, goodness-of-fit parameter ($R^2>0.99$) and the minimized sum of the squared residuals (X^2) [21].

Tail bleeding and rebleeding

The modified procedure of Gui *et al* [22] was used for the tail bleeding test. Two-month-old FIXKO and wild-type (WT) C57BL/6 mice were selected based on matched weight and sex. Infused FIXKO mice were administered with 200 IU/kg r-FIX or 200 IU/kg tg-FIX five minutes before tail transection. Mice were anesthetized with 2.5% avertin. The mice were maintained at 37 ºC, and tail transection was performed at 1.5 mm cross-sectional diameter of the tail. The tail was then placed in saline and kept at 37 ºC where it was allowed to bleed until cessation or until 10 minutes had passed. The time of cessation was recorded. After 10 minutes had passed, 1 minute of pressure was

applied to the tip of the tail to cease bleeding. The clot was stripped after thirty minutes had passed since the initial transection. The tail was then placed in saline and kept at 37 ºC where it was allowed to bleed for 10 minutes until cessation of bleeding occurred. The mice were then allowed to wake up and were observed for 8 hours.

Statistical analysis and curve fitting

Pharmacokinetic parameters were calculated for all studies using a model independent method [23]. The area under the curve (AUC) and the area under the first moment curve (AUMC) with and without extrapolation to infinity were calculated by numerical integration of the exponential decay equation that best fitted each data set using Mathlab 14.0 (PTC, Needham, MA USA). Mean residence time (MRT) was calculated from these parameters according to Shapiro at al [20].

All statistical calculations and curve fitting modeling using non-linear regression methods were done with GraphPad Prism 5.0 software (GraphPad Software, San Diego CA, USA) [21, 24]. Statistical comparison of data sets was done using one-way analysis of variance (ANOVA) with Dunnett's test for multiple comparisons. A P-value > 0.05 was considered not significant.

2.4 Results

Terminal Phase Clearance Study

All FIXKO mice reported on in this study remained healthy during the assay period in both terminal and recovery phase studies. The assays of the antigen concentration and activity levels due to infusions of tg-, r-, and pd-FIX can be seen in in Figure 2.1. Activity clearance times remained approximately the same for all three

species of FIX; however, antigen clearance times for tg-FIX indicate that the tg-FIX in the bloodstream is rapidly cleared. The regression analyses of all three species indicate that the MRT of tg-FIX according to the activity assay is within normal range for a hemophilia B treatment into FIXKO mice (Table 2.1). When applied to the antigen assay, the tg-FIX has a third of the MRT of both commercial variants of FIX (Table 2.1). The specific activities of the samples demonstrate that while r-FIX and pd-FIX remained near 200 IU/mg, the normal activity for FIX, tg-FIX began with very low specific activity and rapidly increased to an above normal specific activity level as the antigen levels rapidly decreased, displaying$P < 0.01$ for tg-FIX compared to r-FIX and pd-FIX, and the activity levels decreased at a normal pace with no significant difference between pharmacokinetics for all samples (P value >> 0.05)(Figure 2.2).

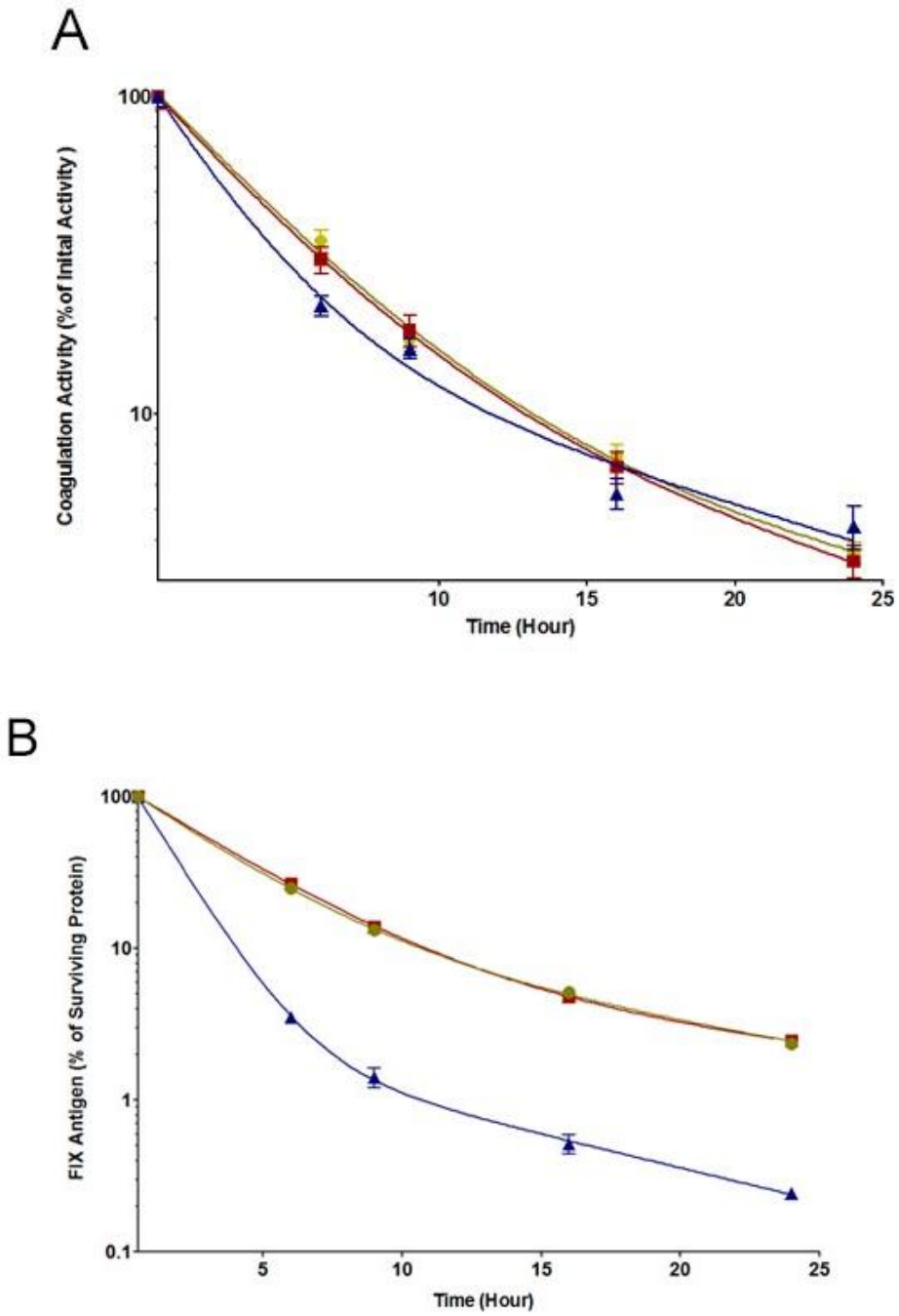

Figure 2.1. Percent of coagulation activity and antigen levels of FIX in circulation during the terminal phase. FIXKO mice were infused at a calculated target dose concentration of 75 µg FIX/mL mouse plasma. Coagulation activity (A) and FIX antigen levels (B) were fitted using a double exponential decay model. ● pd-FIX (n=8), ■ r-FIX (n=8), and ▲ tg-FIX (n=8). Data was normalized using the first data point at time=30 min as the common denominator. Data represent mean values ±SEM.

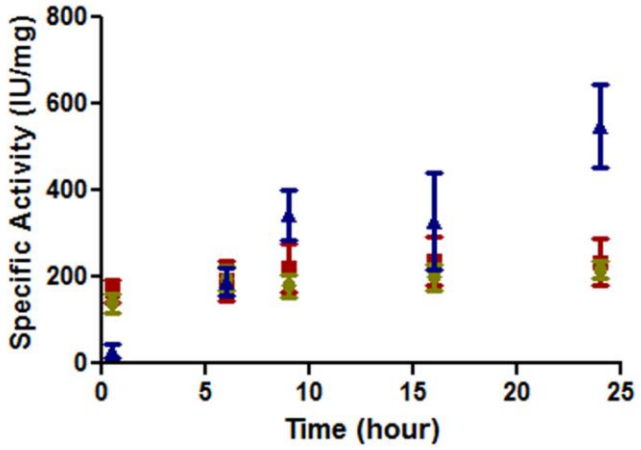

Figure 2.2. Specific activity of FIX during the terminal phase. FIXKO mice were infused at a calculated target dose concentration of 75 µg FIX/mL mouse plasma. ● pd-FIX (n=9), ■ r-FIX (n=8), and ▲ tg-FIX (n=8). Data represent mean values ±SEM.

Table 2.1. Pharmacokinetic variables during the terminal phase. FIXKO mice were infused at a calculated target dose concentration of 75 µg FIX/mL mouse plasma, and pharmacokinetic variables were determined based on aPTT and ELISA measurements.

aPTT						
Treatment	**Specific activity of stock solutions (IU/mg)**	**½t (h)**	**MRT (h)**	**AUC**	**AUMC**	**R^2**
pd-FIX	258	14.2	9.7	599	3740	0.997
r-FIX	137	11.2	8.5	578	3550	0.999
tg-FIX	252	10.8	9.4	514	3310	0.997
ELISA						
Treatment	**Specific activity of stock solutions (IU/mg)**	**½t (h)**	**MRT (h)**	**AUC**	**AUMC**	**R^2**
pd-FIX	258	9.7	7.1	483	2400	1
r-FIX	137	13.8	8.2	487	2450	1
tg-FIX	252	6.8	2.4	222	468	0.998

Recovery Phase Clearance Study

The recovery phase studies showed distinct pharmacokinetic regimes for each FIX variant. Activity levels and antigen levels decreased the most rapidly in tg-FIX, followed by pd-FIX, and r-FIX (Figure 2.3). The rapid decrease in antigen levels witnessed in the terminal tg-FIX study contrasts mildly with the moderate decrease in this study. The specific activities also formed three overlapping regimes for each variant (Fig. 4). These regimes maintained approximately constant specific activity for each species for all time points, indicating the rate of clearance according to both antigen and activity assays is equivalent. MRT for all samples decreased to approximately 3 hours for all samples according to both activity and antigen assays (Table 2.2).

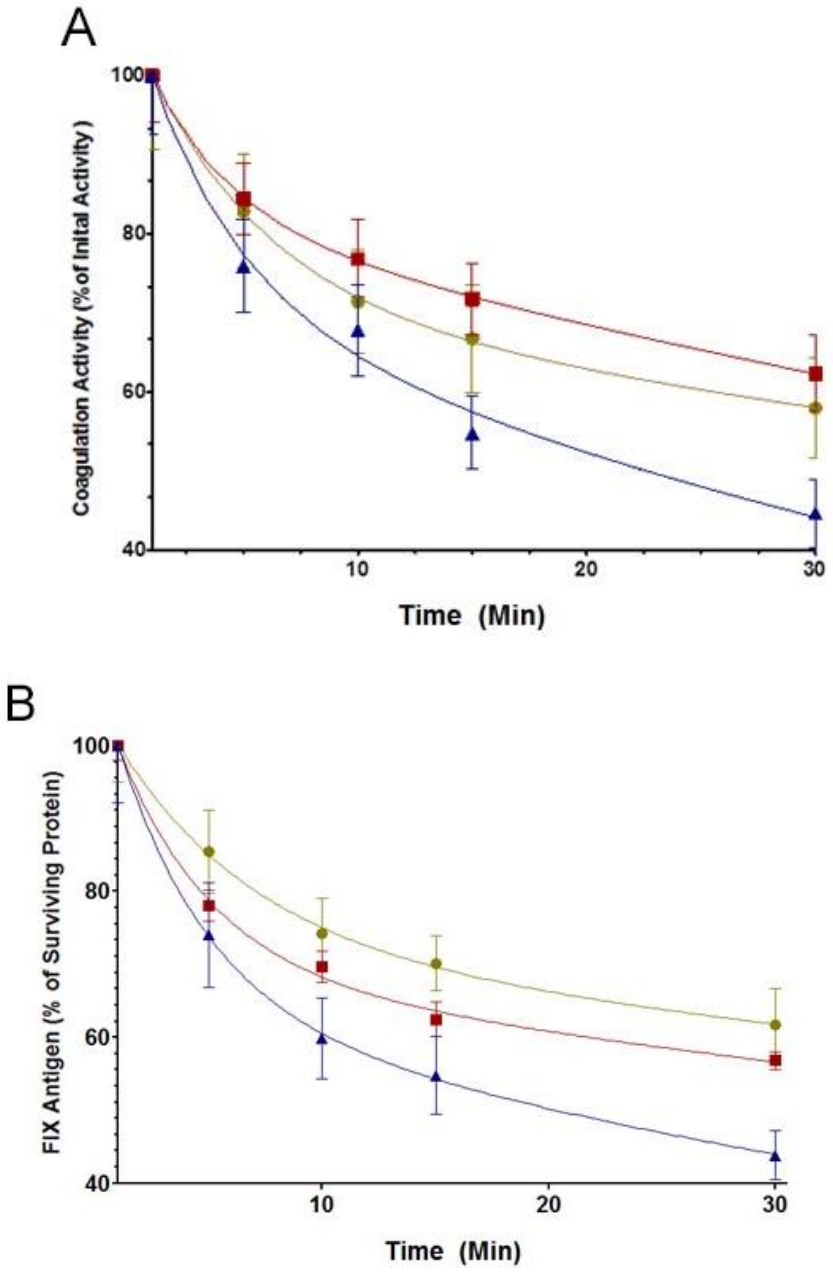

Figure 2.3. Percent of coagulation activity and antigen levels of FIX in circulation during the recovery phase FIXKO mice were infused at a calculated target dose concentration of 35 µg FIX/mL mouse plasma. Coagulation activity (A) and FIX antigen levels (B) were fitted using a double exponential decay model. ● pd-FIX (n=9), ■ r-FIX (n=8), and ▲ tg-FIX (n=8). Data was normalized using the first data point at time=30 min as the common denominator. Data represent mean values ±SEM.

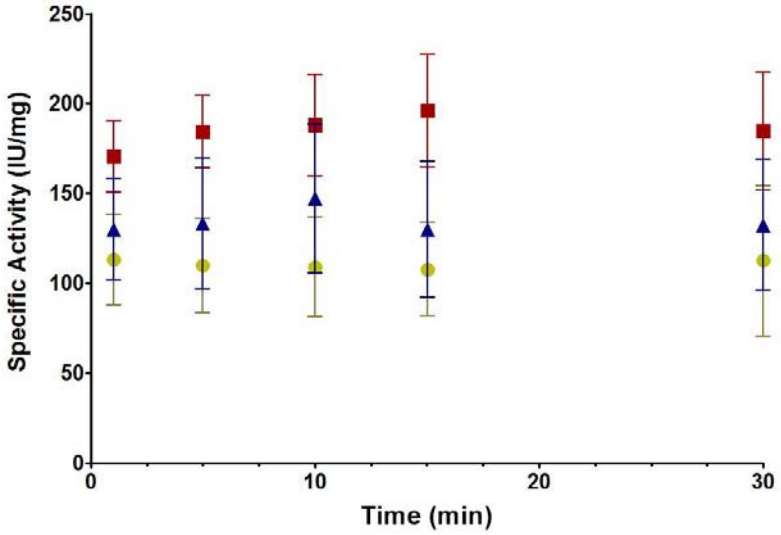

Figure 2.4. Specific activity of FIX during the terminal phase. FIXKO mice were infused at a calculated target dose concentration of 35 µg FIX/mL mouse plasma. ● pd-FIX (n=9), ■ r-FIX (n=8), and ▲ tg-FIX (n=8). Data represent mean values ±SEM.

Table 2.2. Pharmacokinetic variables during the recovery phase. FIXKO mice were infused at a calculated target dose concentration of 35 µg FIX/mL mouse plasma, and pharmacokinetic variables were determined based on aPTT and ELISA measurements.

aPTT						
Treatment	**Specific activity of stock solutions (IU/mg)**	**½t (h)**	**MRT (h)**	**AMC**	**AUMC**	**R^2**
pd-FIX	205	1.6	2.3	35.3	482	0.999
r-FIX	282	1.2	1.8	37.4	519	0.999
tg-FIX	207	0.7	1	31	403	0.989
ELISA						
Treatment	**Specific activity of stock solutions (IU/mg)**	**½t (h)**	**MRT (h)**	**AMC**	**AUMC**	**R^2**
pd-FIX	205	2.1	3	36.8	507	0.999
r-FIX	282	1.7	2.5	34.1	466	0.997
tg-FIX	207	0.9	1.3	29.1	288	0.999

Bleeding time

Tail cut studies confirmed that infusions of tg-FIX and r-FIX are capable of restoring hemostasis in FIXKO mice to levels similar to WT mice at both 5 (immediate hemostasis) and 30 minutes (secondary bleeding) (Fig. 2.5). All infused mice and WT mice had significantly faster clotting than untreated FIXKO mice while the clotting times for infused mice and WT mice were not significantly different. Rebleeding was seen in approximately half of the treated and WT mice, while all but one of the untreated FIXKO mice was observed to rebleed (Table 2.3). All treated FIXKO and WT mice survived and displayed no sign of distress during the 8 hour observation period in contrast to two of the eight mice from the untreated FIXKO group which were euthanized in compliance with the animal protocol.

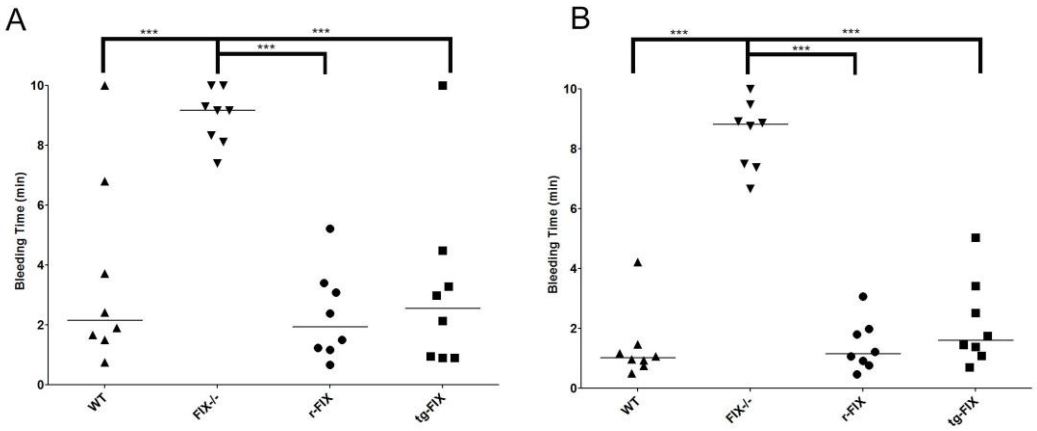

Figure 2.5. Bleeding time after tail transection. Hemostatic effect *in vivo* of tg-FIX in infused hemophilia B knockout mice. Time from tail transection to bleeding termination (A). After 10 minutes, bleeding was ended by application of firm pressure. After 30 minutes from time of bleeding termination, the clot was removed and secondary bleeding was recorded until bleeding termination (B). In infused mice, 200 IU/kg of either r-FIX or tg-FIX was infused five minutes prior to infusion. Significant variance ($P < 0.001$) was indicated by WT, r-FIX, and tg-FIX when compared to FIX-/- for both tail cuts [WT (n=8), FIX -/- (n=8), r-FIX (n=8), and tg-FIX (n=8)].

Table 2.3. Tail Transection Bleeding and Rebleeding. FIXKO mice were infused with 200 IU/kg r-FIX or tg-FIX. 5 minutes after infusion, a tail transection was performed on the infused mice, untreated FIXKO mice, and WT mice. Time of bleeding cessation was recorded and if no cessation occurred in 10 minutes before, pressure was used to terminate bleeding. 30 minutes after transection, the clots were stripped and secondary bleeding time was recorded. Mice were observed for at least 8 hours for rebleeding.

	1st Bleeding Time (5 Minutes Post Infusion)		2nd Bleeding Time (30 Minutes Post Infusion)		Delayed Rebleeding (8 hours post transection)
Treatment Group	**Average (min)**	**Standard Deviation**	**Average (min)**	**Standard Deviation**	**Bleeding/Sample Size (%)**
r-FIX	**2.33**	**1.51**	**1.41**	**0.84**	3/8 (38%)
tg-FIX	**3.20**	**3.04**	**2.17**	**1.44**	4/8 (50%)
WT	**3.60**	**3.20**	**1.39**	**1.18**	3/8 (38%)
FIX-/-(untreated)	**8.94**	**0.92**	**8.45**	**1.15**	7/8 (88%)

2.5 Discussion

The comparative pharmacokinetic studies of pd-FIX, r-FIX, and tg-FIX have revealed that tg-FIX demonstrates reduced MRT in both the recovery and terminal phases following injection of FIX into FIXKO mice. However, tail clip studies revealed that tg-FIX restored hemostasis to FIXKO mice similarly to r-FIX, and the treated FIXKO mice had bleeding times nearly identical to WT mice. Interestingly, FIXKO mice treated with tg-FIX in the long-term, higher dose study maintained pharmacokinetic variables nearly identical to r-FIX and pd-FIX. This is in stark contrast to the antigen levels of the mice from the same studies which had a significant drop in the pharmacokinetic variables. This phenomenon has been observed elsewhere in literature, and is attributed to extravascular partitioning of the FIX [25-27]. This extravascular partitioning in previous literature was caused by a modification to the Gla domain of FIX. FIX contains 12 Gla residues which can are γ-carboxylated in pd-FIX [15]; however, tg-FIX has been found to

have an average of 10-11 γ-carboxylated Gla residues [12] and while r-FIX has been previously be characterized to have an 11-12 γ-carboxylated Gla residues with Gla residue 11 or 12 being under γ-carboxylated [28]. As r-FIX provides normal pharmacokinetics in FIXKO mice, tg-FIX is most likely under γ-carboxylated in a different region of the Gla Domain.

Despite the effect of the changed conformation of tg-FIX on pharmacokinetic variables, bleeding times indicated that tg-FIX provided safe and effective treatment to FIXKO mice. WT, r-FIX infused FIXKO, and tg-FIX infused FIXKO mice had significantly reduced bleeding times compared to untreated FIXKO mice, while r-FIX and tg-FIX infused FIXKO mice regained hemostasis in a range of time that was insignificantly different from WT mice. These results indicate that the dose of tg-FIX delivered to these FIXKO mice was sufficient to maintain hemostasis for two bleeding events in the recovery phase. While rebleeding was an issue in mice treated with tg-FIX, the occurrence of rebleeding was not significantly different than FIXKO mice treated with r-FIX or WT mice.

These results indicate that tg-FIX has potential use as a pharmacological agent. While further studies will need to be performed to establish the pharmacokinetics of multiple infusions, the ability of tg-FIX to restore hemostasis to FIXKO mice who have been induced with a lethal injury for normal FIXKO mice shows the potential of tg-FIX as a treatment option. In the most conservative case, tg-FIX could be of use for treatment of hemophilia B patients undergoing surgery [29, 30], where large doses of FIX are traditionally administered to ensure that primary initial clotting occurs and that secondary internal bleeding is prevented. Clinical studies have also shown that continuous infusions

of FIX result in higher antigen response levels at lower doses of FIX over time [31], a phenomenon attributed to extravascular filling [26]. The antigen clearance times of tg-FIX, which are similar to the high-extravascular affinity K5A FIX of Gui et al. [27], indicate that tg-FIX has increased extravascular sequestration compared to pd- and r-FIX. The medical relevance of extravascular partitioning of FIX is still an object of current debate, and thus the fate of tg-FIX compared to pd-FIX and r-FIX as a prophylactic agent is intimately linked to the determination of the roles sequestered and plasma FIX play in hemostasis.

2.6 Acknowledgements

I would like to thank the large team responsible for the production, care, and characterization of the factor IX pigs and their milk. I would also like to thank Genlin Hu, Tong Gui, and Dr. Paul Monahan for their role in the mouse trials. Most importantly, I would like to thank Raffet Velarde, Weijie Xu, and Mostafa Fatemi for introducing me to the materials necessary to complete this research. This project was supported by NIH Heart, Lung, and Blood Institute grant "cGMP Recombinant FIX for IV and Oral Hemophilia B Therapy" (R01 JL078944).

2.7 References

1 Kasthuri RS, Roberts HR, Monahan PE. Factor IX Deficiency or Hemophilia B: Clinical Manifestations and Management. ***Hemostasis and Thrombosis: Practical Guidelines in Clinical Management*****. 2014: 57.**

2 Furie B, Furie BC. The molecular basis of blood coagulation. ***Cell*****. 1988; 53: 505-18.**

3 Thompson AR, Chen S-H. Characterization of factor IX defects in hemophilia B patients. ***Methods in enzymology*****. 1993; 222: 143-69.**

4 Berntorp E, Astermark J, Baghaei F, Bergqvist D, Holmström M, Ljungberg B, Norlund A, Palmblad J, Petrini P, Stigendal L. Treatment of haemophilia A and B and von Willebrand's disease: summary and conclusions of a systematic review as part of a Swedish health-technology assessment. *Haemophilia*. 2012; 18: 158-65.

5 Collins P, Fischer K, Morfini M, Blanchette V, Björkman S. Implications of coagulation factor VIII and IX pharmacokinetics in the prophylactic treatment of haemophilia. *Haemophilia*. 2011; 17: 2-10.

6 White GC, 2nd, Beebe A, Nielsen B. Recombinant factor IX. *Thromb Haemost*. 1997; 78: 261-5.

7 Fischer K, Van Der Bom J, Molho P, Negrier C, Mauser-Bunschoten E, Roosendaal G, De Kleijn P, Grobbee D, Van Den Berg H. Prophylactic versus on-demand treatment strategies for severe haemophilia: a comparison of costs and long-term outcome. *Haemophilia*. 2002; 8: 745-52.

8 Kelley K, Verma I, Pierce G. Gene therapy: reality or myth for the global bleeding disorders community? *Haemophilia*. 2002; 8: 261-7.

9 Kurachi K, Kurachi S, Furukawa M, Yao S. Biology of factor IX. *Blood coagulation & fibrinolysis*. 1993; 4: 953-73.

10 Echelard Y, Ziomek CA, Meade HM. Production of recombinant therapeutic proteins in the milk of transgenic animals. *BioPharm international*. 2006; 19.

11 Velander WH, Lubon H, Drohan WN. Transgenic livestock as drug factories. *Scientific American*. 1997; 276: 54-8.

12 Van Cott KE, Butler SP, Russell CG, Subramanian A, Lubon H, Gwazdauskas F, Knight J, Drohan WN, Velander WH. Transgenic pigs as bioreactors: a comparison of gamma-carboxylation of glutamic acid in recombinant human protein C and factor IX by the mammary gland. *Genetic analysis: biomolecular engineering*. 1999; 15: 155-60.

13 Baruah GL, Belfort G. A Predictive Aggregate Transport Model for Microfiltration of Combined Macromolecular Solutions and Poly-Disperse Suspensions: Model Development. *Biotechnology Progress*. 2003; 19: 1524-32.

14 Lindsay M, Gil G-C, Cadiz A, Velander WH, Zhang C, Van Cott KE. Purification of recombinant DNA-derived factor IX produced in transgenic pig milk and fractionation of active and inactive subpopulations. *Journal of Chromatography A*. 2004; 1026: 149-57.

15 Furie B, Furie BC. Molecular basis of vitamin K-dependent gamma-carboxylation. *Blood*. 1990; 75: 1753-62.

16 Monahan PE. Factor IX: Insights from knock-out and genetically engineered mice. *Thromb Haemost*. 2008; 100: 563-75.

17 Lin H-F, Maeda N, Smithies O, Straight DL, Stafford DW. A coagulation factor IX-deficient mouse model for human hemophilia B. *Blood*. 1997; 90: 3962-6.

18 Agah S, Sutton A, Velander WH, Bajaj SP. Role of Mg2+ in Extrinsic and Intrinsic Coagulation Under Physiologic Conditions. *Blood*: American Society of Hematology, 2008, 705-6.

19 Jin D-Y, Zhang T-P, Gui T, Stafford DW, Monahan PE. Creation of a mouse expressing defective human factor IX. *Blood*. 2004; 104: 1733-9. 10.1182/blood-2004-01-0138.

20 Shapiro A, Korth-Bradley J, Poon MC. Use of pharmacokinetics in the coagulation factor treatment of patients with haemophilia. *Haemophilia*. 2005; 11: 571-82.
21 Motulsky H. Prism 5 Statistics Guide, 2007. *GraphPad Software*. 2007.
22 Gui T, Reheman A, Funkhouser WK, Bellinger DA, Hagaman JR, Stafford DW, Monahan PE, Ni H. In vivo response to vascular injury in the absence of factor IX: examination in factor IX knockout mice. *Thrombosis Research*. 2007; 121: 225-34.
23 Gibaldi M, Perrier D. Pharmacokinetics: revised and expanded. *Drugs and the pharmaceutical sciences*. 1999; 92: 15-.
24 Motulsky H. Prism 5 Regression Guide, 2007. *GraphPad Software*. 2007.
25 Stern DM, Knitter G, Kisiel W, Nawroth PP. In vivo evidence of intravascular binding sites for coagulation factor IX. *British journal of haematology*. 1987; 66: 227-32.
26 Feng D, Stafford KA, Broze GJ, Stafford DW. Evidence of clinically significant extravascular stores of factor IX. *Journal of Thrombosis and Haemostasis*. 2013; 11: 2176-8.
27 Gui T, Lin H-F, Jin D-Y, Hoffman M, Straight DL, Roberts HR, Stafford DW. Circulating and binding characteristics of wild-type factor IX and certain Gla domain mutants in vivo. *Blood*. 2002; 100: 153-8. 10.1182/blood.V100.1.153.
28 Gillis S, Furie BC, Furie B, Patel H, Huberty MC, Switzer M, Barry Foster W, Scoble HA, Bond MD. γ-Carboxyglutamic acids 36 and 40 do not contribute to human factor IX function. *Protein science*. 1997; 6: 185-96.
29 Craddock Jr CG, Fenninger LD, Simmons B. Hemophilia: problem of surgical intervention for accompanying diseases review of the literature and report of a case. *Annals of surgery*. 1948; 128: 888.
30 Löfqvist T, Nilsson IM, Petersson C. Orthopaedic surgery in hemophilia: 20 years' experience in Sweden. *Clinical orthopaedics and related research*. 1996; 332: 232-41.
31 Uprichard J, Adamidou D, Goddard N, Mann H, Yee T. Factor IX replacement to cover total knee replacement surgery in haemophilia B: a single-centre experience, 2000–2010. *Haemophilia*. 2012; 18: 46-9.

Chapter 3:

Extravascular Filling by Novel Recombinant FIX used as a Vehicle to Lengthen Plasma Residence Time

Nicholas C. Vanderslice*, Weijiu Xu*, Mostafa Fatemi*, Tong Gui†, Genlin Hu†, Amanda S. Messer[§], Nick Masiello‡, Paul E. Monahan†, Elizabeth P. Merricks**, Kevin E. Van Cott*, Timothy Nichols**, S. Paul Bajaj[§], William H. Velander*

*Department of Chemical and Biomolecular Engineering, University of Nebraska-Lincoln, Lincoln, Nebraska; † Department of Pediatrics, University of North Carolina at Chapel Hill, Chapel Hill, North Carolina; § Department of Orthopaedic Surgery, David Geffen School of Medicine at UCLA, Los Angeles; ‡Revobiologics, Framingham MA ; **Department of Pathology and Laboratory Medicine, University of North Carolina at Chapel Hill, Chapel Hill, North Carolina

3.1 Abstract

Background: Multiple gene transgenesis was used to produce a non-processionally carboxylated, biologically active, recombinant human factor IX (tg-FIX) protein from the milk of transgenic pigs.

Objective: The manipulation of FIX circulation residence time by extravascular reservoir filling versus permanent clearance was studied in hemophilic B dogs using crossover infusion of tg-FIX and pd-FIX.

Methods: Mass spectrometry and metal-dependent monoclonal antibody mapping by Biacore were used to characterize the Gla domain of tg-FIX. The cross-over, IV infusion

of plasma-derived FIX (pd-FIX) and tg-FIX were administered at 50 IU/kg to hemophilic B dogs as follows:

- Dog O06 was infused with a single dose of active tg-FIX;
- Dog O25 was infused with pd-FIX and at 48 hours was reinfused with active tg-FIX;
- Dog O05 was infused with active tg-FIX and at 48 hours was reinfused with pd-FIX;
- Dog O66 was infused with active tg-FIX and at 72 hours was reinfused with whole population tg-FIX.

For all studies, plasma antigen, one-stage clotting activity, and whole blood clotting times (WBCT) were assessed. Recovery phase half-life and terminal phase mean residence time (MRT) were calculated.

Results: The tg-FIX possesses *in vitro* coagulation activity comparable to therapeutic grade pd-FIX while containing a unique, non-processive γ-carboxylation in positions 7-10 of the Gla domain. The pharmacokinetics observed during cross-over infusion studies between pd-FIX and tg-FIX showed a strong dependence on the FIX species first infused: the latter infused species presented a >2-fold lengthened recovery phase and mean residence time (MRT) from <30 hours to about 40 hours. The time course coagulation activity by WBCT was also lengthened and sustained in excess of 100 hours for all tg-FIX/ pd-FIX cross-over infusions, reflecting an increased plasma side partitioning relative to extravascular storage. The tg-FIX had rapid plasma concentration fall-off for all dogs having no prior exposure to exogenous FIX and thus presented a much faster extravascular partitioning kinetics relative to pd-FIX.

Conclusion: These IV infusion studies show that extravascular filling phenomena can be used as a vehicle to substantially lengthen circulation residence time for FIX.

3.2 Introduction

Hemophilia B (HB) is a bleeding disorder characterized by the deficiency of biologically active coagulation factor IX (FIX) [1, 2]. Periodic replacement therapy by intravenous (IV) infusion is recommended to decrease the occurrence of bleeding episodes in most patients. However, this therapy is complicated by the rapid clearance of FIX from circulation [3, 4], the development of inhibitors which can dramatically increase the volume of FIX needed for periodic replacement therapy [5], and the differences in FIX biotherapuetics which are currently derived from pooled human plasma (pd-FIX) and recombinant animal cell culture bioreactors (r-FIX) [6-11]. As a result, current FIX bioengineering seeks to lengthen its plasma residence time using modifications such as PEGylation [12], the addition of additional glycosylation sites [13], albumin fusion [14], and FIX immunoglobulin fusion [15]. In parallel, new recombinant production methods are being developed to increase the abundance of FIX by using higher animal cell culture density bioreactors [16] and also the milk of transgenic livestock [17-19]. Transgenic livestock is viewed as a modern method to overcome traditional limitations of cell density in mammalian cell reactors [20], and with the advent of new tools for genetic manipulation, a way to create functional posttranslational modifications despite rate limitations [21, 22].

The above efforts to improve HB therapy would be advanced by a deeper understanding of the vascular transport phenomena that determine extravascular storage

levels of FIX [23, 24]. For example, the molecular engineering that lengthens FIX circulation residence times should also avoid an adverse impact on the hemostatic role that FIX likely plays while residing in extravascular reservoirs. Importantly, in the context of replacement HB therapy, the hemostatic balance associated with FIX in extravascular reservoirs with that of permanent hepatic clearance by the liver is not yet known [24, 25]. This important physiology is obscured by the fact that the liver is both responsible for permanent clearance of plasma proteins and is a highly vascularized organ that can be a major endothelial and extravascular reservoir for FIX [3, 26]. In mouse [3, 4], rat [27], and baboon studies[26], high levels of radio-labeled FIX accumulated in the liver shortly after IV infusion. While a component of the clearance mechanism of glycoproteins like FIX by the liver has been attributed to hepatic asialoglycoprotein receptors, a detailed understanding of permanent clearance from plasma has not been described [18]. Moreover, the nature of the occupation of IV infused FIX within the liver is not yet known in the context of permanently cleared FIX versus that which is hemostatically present in hepatic or other extravascular reservoirs.

The pharmacokinetic (PK) behavior of pd- and r-FIX in plasmin is well characterized in HB dog [8] and humans [28-35]. However, the endothelial and extravascular partitioning of FIX is still being characterized. One attempt to characterize this phenomenon was a study in which pd-FIX and r-FIX variants were IV infused into the saphenous veins of HB mice [4, 36]. In addition, Gui et al. has established that the vitamin K-dependent γ-carboxyglutamic acid (Gla) domain of pd-FIX [37, 38] strongly interacted with collagen IV found in the extracellular matrix (ECM) of endothelial cells [4, 39]. These studies demonstrated that the collagen binding affinity of FIX could be

enhanced or decreased by changes in Gla domain conformation or mutations in the Gla domain [4, 40]. More recently, HB mice studies by Feng et al. [23] have shown that pd-FIX can occupy endothelial and extracellular reservoirs for more than seven days while being undetected in plasma, and concluding that three-fold more FIX is contained in these extravascular reservoirs than in circulation. Importantly, the above studies *in vivo* showed that differences in Gla domains between pd-FIX and bioengineered r-FIX affect the relative balance of extravascular storage and plasma residence time.

Recently, the evidence of the large amounts of FIX residing in the extravascular reservoirs of different organs of normal baboons was further illuminated [12]. This recent analysis readdressed the data from Stern et al. [26] that studied bovine FIX infused at high levels into a normal baboon. This study reported displacement of endogenous baboon FIX into circulation: when high levels of IV bovine FIX were infused, the antigen levels of baboon FIX were found to rise to over twice normal levels. Thus, there exists important evidence in a primate model that large amounts of FIX both exist and are displaceable from extravascular reservoirs. While no comparable study has been made in normal or HB human subjects, those patients who express no plasma FIX antigen need more FIX administered to achieve the equivalent plasma antigen levels during the recovery PK phase than those who express antigen [23, 24]. These HB patients potentially present an antigen structure that still has significant endothelial avidity and the ability to load extravascular space, but has defective coagulation activity.

Collectively, the above data in HB mice, rats and normal baboons led us to infuse r-FIX made in the milk of transgenic pigs (tg-FIX) in a crossover study with pd-FIX. This

paper details the preclinical administration of tg- and pd-FIX to HB dogs, a standard large animal model for hemophilia [41-43].

3.3 Materials and Methods

Hemophilia B Dogs

This crossover study between pd-FIX and tg-FIX was conducted on four HB dogs at the Francis Owen Blood Research Laboratory at the University of North Carolina at Chapel Hill. All studies were approved by the Institutional Animal Care and Use Committee at the University of North Carolina at Chapel Hill. Exclusion criteria were clinically overt illness, abnormal clinical serum chemistry or hematology parameters (i.e. complete blood counts and platelet counts), and treatment with FIX in the 3 weeks prior [44].

Materials

All buffer components were purchased from VWR International LLC (Radnor, PA, USA), Thermo Fisher Scientific (Waltham, MA, USA) or Sigma (St. Louis, MO, USA) unless otherwise stated. For these studies, tg-FIX was purified using a modified version of the procedure of Lindsay et al. [17]. Size exclusion chromatography (SEC) was used to polish the purified sample into inactive, active, and activated populations. Whole population tg-FIX contained 20% inactive tg-FIX and 80% active tg-FIX population with activity calculated based on one-stage clotting assay and ELISA of the tg-FIX before recombining the two fractions. Freshly immunopurified stocks of pd-FIX were provided by Revobiologics, Framingham MA. The integrity of the purified pd-FIX and tg-FIX was verified by SEC and 12% sodium dodecyl sulfate-polyacrylamide gel

electrophoresis (SDS-PAGE) under non-reduced and reduced conditions and Western blot detection using an anti-human FIX rabbit polyclonal (Sigma, St Louis, MO, US) paired with a goat anti-rabbit IgG H&L peroxidase conjugate (Sigma, St Louis, MO, US). The procoagulant activity of the stock protein solutions was measured with a one-stage clotting assay as previously described [17]. The stocks of therapeutic grade r-FIX (BeneFIX, Pfizer, USA) were expired for clinical use, but when used in experiments, exhibited full procoagulant activity by one-stage clotting assay. FIX activity was measured in international units, with 1 unit corresponding to the activity of FIX in 1 mL of plasma which corresponds to a value of 200 IU/mg. All active FIX species were measured with activities between 150-250 IU/mg.

Affinity Separation of Purified tg-FIX

A human factor IX affinity column was constructed using a custom Gla domain anti-FIX Mg^{2+}-dependent 1G7 monoclonal antibody (mAb) (Green Mountain Antibodies, USA) which was bound to Streamline rProtein A (GE Healthcare, USA). tg-FIX, r-FIX, and pd-FIX were dialyzed into an equilibrium buffer containing 20 mM imidazole, 50mM NaCl, 1.1 mM $CaCl_2$, and 0.6 mM $MgCl_2$ at pH 7.4 in snake-like dialysis membranes. The dialyzed FIX species were loaded onto the 1G7 mAb column and equilibrated with two column volumes (CV) of equilibrium buffer and washed with three CV of high salt equilibrium buffer containing 500 mM NaCl. Unbound FIX was collected and then concentrated using Amicon Ultra 10 kDa molecular cut-off centrifugal filter (Millipore, Billerica, MA, USA). The loaded 1G7 mAb column was then equilibrated with 2 CV of equilibrium buffer and eluted with six CV of 20 mM imidazole, 50 mM NaCl, and 5 mM EDTA at pH 7.4. Bound FIX was collected and then

concentrated using Amicon Ultra 10 kDa molecular cut-off centrifugal filter (Millipore, Billerica, MA, USA). The chromatography and fraction collection was performed on a BioCad Vision chromatography station equipped with an integrated fraction collector (Applied Biosystems, Carlsbad, Ca, USA).

Biacore binding interaction of factor IX to Gla domain monoclonal antibodies.

A Biacore T100 Series S CM5 chip was coupled with protein A/G (Pierce Biotechnology, Rockford IL) in 10mM sodium acetate pH 4.0 using the amine coupling procedure with a target of 1000 Response Units (RU) as described by Biacore (Uppsala, Sweden). On average we obtained 1015 RU protein A/G covalently bound to the chip. For a control surface, the flow cell was activated with EDC (1-ethyl-3-(3-dimethylaminopropyl) carbodiimide hydrochloride) and NHS (N-hydroxysuccinimide) and blocked by 1M ethanolamine-HCl pH 8.5. The Biacore chip, EDC, NHS and ethanolamine were all purchased from GE Healthcare (Piscataway, NJ). 100 nM factor IX Gla domain Mg^{2+}-dependent mAb, 1G7, in screen buffer (12mg/mL carboxymethyl-dextran sodium salt, 12mg/mL bovine serum albumin, and HEPES buffered saline with 0.005% (v/v) P20 pH 7.4) or the Ca^{2+}-dependent mAb, SB 249417, were captured separately onto the protein A/G surface. Using a 5 µl/min flow rate and a contact time of 2 minutes, we obtained on average 3500 RU captured mAb. On the control surface we used screen buffer with no mAb under the same conditions. After sensogram stabilization on both surfaces, varying concentrations of pd-FIX, r-FIX, inactive tg-FIX, or active tg-FIX (12.5-200nM) in running buffer (5mM calcium HBS-P pH 7.4) were flowed over the control and mAb surfaces at 30 µl/min for 2 minutes. Dissociation of FIX was monitored for 5 minutes using running buffer at the same flow rate. Surfaces were

regenerated using 10mM glycine pH 1.5 for half a minute at 30µl/min. Both surfaces were washed with running buffer for 2 minutes before the next run. Analysis was performed using the Biacore T100 evaluation software v1.1.1 (Biacore Uppsala, Sweden) and sensograms displayed using Microsoft Excel.

Mass Spectrometry

Samples of r-FIX and active tg-FIX were activated with factor XIa (FXIa) (Haemtech, Essex Junction, VT) using a 1:100 (w:w) enzyme to substrate ratio in 5mM $CaCl_2$, 1X TBS, pH 7.4 at 37°C for 1.0 hour. After activation, the samples were quenched with 1.2 moles of EDTA per mole of Calcium and stored at -80^{o}C until further analysis.

LC-ESI-TOF mass spectrometry (MS) analysis was performed on an Agilent 1200 capLC system with an Agilent 6210 ESI-TOF MS. Solvent A was 0.1% formic acid (Fluka) (v/v) in deionized water. Solvent B was 0.1% formic acid (v/v) in acetonitrile (Burdick and Jackson). The column was an Agilent 300SB-C8 Poroshell column: 7.5 cm L x 0.5 mm ID, 5 micron particle size. The samples were diluted in Solvent A in the HPLC vial and loaded in the autosampler. Approximately 35 pmol of sample was injected on the column in a 40 microliter injection volume. The column was pre-equilibrated with 5%B; the flow rate was 20 microliters/minute; the column oven was set at 37^{o}C; the autosampler was set at 10^{o}C. After injection, the column was washed for 5 minutes with 5% B, then a linear gradient up to 20%B over 10 minutes, followed by a linear gradient up to 55% B over 70 minutes. The column was then cleaned by ramping up to 95% B for 5 minutes and then a series of three cycles of 10%B to 70% B, and then the column was re-equilibrated for >10 CV with 0 %B for the next injection. A blank injection was performed in between each sample to minimize column carryover. MS data

were acquired with MassHunter in positive mode with the following parameters: 4000 V source voltage, 325^{o}C nebulizing gas temperature, 7 L/min gas flow rate, internal reference mass of 922.01 m/z. MS data were analyzed using Agilent's Qualitative Analysis (version B.01.03).

Hemophilia B Dog Studies

Four different HB dogs were IV infused with 50 IU/kg body weight with either pd-FIX or tg-FIX as follows:

- Dog O06 was infused with a single dose of active tg-FIX;
- Dog O25 was infused with pd-FIX and at 48 hours was reinfused with active tg-FIX;
- Dog O05 was infused with active tg-FIX and at 48 hours was reinfused with pd-FIX;
- Dog O66 was infused with active tg-FIX and at 72 hours was reinfused with whole population tg-FIX.

Native and citrated whole blood (for preparing plasma) samples were taken at 15 and 30 minutes then at 1, 2, 4, 8, 12, 24, 48 hours post FIX infusion. At 48 hours (O25 and O05) and 72 hours (O66), FIX concentrations had returned to near baseline levels for all dogs. The same time points were taken after the second infusion and additional sampling was done twice daily until ~360 hours post infusion. PK parameters were calculated for both studies using a model independent method [45]. Mean residence time (MRT) was calculated from these parameters according to Shapiro et al. [46].

Pharmacokinetic Assays

Human FIX antigen concentration, activity, and whole blood clotting time (WBCT) were assayed for all plasma samples collected. FIX antigen plasma concentration was evaluated by a FIX-ELISA kit (Kordia), and FIX activity level was evaluated using a one-stage clotting assay based on the Behring Coagulation Timer (Siemens Healthcare, Diagnostics Products GmbH, Marburg, Germany) [47]. Procedures for both the one-stage clotting assay and ELISA have been described previously in Nolte et al. [47]. WBCT was assayed as previously described using the 'two-tube' method using silicone-coated tubes which were tilted every 30 seconds. [44, 48, 49].

3.4 Results

γ-Carboxylation of the Gla domain

Previous analysis of pd-FIX showed that normal human donors produce exclusively 12 Gla pd-FIX under normal conditions [50]. However, both r-FIX and tg-FIX samples contain more varied under-carboxylated Gla populations. Previous amino acid analysis of FIX after basic hydrolysis has stated that pd-FIX contains on average 10.5 mol Gla/mol pd-FIX, r-FIX contains on average 6.5 moles Gla/mol r-FIX, and tg-FIX contains on average 6.0 mol Gla/mol tg-FIX [17]. The MS structural characterization of the r-FIX revealed the presence of a mixed population of 10, 11, and 12 Gla r-FIX (Fig. 3.1A). 12 Gla r-FIX was the predominant species for the sample, containing an estimated ~67% of the sample, followed by ~31% of 11 Gla r-FIX, and ~2% 10 Gla r-FIX. For active tg-FIX, 9, 10, 11, and 12 Gla species are present at an estimated ~9%, ~47%, ~28%, and ~16% of the sample respectively (Fig. 3.1D), all of which contain γ-carboxylated 1-6 Gla domains according to MS and SB 249417-

conjugated Biacore (Table 3.1). Each FIX Gla species contains two peaks due to ±beta-hydroxylation.

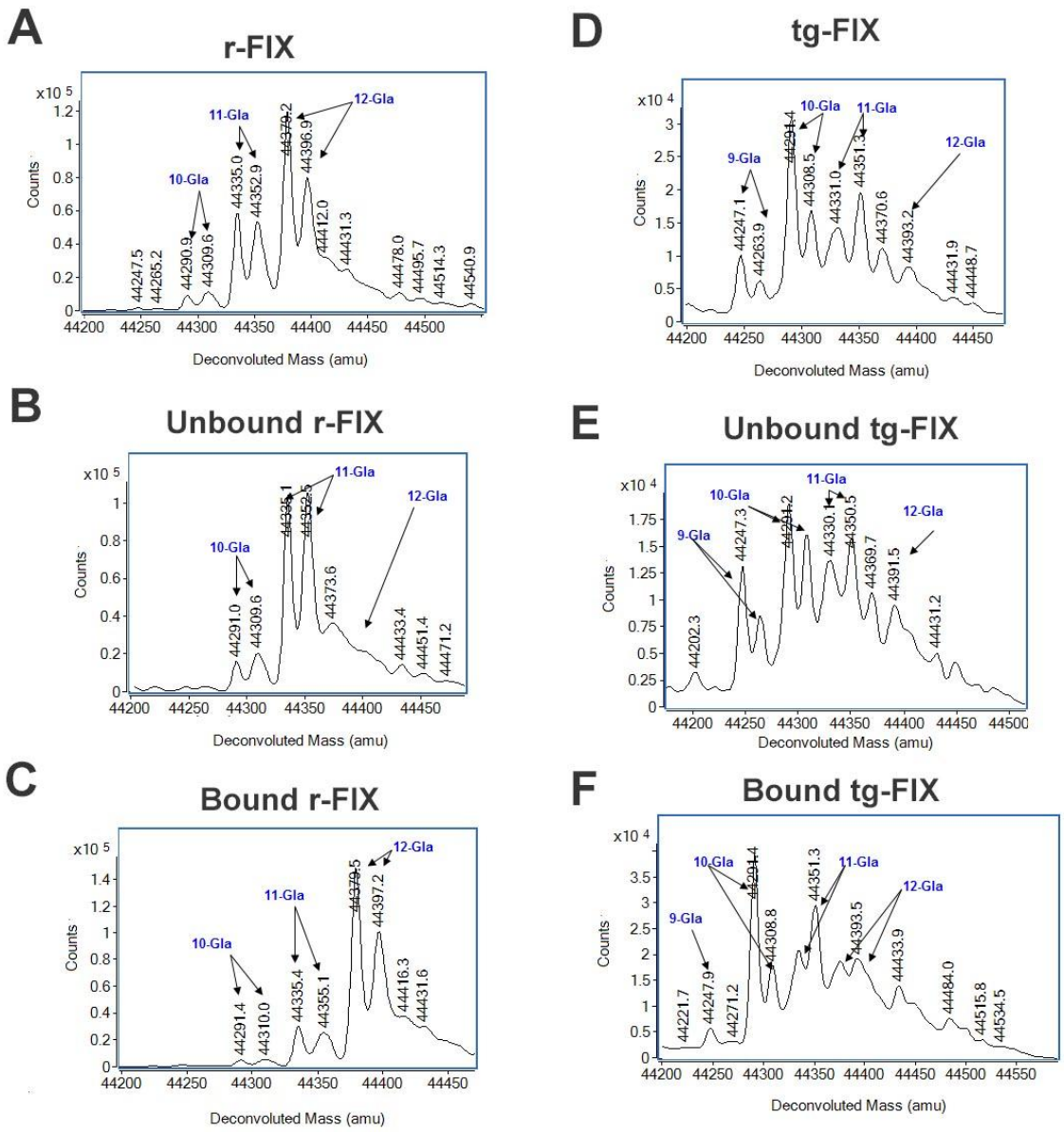

Figure 3.1. LC-ESI-TOF mass spectrometry analysis of FIX gla content. (A, B, C) r-FIX and (D, E, F) tg-FIX were analyzed using 1G7 mAb affinity column. (r-FIX: A; tg-FIX: D) Active FIX was loaded onto the 1G7 affinity column where the (r-FIX: B; tg-FIX: E) unbound FIX and (r-FIX: C; tg-FIX: E) eluted bound FIX were collected. Samples were treated with factor XIa to activate the FIX and analyzed with LC-ESI-TOF mass spectrometry.

Table 3.1. Characteristics of pd-FIX, r-FIX, and tg-FIX

Characteristic	**pd-FIX [11]**	**r-FIX [11]**	**tg-FIX**
Primary structure	Ala^{148}/Thr^{148}	Ala^{148}	Thr^{148}
Specific Activity (IU/mg)	200	150-200	150-250
Total γ-carboxyglutamic acid content	100%	60%	Minor Species
12 of 12 Gla	0	35%	Major Species
11 of 12 Gla	0	5%	Major Species
10 of 12 Gla		0	Minor Species
<10 of 12 Gla			
Biacore: Steady-State KD (nM)			
Ca^{2+}-dependent mAb	7.5E-8	3.8E-8	9.9E-8
Mg^{2+}-dependent mAb	1.7E-7	9.3E-8	3.9E-7
γ-carboxylated Gla Residues			
1-6	Majority γ-Carboxylated	Majority γ-Carboxylated	Majority γ-Carboxylated
7-10	Majority γ-Carboxylated	Majority γ-Carboxylated	Minority γ-Carboxylated
11-12	Majority γ-Carboxylated	Minority γ-Carboxylated	Majority γ-Carboxylated
β-hydroxyaspartic acid (Asp 64)	37%	46%	40-50%
Pro-peptide content	None detected	None detected	None detected
Activated FIX	0.21% ±0.010%	0.11% ±0.0019%	None detected
Tyr 155 sulfation	>90%	<15%	10-15%
Ser 158 phosphorylation[18, 51]	>90%	<1%	70%
Sialylation (nmol/mol FIX)[18, 51]	8.8	6.5	4-5.5

1G7 mAb column purification of pd-FIX, r-FIX, and tg-FIX resulted in starkly different chromatography profiles. The 1G7 column was capable of binding 100% of the pd-FIX; however, for r-FIX and tg-FIX, 30-50% of the FIX remained unbound to the column and was removed by the salt wash. MS revealed that the purification of the r-FIX

by 1G7 mAb column successfully removed over 70% of the FIX species with less than 12 Gla (Fig. 3.1B and 3.1C). In contrast, 1G7 mAb purification of tg-FIX showed retention of 10, 11, and 12 Gla species in the eluate while also containing unbound populations of 9, 10, 11, and 12 Gla species in the salt wash (Fig. 3.1E and 3.1F). The differences in the binding of the under-carboxylated species of r-FIX and tg-FIX to 1G7 mAb indicate that the order of γ-carboxylation in each FIX species is different. The MS analysis indicates from the diversity of under-carboxylated species in the tg-FIX that the 11-12 Gla domain detected by 1G7 is γ-carboxylated more consistently than r-FIX; however, tg-FIX is more consistently missing at least one Gla domain in the 7-10 Gla residue range according to both Biacore and MS. These differences in the Gla domain conformation between species is likely to exhibit stark differences in extravascular binding [4, 39].

Pharmacokinetics of single-dose of active tg-FIX (O06)

When tg-FIX was infused into HB dog without a transfusion in the previous three weeks (Fig. 3.2), quantitative pharmacokinetic variables were unobtainable at an acceptable degree of certainty. Qualitatively, both the antigen concentration and activity levels exhibited a rapid decrease in FIX presence. The 50 IU/kg dose of tg-FIX resulted in an immediate response corresponding to a concentration 12% of normal and an activity level 15% of normal. However, FIX antigen concentration and activity levels were undetectable by 8 and 24 hours respectively. Comparatively, this single infusion of tg-FIX corresponded to the pharmacokinetic behavior of a FIX K5R mutant produced by Gui et al. [4] which was found to have increased binding to the extravascular reservoirs in mice.

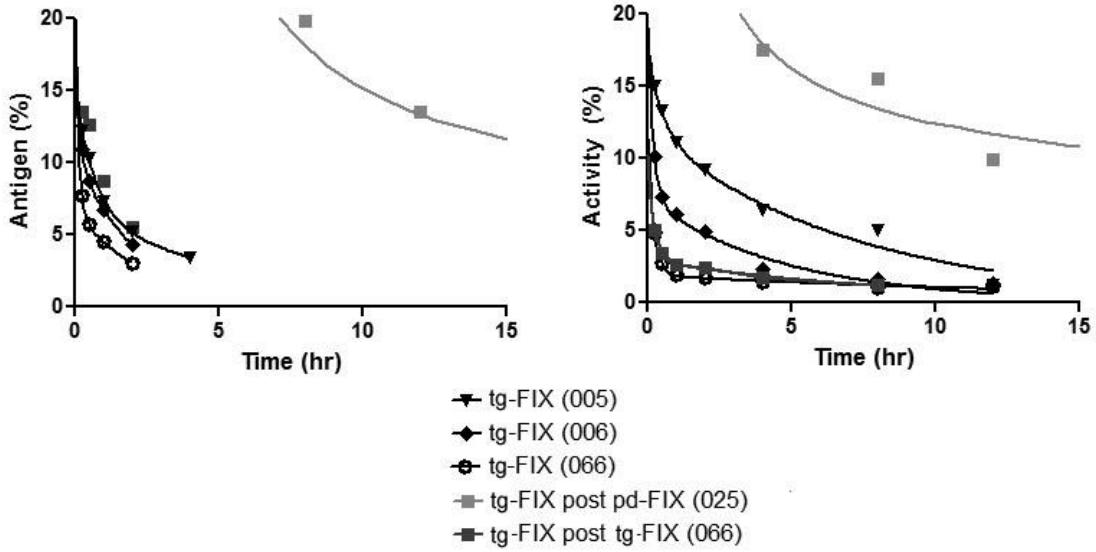

Figure 3.2. Effect of tg-FIX on plasma activity and antigen levels in hemophilia B dog. FIX activity measured by (A) antigen measured by ELISA and (B) one stage clotting assay. Each line represents an individual trial of 50 U/kg tg-FIX administered to a hemophilia B dog.

Pharmacokinetics of crossover-dosing of pd-FIX followed by active tg-FIX (O25) The initial dosing of 50 IU/kg of pd-FIX responded within the normal pharmacokinetic range for FIX replacement therapy (Table 3.2 and 3.3). Peak antigen concentration and activity levels were 80% and 68% of normal respectively, and by 48 hours the majority of the pd-FIX had been cleared from the plasma, with antigen and activity levels between 10-11% of normal (Fig. 3.3). The infusion of tg-FIX at 48 hours post pd-FIX infusion also produced elevated antigen concentration and activity levels (Table 3.2 and 3.3). The MRT of the tg-FIX surprisingly surpassed the initial infusion of pd-FIX for this trial, although the tg-FIX only reached peak antigen and activity levels of 70% and 36% of normal respectively. The tg-FIX activity level and antigen concentration remained

detectable for over 72 hours post infusion, sharply contrasting the rapid decrease in these parameters seen in the single infusion trial (Fig. 3.2 and 3.3).

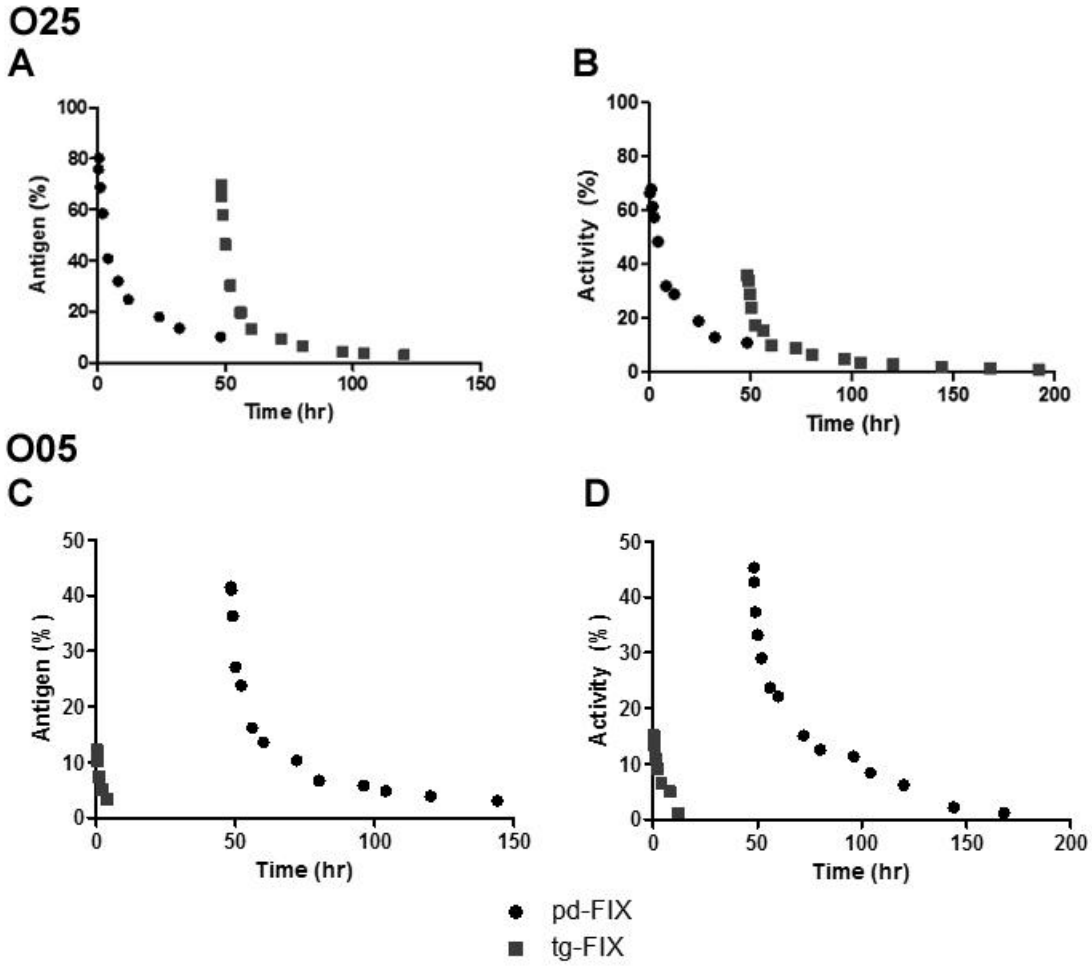

Figure 3.3. The crossover pharmacokinetics of IV injected pd- and tg-FIX in Hemophilia B dog. (A, B) 50 U/kg of pd-FIX was initially IV delivered to a hemophilia B dog (O25), followed by 50 U/kg of tg-FIX delivered 48 hours after initial delivery of pd-FIX. (C, D) 50 U/kg of tg-FIX was initially IV delivered to a hemophilia B dog (O25), followed by 50 U/kg of pd-FIX then delivered 48 hours after initial delivery of pd-FIX. Antigen concentration and activity levels were determined by (A, C) ELISA and (B, D) one stage clotting assay respectively.

Table 3.2. Pharmacokinetic properties of pd- and tg-FIX crossover studies as measured by ELISA.

FIX Infused	Recovery Half-Life (hour)	Terminal Half-Life (hour)	MRT (hour)	AUC	AUMC	R^2
pd-FIX (O25)	1.9	24	31	1200	14000	.994
pd-FIX post tg-FIX (O05)	1.9	30	40	450	8200	.994
tg-FIX (O05)	0.5	4.3	5.5	46	240	.999
tg-FIX post pd-FIX (O25)	4.9	34	39	1300	41000	.998

Table 3.3. Pharmacokinetic properties of pd- and tg-FIX crossover studies as measured by aPTT.

FIX Infused	Recovery Half-Life (hour)	Terminal Half-Life (hour)	MRT (hour)	AUC	AUMC	R^2
pd-FIX (O25)	3.1	22	28	1400	16000	.993
pd-FIX post tg-FIX (O05)	1.1	30	42	650	8300	.996
tg-FIX (O05)	0.4	4.9	6.8	86	550	.983
tg-FIX post pd-FIX (O25)	2.7	29	38	1900	64000	.995

Pharmacokinetics of crossover-dosing of active tg-FIX followed by pd-FIX (O05)

Initial dosing of tg-FIX responded similarly to Dog 066 as expected; however, a slightly longer detectable plasma residence time allowed for quantification of the pharmacokinetic variables (Tables 3.2 and 3.3). The MRT of the tg-FIX infused into dog O05 based on both activity and antigen assays was less than 18% of the tg-FIX infused into dog O25, with the change in procedure being the prior infusion of pd-FIX in dog O25 (Fig. 3.2 and 3.3). FIX composition of the tg-FIX samples delivered to both animals

was confirmed by one-stage clotting assay, SDS-PAGE, and SEC to be functionally identical. In dog O05, the pd-FIX sample administered 48 post tg-FIX infusion exhibited a lower peak response; however, it also exhibited an MRT increased by 29% based on antigen levels and 50% based on activity levels (Fig. 3.3).

Pharmacokinetics of crossover-dosing of active tg-FIX followed by whole population tg-FIX (O66)

Both tg-FIX infusions in the crossover-study were cleared from the plasma at rates too rapid for quantification (Fig. 3.2). Interestingly, activity levels and antigen concentration both showed clearance times for both active tg-FIX contained in the first infusion of tg-FIX into dog O66 and whole population tg-FIX that remained identical despite the 20% increase in concentration of total FIX in whole population tg-FIX from active tg-FIX.

Whole Blood Clotting Times

In stark contrast with the low pharmacokinetic variables obtained by one-stage clotting assay and ELISA for tg-FIX, all treatments maintained WBCT of less than 20 minutes for at least 48 hours (Fig. 3.4). Interestingly, all treatments with a prior infusion maintained WBCT of less than 20 minutes for at least 72 hours and remained under 60 minutes for over 100 hours. Steady-state values were maintained for the longest time period in the crossover-dosing of pd-FIX followed by active tg-FIX (O25).

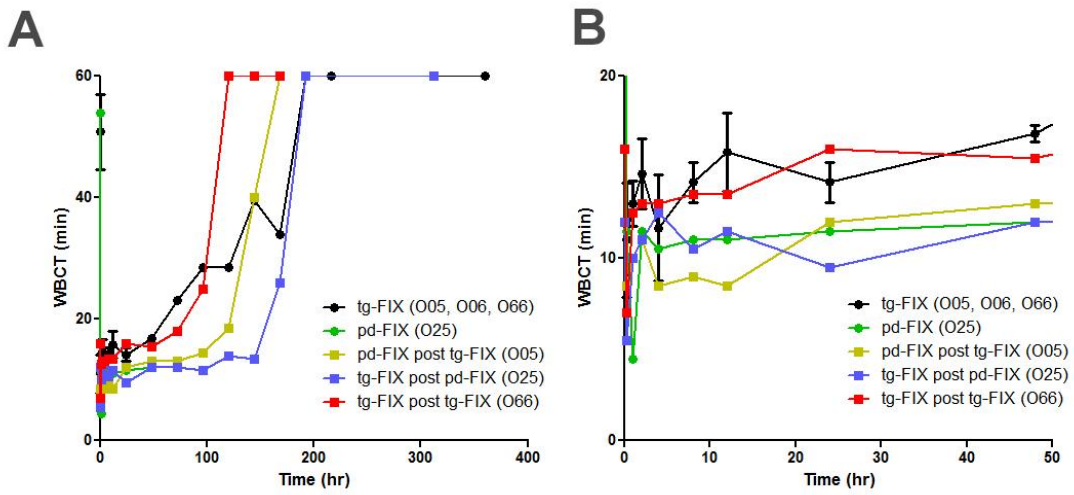

Figure 3.4. Effect of tg- and pd-FIX on the WBCT in hemophilia B dog. Time course plotted from infusion time until (A) 400 hours and (B) 50 hours. Circles indicate dogs with no prior infusion in the preceding 3 weeks, and squares indicate an infusion of a FIX species given 48 hours before administration.

Safety

Throughout the study, all animals remained in healthy conditions and showed no sign of fever or systemic reaction to the infused materials.

3.5 Discussion

These preclinical studies were performed in order to test the safety and efficacy of tg-FIX produced in the milk of swine. In these studies, the tg-FIX was characterized to have two vastly different pharmacokinetic profiles based on the prior infused species. Based on the similarity of this data to previous research on designed FIX mutants [4, 26, 39], we believe that these changes in pharmacokinetic are due changes in the Gla domain of the tg-FIX and in the filling of the extravascular reservoir.

While the specific activity by one-stage clotting assay is similar for pd-FIX, r-FIX and tg-FIX, it is important to note that the Gla conformation of the tg-FIX versus the pd-FIX and r-FIX is different due to the differences in Gla domain γ-carboxylation [17, 27, 52]. All major populations of pd-FIX, r-FIX, and tg-FIX were confirmed to contain γ-carboxylated 1-6 Gla domains by both MS and SB 249417-conjugated Biacore. MS has revealed that the tg-FIX has an average carboxylation content 10-11 Gla residues as opposed to the 12 fully γ-carboxylated Gla residues found in pd-FIX. When pd-FIX, r-FIX, and tg-FIX were purified using a column designed with a mAb that targets a magnesium dependent, tg-FIX was shown to contain different sub-populations of under-carboxylated FIX than r-FIX. Previous literature has stated that r-FIX [53], when under-carboxylated, typically does not contain Gla 11 or 12 and this under-carboxylation does not affect the function of the r-FIX. Combined with the exclusive affinity of the 1G7 mAb to 12 Gla r-FIX compared to other subpopulations of r-FIX, previous literature on r-FIX and our current data indicate that 1G7 mAb targets either the 11 or 12 Gla site of FIX. The diversity of tg-FIX that bound to the 1G7 mAb indicates that Gla 11 and 12 are present in most subpopulations of tg-FIX and that under-carboxylation in tg-FIX occurs at Gla 7-10. As a result, it can be stated that tg-FIX is produced using non-processive carboxylation [53-55]. This non-processive under-carboxylation can directly impact the tertiary structure of the Gla domain, which is responsible for the binding of FIX to the endothelium [4, 39, 40, 56].

These changes in the Gla domain of tg-FIX can be seen in its high avidity for endothelium and extravascular reservoirs as evidenced by its rapid plasma falloff when exposed to HB dog vasculature which had no prior exposure to FIX. This avidity is also

demonstrated when whole population tg-FIX is administered 72 hours after a tg-FIX infusion. Despite the whole population tg-FIX containing 20% more total FIX, the clearance time of the active tg-FIX remained unchanged. This likely indicates two separate mechanisms for the removal of FIX from plasma: the storage of active FIX in the extravascular reservoirs and hepatic clearance of inactive FIX.

The storage of both tg- and pd-FIX in the extravascular reservoirs can be seen in dog studies O25 and O05. The filling of the vascular space by first species infused in three weeks can be seen in the dramatically increased pharmacokinetic properties of the second infusion compared to an infusion with no prior infusion in the last three weeks. Quantitatively, over a 7-fold increase in residence time can be seen in the tg-FIX that was presented with a prior infusion of pd-FIX 48 hours prior earlier, and a 30% increase for pd-FIX when presented with a prior infusion of tg-FIX 48 hours earlier.

Most importantly, WBCT indicate that tg-FIX is capable of providing acceptable hemostasis for over 48 hours despite the presences of antigen or activity in the plasma. All HB dogs studied remained in healthy condition during the study, indicating that tg-FIX is both safe and efficacious in HB dogs. These HB dog studies strongly supports the impact of extravascular binding described in molecular and PK terms by Gailani [39] and Feng et al. [23]. It further explains the reduced amount of FIX needed over time in patients who receive continuous infusions of FIX [24]. We did not document the occupation of the extravascular compartment by the FIX species so a direct correlation with the PK behavior cannot be performed. However, our results are consistent with the effects of the extravascular space loading and its influence on subsequent infusions of FIX [4, 26]. Importantly, this effect continued even after plasma levels of FIX antigen

and activity have reached a near non-detectable level. This information provides the continued impetus to further detail the potentially profound impact that reservoir phenomena have on the general dosing strategy for treating HB and especially in the context of design strategies used to achieve longer lasting FIX biotherapuetics.

3.6 Acknowledgements

I would like to thank Dr. Nichols, Dr. Merricks, and all those responsible for the Hemophilia B dog colony at the Francis Owen Blood Laboratory of University of North Carolina-Chapel Hill for their aid in the dog trial. I would also like to thank Laura Smoyer and Dr. Van Cott for providing of the mass spectrometry of the material.

3.7 References

1 Furie B, Furie BC. The molecular basis of blood coagulation. *Cell*. 1988; **53**: 505-18.

2 Osterud B, Bouma B, Griffin J. Human blood coagulation factor IX. Purification, properties, and mechanism of activation by activated factor XI. *Journal of Biological Chemistry*. 1978; **253**: 5946-51.

3 Fuchs H, Trapp H, Griffith M, Roberts H, Pizzo S. Regulation of factor IXa in vitro in human and mouse plasma and in vivo in the mouse. Role of the endothelium and the plasma proteinase inhibitors. *Journal of Clinical Investigation*. 1984; **73**: 1696.

4 Gui T, Lin H-F, Jin D-Y, Hoffman M, Straight DL, Roberts HR, Stafford DW. Circulating and binding characteristics of wild-type factor IX and certain Gla domain mutants in vivo. *Blood*. 2002; **100**: 153-8. 10.1182/blood.V100.1.153.

5 Kasthuri RS, Roberts HR, Monahan PE. Factor IX Deficiency or Hemophilia B: Clinical Manifestations and Management. *Hemostasis and Thrombosis: Practical Guidelines in Clinical Management*. 2014: 57.

6 Morfini M. Secondary prophylaxis with factor IX concentrates: continuous infusion. *Blood Transfusion*. 2008; **6**: s21.

7 Monahan PE, Di Paola J. Recombinant factor IX for clinical and research use. *Seminars in thrombosis and hemostasis*: © Thieme Medical Publishers, 2010, 498-509.

8 Brinkhous K, Sigman J, Read M, Stewart P, McCarthy K, Timony G, Leppanen S, Rup B, Keith JJ, Garzone P. Recombinant human factor IX: replacement therapy, prophylaxis, and pharmacokinetics in canine hemophilia B. *Blood*. 1996; **88**: 2603-10.

9 Chowdary P, Dasani H, Jones J, Loran C, Eldridge A, Hughes S, Collins P. Recombinant factor IX (BeneFix®) by adjusted continuous infusion: a study of stability, sterility and clinical experience. *Haemophilia*. 2001; **7**: 140-5.
10 Kaufman R, Wasley L, Furie B, Furie B, Shoemaker C. Expression, purification, and characterization of recombinant gamma-carboxylated factor IX synthesized in Chinese hamster ovary cells. *Journal of Biological Chemistry*. 1986; **261**: 9622-8.
11 White GC, 2nd, Beebe A, Nielsen B. Recombinant factor IX. *Thromb Haemost*. 1997; **78**: 261-5.
12 Østergaard H, Bjelke JR, Hansen L, Petersen LC, Pedersen AA, Elm T, Møller F, Hermit MB, Holm PK, Krogh TN, Petersen JM, Ezban M, Sørensen BB, Andersen MD, Agersø H, Ahmadian H, Balling KW, Christiansen MLS, Knobe K, Nichols TC, Bjørn SE, Tranholm M. Prolonged half-life and preserved enzymatic properties of factor IX selectively PEGylated on native N-glycans in the activation peptide. *Blood*. 2011; **118**: 2333-41. 10.1182/blood-2011-02-336172.
13 Brooks A, Sim D, Gritzan U, Patel C, Blasko E, Feldman R, Tang L, Ho E, Zhao XY, Apeler H. Glycoengineered factor IX variants with improved pharmacokinetics and subcutaneous efficacy. *Journal of Thrombosis and Haemostasis*. 2013; **11**: 1699-706.
14 Schulte S. Half-life extension through albumin fusion technologies. *Thrombosis Research*. 2009; **124, Supplement 2**: S6-S8. 10.1016/s0049-3848(09)70157-4.
15 Peters RT, Low SC, Kamphaus GD, Dumont JA, Amari JV, Lu Q, Zarbis-Papastoitsis G, Reidy TJ, Merricks EP, Nichols TC, Bitonti AJ. Prolonged activity of factor IX as a monomeric Fc fusion protein. *Blood*. 2010; **115**: 2057-64. 10.1182/blood-2009-08-239665.
16 Windyga J, Lissitchkov T, Stasyshyn O, Mamonov V, Rusen L, Lamas J, Oh MS, Chapman M, Fritsch S, Pavlova B. Pharmacokinetics, efficacy and safety of BAX326, a novel recombinant factor IX: a prospective, controlled, multicentre phase I/III study in previously treated patients with severe (FIX level< 1%) or moderately severe (FIX level≤ 2%) haemophilia B. *Haemophilia*. 2013.
17 Lindsay M, Gil G-C, Cadiz A, Velander WH, Zhang C, Van Cott KE. Purification of recombinant DNA-derived factor IX produced in transgenic pig milk and fractionation of active and inactive subpopulations. *Journal of Chromatography A*. 2004; **1026**: 149-57.
18 Gil G-C, Velander WH, Van Cott KE. Analysis of the N-glycans of recombinant human Factor IX purified from transgenic pig milk. *Glycobiology*. 2008; **18**: 526-39. 10.1093/glycob/cwn035.
19 Van Cott K, Monahan PE, Nichols TC, Velander WH. Haemophilic factors produced by transgenic livestock: abundance that can enable alternative therapies worldwide. *Haemophilia*. 2004; **10**: 70-6.
20 Morcöl T, Akers RM, Johnson JL, Williams BL, Gwazdauskas FC, Knight JW, Lubon H, Paleyanda RK, Drohan WN, Velander WH. The Porcine Mammary Gland as a Bioreactor for Complex Proteinsa. *Annals of the New York Academy of Sciences*. 1994; **721**: 218-33.
21 Subramanian A, Paleyanda RK, Lubon H, Williams BL, Gwazdauskas FC, Knight JW, Drohan WN, Velander WH. Rate Limitations in Posttranslational Processing by the Mammary Gland of Transgenic Animalsa. *Annals of the New York Academy of Sciences*. 1996; **782**: 87-96.

22 Velander WH, Lubon H, Drohan WN. Transgenic livestock as drug factories. *Scientific American*. 1997; **276**: 54-8.
23 Feng D, Stafford KA, Broze GJ, Stafford DW. Evidence of clinically significant extravascular stores of factor IX. *Journal of Thrombosis and Haemostasis*. 2013; **11**: 2176-8.
24 Uprichard J, Adamidou D, Goddard N, Mann H, Yee T. Factor IX replacement to cover total knee replacement surgery in haemophilia B: a single-centre experience, 2000–2010. *Haemophilia*. 2012; **18**: 46-9.
25 Liebman H, Rosenwald-Zuckerman T, Retzios A, Yasmin S, Kasper C. Kinetics of factor IX activity differ from that of factor IX antigen in patients with haemophilia B receiving high-purity factor IX replacement. *Haemophilia: the official journal of the World Federation of Hemophilia*. 1999; **5**: 174-80.
26 Stern DM, Knitter G, Kisiel W, Nawroth PP. In vivo evidence of intravascular binding sites for coagulation factor IX. *British journal of haematology*. 1987; **66**: 227-32.
27 Chang C-H, Chow T-K, Yang C-Y, Chang T-J, Wu Y-H, Lee T-W. Biodistribution and Pharmacokinetics of Transgenic Pig-produced Recombinant Human Factor IX (rhFIX) in Rats. *In Vivo*. 2008; **22**: 693-7.
28 Björkman S. Prophylactic dosing of factor VIII and factor IX from a clinical pharmacokinetic perspective. *Haemophilia*. 2003; **9**: 101-10.
29 Chang H-H, Yang Y-L, Hung M-H, Tsay W, Shen M-C. Pharmacokinetic study of recombinant human factor IX in previously treated patients with hemophilia B in Taiwan. *Journal of the Formosan Medical Association*. 2007; **106**: 281-7.
30 Morfini M, Laguna P, Leissinger C. Factor IX pharmacokinetics: differences between plasma-derived and recombinant products and the clinical and economic implications: a meeting report. *Haemophilia*. 2008; **14**: 873-5.
31 Poon MC. Pharmacokinetics of factors IX, recombinant human activated factor VII and factor XIII. *Haemophilia*. 2006; **12**: 61-9.
32 Ruiz-Sáez A, Hong A, Arguello A, Echenagucia M, Boadas A, Fabbrizzi F, Minichilli F, Bosch N. Pharmacokinetics, thrombogenicity and safety of a double viral inactivated factor IX concentrate compared with a prothrombin complex concentrate. *Haemophilia*. 2005; **11**: 583-8.
33 Morfini M. Pharmacokinetics of factor VIII and factor IX. *Haemophilia*. 2003; **9**: 94-100.
34 Björkman S. A commentary on the differences in pharmacokinetics between recombinant and plasma-derived factor IX and their implications for dosing. *Haemophilia*. 2011; **17**: 179-84.
35 Ewenstein BM, Joist JH, Shapiro AD, Hofstra TC, Leissinger CA, Seremetis SV, Broder M, Mueller-Velten G, Schwartz BA. Pharmacokinetic analysis of plasma-derived and recombinant F IX concentrates in previously treated patients with moderate or severe hemophilia B. *Transfusion*. 2002; **42**: 190-7.
36 Gui T, Reheman A, Ni H, Gross P, Yin F, Monroe D, Monahan P, Stafford D. Abnormal hemostasis in a knock-in mouse carrying a variant of factor IX with impaired binding to collagen type IV. *Journal of Thrombosis and Haemostasis*. 2009; **7**: 1843-51.
37 Furie B, Furie BC. Molecular basis of vitamin K-dependent gamma-carboxylation. *Blood*. 1990; **75**: 1753-62.

38 Vermeer C. Gamma-carboxyglutamate-containing proteins and the vitamin K-dependent carboxylase. *Biochemical journal*. 1990; **266**: 625.
39 Gailani D. Factor IX binding to collagen. *Journal of Thrombosis and Haemostasis*. 2009; **7**: 1840-2.
40 Toomey JR, Smith KJ, Roberts HR, Stafford DW. The endothelial cell binding determinant of human factor IX resides in the. gamma.-carboxyglutamic acid domain. *Biochemistry*. 1992; **31**: 1806-8.
41 Nichols TC, Dillow AM, Franck HW, Merricks EP, Raymer RA, Bellinger DA, Arruda VR, High KA. Protein replacement therapy and gene transfer in canine models of hemophilia A, hemophilia B, von willebrand disease, and factor VII deficiency. *ILAR Journal*. 2009; **50**: 144-67.
42 Mauser A, Whitlark J, Whitney K, Lothrop CJ. A deletion mutation causes hemophilia B in Lhasa Apso dogs. *Blood*. 1996; **88**: 3451-5.
43 Evans JP, Brinkhous KM, Brayer GD, Reisner HM, High KA. Canine hemophilia B resulting from a point mutation with unusual consequences. *Proceedings of the National Academy of Sciences*. 1989; **86**: 10095-9.
44 Nichols T, Franck H, Franck C, De Friess N, Raymer R, Merricks E. Sensitivity of whole blood clotting time and activated partial thromboplastin time for factor IX: relevance to gene therapy and determination of post-transfusion elimination time of canine factor IX in hemophilia B dogs. *Journal of Thrombosis and Haemostasis*. 2012; **10**: 474-6.
45 Gibaldi M, Perrier D. Pharmacokinetics: revised and expanded. *Drugs and the pharmaceutical sciences*. 1999; **92**: 15-.
46 Shapiro A, Korth-Bradley J, Poon MC. Use of pharmacokinetics in the coagulation factor treatment of patients with haemophilia. *Haemophilia*. 2005; **11**: 571-82.
47 Nolte M, Nichols T, Mueller-Cohrs J, Merricks E, Pragst I, Zollner S, Dickneite G. Improved kinetics of rIX-FP, a recombinant fusion protein linking factor IX with albumin, in cynomolgus monkeys and hemophilia B dogs. *Journal of Thrombosis and Haemostasis*. 2012; **10**: 1591-9.
48 Arruda VR, Stedman HH, Haurigot V, Buchlis G, Baila S, Favaro P, Chen Y, Franck HG, Zhou S, Wright JF. Peripheral transvenular delivery of adeno-associated viral vectors to skeletal muscle as a novel therapy for hemophilia B. *Blood*. 2010; **115**: 4678-88.
49 Herzog RW, Yang EY, Couto LB, Hagstrom JN, Elwell D, Fields PA, Burton M, Bellinger DA, Read MS, Brinkhous KM. Long-term correction of canine hemophilia B by gene transfer of blood coagulation factor IX mediated by adeno-associated viral vector. *Nature medicine*. 1999; **5**: 56-63.
50 Freedman SJ, Furie BC, Furie B, Baleja JD. Structure of the Calcium Ion-Bound. gamma.-Carboxyglutamic Acid-Rich Domain of Factor IX. *Biochemistry*. 1995; **34**: 12126-37.
51 Gil GC, Velander WH, Van Cott KE. N-glycosylation microheterogeneity and site occupancy of an Asn-X-Cys sequon in plasma-derived and recombinant protein C. 2009; **9**: 2555-67. 10.1002/pmic.200800775.
52 Van Cott KE, Butler SP, Russell CG, Subramanian A, Lubon H, Gwazdauskas F, Knight J, Drohan WN, Velander WH. Transgenic pigs as bioreactors: a comparison of

gamma-carboxylation of glutamic acid in recombinant human protein C and factor IX by the mammary gland. *Genetic analysis: biomolecular engineering*. 1999; **15**: 155-60.
53 Gillis S, Furie BC, Furie B, Patel H, Huberty MC, Switzer M, Barry Foster W, Scoble HA, Bond MD. γ-Carboxyglutamic acids 36 and 40 do not contribute to human factor IX function. *Protein science*. 1997; **6**: 185-96.
54 Suttie JW. Vitamin K-dependent carboxylase. *eLS*. 1985.
55 Morris DP, Stevens RD, Wright DJ, Stafford DW. Processive Post-translational Modification Vitamin K-Dependent Carboxylation of a Peptide Substrate. *Journal of Biological Chemistry*. 1995; **270**: 30491-8.
56 Cheung W-F, Van Den Born J, Kühn K, Kjellen L, Hudson BG, Stafford DW. Identification of the endothelial cell binding site for factor IX. *Proceedings of the National Academy of Sciences*. 1996; **93**: 11068-73.

Chapter 4:

Oral and Buccal Delivery Raises Circulating Levels of Factor IX in Mouse and Dog Models

Nicholas C. Vanderslice*, Weijiu Xu*, Tong Gui†, Genlin Hu†, Tülin Morcöl‡, Paul E. Monahan†, Timothy Nichols**, William H. Velander*

*Department of Chemical and Biomolecular Engineering, University of Nebraska-Lincoln, Lincoln, Nebraska; † Department of Pediatrics, University of North Carolina at Chapel Hill, Chapel Hill, North Carolina; ‡ CaPtivate Pharmaceuticals, Philadelphia, PA; **Department of Pathology and Laboratory Medicine, University of North Carolina at Chapel Hill, Chapel Hill, North Carolina

4.1 Abstract

Deliveries of human factor IX (FIX) to the mucosal lining of the mouth (buccal) or gut (oral) are non-intravenous administration methods with inherently low bioavailability. The aim of this probative study was to investigate the potential of oral and buccal delivery of plasma-derived (pd-) and transgenic milk derived (tg-) FIX in mice and dogs. To survey oral versus buccal delivery, raw milk containing tg-FIX and calcium phosphate (CaP) formulated FIX was administered to study animals. ELISA and one stage coagulation assays were used to determine FIX bioavailability. FIX coagulation activity levels of CRM- hemophilic mice increased to 2.7%-4.6% 1 hour after feeding 2000 IU/kg raw milk containing tg-FIX, indicating a bioavailability of <0.2%. Furthermore, in 1 of 2 normal dogs the level of FIX antigen and coagulation activity increased >13% after 1 hours post-feeding of 250 IU/kg of tg-FIX milk,

indicating a minimum of 2% bioavailability. The CaP microparticles were used to buccally deliver pd-FIX, which resulted in a >150 ng/mL FIX antigen level rise in 3 of 4 normal mice. In CRM+ hemophilic mice fed CaP:tg-FIX, antigen levels rose >400 ng/mL after 15 minutes and remained >300 ng/mL for 24 hours. The bioavailability of CaP formulations in both CRM- and CRM+ mice was <0.2%. Evidence of the displacement of bioengineered FIX from the endothelial reservoirs of CRM+ mice was observed after the buccal administration of CaP:tg-FIX. This work justifies further studies in hemophilic dog models through the oral delivery of tg-FIX by lipophilic carrier to the normal dog model.

4.2 Introduction

Hemophilia B [1-5] is currently treated using prophylactic treatment of either plasma-derived (pd-) [6, 7] or recombinant FIX [6-8] delivered intravenously (IV) [5, 9-11]. However, the routine treatment of children frequently requires administration by central-venous catheter, which has the risk of complication, including deep-vein thrombosis and infection [12, 13]. In addition, the risk of inhibitor development increases with each successive FIX infusion during the course of IV therapy [14-16].

Recent studies on the accumulation of FIX in endothelial reservoirs of hemophilia B mice have provided new insight into the pharmacokinetic behavior that occurs after IV administration of FIX [3, 17-20]. These studies have shown that point mutations in the Gla domain alter the partitioning of FIX into the endothelial reservoirs and, therefore alter its pharmacokinetic behavior in circulation, revealing the central role of the Gla domain in the reservoir phenomena.

A formidable barrier to the development of non IV delivery of hemophilia factors is the combination of low bioavailability and the correspondingly inadequate production methods for FIX and FVIII. However, the oral delivery of 800 units in a single dose of liposome encapsulated pd-FVIII into a single hemophilia A patient was previously demonstrated to raise FVIII plasma activity levels to 5-10% of normal within 2 hours after ingestion [21], and 5% after about 25 hours, establishing a bioavailability of 20%. Few studies have reported patient-friendly methods such as buccal administration for mouth absorption and oral delivery for gastrointestinal absorption due to the large amounts of factor needed for development of these methods.

The use of transgenic production methods in the milk of livestock or in plants can potentially produce >100-fold more recombinant factor than is possible by current large-scale manufacturing methods [22-25]. For example, FIX antigen that does not have coagulation activity has been made in large amounts by transgenic plants and used to reduce the formation of inhibitors by oral delivery in hemophilic B mice despite low bioavailability [14, 26] . Furthermore, biologically active FIX has been successfully purified from the milk of transgenic (tg-) swine [23]. This probative study reports on the administration of active tg-FIX in oral and buccal delivery into normal mice and dogs as well as hemophilia B mice.

4.3 Materials and Methods

All buffer components were purchased from VWR International LLC (Radnor, PA, USA), Thermo Fisher scientific (Waltham, MA, USA) or Sigma (St. Louis, MO, USA) unless otherwise stated. Transgenic pig milk was collected as previously described

[23]. In order to minimize degradation, purification processes were performed at 4^0C. The stocks of pd-FIX (Mononine®, CSL Behring, USA) were expired for clinical use; however, when used in experiments, exhibited full procoagulant activity. Blood samples were assayed for absorption of FIX into blood circulation by h-FIX-ELISA [27] and single stage coagulation assay [28].

Oral delivery of raw tg-FIX milk to mice

CRM- FIX knock-out (FIXKO) hemophilic B mice were fed 0.5 mL raw tg-FIX milk containing 100 IU FIX/mL after a meal (postprandial) (n=4). Post-administration, plasma samples were collected one hour after dosing.

Oral delivery of raw tg-FIX milk to dogs

The study was conducted on one haemostatically normal dog at ProGenetics LLC. The protocol was approved by the Institutional Animal Care and Use Committee of ProGenetics. Exclusion criteria were clinically overt illness, abnormal clinical serum chemistry or hematology parameters, prior treatment with FIX, and any medical treatment, including plasma transfusion, fewer than 14 days prior to inclusion. The normal dog was fed raw tg-FIX milk that provided 250 IU FIX/kg. Post-administration, plasma samples were collected at 1, 2 and 10 hours.

Purification of tg-FIX

Whole tg-FIX milk was purified using a modified version of the procedure of Lindsay et al. [23]. The modified procedure included centrifugation, affinity chromatography, and size-exclusion chromatography. Affinity chromatography was carried out using a Heparin Sepharose 6 Fast Flow (GE Healthcare, Uppsala, Sweden) column and a Macro Prep Ceramic Hydroxyapatite Type II – 40 μm (Bio Rad - Hercules,

CA, USA), column while size-exclusion chromatography was carried out on a TSK gel G3000SWxl (Tosoh Bioscience, King of Prussia, PA, USA) column.

Analysis of purified FIX

The integrity of the purified tg-FIX was verified by standard 12% sodium dodecyl sulfate-polyacrylamide gel electrophoresis (SDS-PAGE) under non-reduced and reduced conditions; and Western blot detection using an anti-human factor IX rabbit polyclonal (Sigma, St Louis, MO, US) paired with a goat anti-rabbit IgG H&L peroxidase conjugate (Sigma, St Louis, MO, US). The procoagulant activity of the stock protein solutions was measured with a single stage coagulation assay as previously described [23].

Formulation of Calcium phosphate (CaP) encapsulated FIX

CaP particles containing FIX as the active drug were synthesized by co-precipitation of FIX with the inorganic salt solutions of calcium and phosphate at 4°C based on protocols of He et al. [29].

Determination of tg-FIX binding efficiency

FIX binding efficiency to CAP was estimated by the Bradford's method using a Bio-Rad protein assay kit. In most cases, >75% binding efficiency was obtained. While in suspension, these formulations contained 190 to 200 IU FIX/mL which were adjusted to 150 IU/mL.

Determination of particle size.

Particle size was determined using a Beckman Coulter N4 Plus submicron particle sizing machine. Distilled water was used as the diluent. Particle size was analyzed at two different angles (60 and 90 degrees).

Buccal delivery of CaP:pd-FIX

CaP:pd-FIX particle suspension containing 191 IU FIX/mL with 1800 nm average particle size was administered buccally to normal CD-1 mice, delivering a total of 49 IU. At 1, 2, 4, 6, 24, 48, and 72 hours post-treatment, blood samples were collected.

Buccal delivery of CaP:tg-FIX

CaP microparticles were sprayed into the mouths of CRM-FIXKO (n=5) mice [30] and CaP:tg-FIX was fed to CRM+ R333Q-hFIX mice (n=7) via the buccal route. Post-administration, plasma samples were collected at 15 min, 2hr, and 24hr.

Dose response of CRM+ R333Q –hFIX mice to buccal delivery of CaP:tg-FIX

The CaP:tg-FIX was fed at 0, 2000, and 6000 IU/kg to R333Q mice (n=8). Post-administration, plasma samples were collected at 15 min, 2hr, and 24hr and the absorption of FIX into blood circulation was determined by ELISA using FIX-T148 antibodies (Green Mountain Antibodies) and Anti-human factor IX (Haematologic Technologies Inc.).

Tail bleeding and rebleeding

The modified procedure of Gui *et al.* [3] was used for the tail bleeding test. Two-month-old R333Q mice were selected based on matched weight and sex. R333Q mice were administered CaP, 2000 IU/kg CaP:tg-FIX, or 6000 IU/kg CaP:tg-FIX 24 hours before tail transection. Mice were anesthetized with 2.5% avertin. The tail transection was performed at 1.5 mm cross-sectional diameter of the tail. The tail was then placed in saline and kept at 37 ºC where it was allowed to bleed until cessation or until 10 minutes had passed. The time of cessation was recorded. After 10 minutes had passed, 1 minute of pressure was applied to the tip of the tail to cease bleeding. The clot was stripped

after thirty minutes had passed since the initial transection. The tail was then placed in saline and kept at 37 ºC where it was allowed to bleed for 10 minutes until cessation of bleeding occurred. The mice were then allowed to wake up and were observed for 8 hours.

Statistical analysis

All statistical calculations were done with GraphPad Prism 5.0 software (GraphPad Software, San Diego CA, USA) [31]. Statistical comparison of data sets was done using one-way analysis of variance (ANOVA) with Dunnett's test for multiple comparisons. A P-value > 0.05 was considered not significant.

4.4 Results

Oral delivery of raw milk containing tg-FIX to mice and dogs

We chose CRM- hemophilic mice for oral delivery studies due to the absence of baseline FIX antigen and activity detected in these animals. One hour after a single feeding of 0.5 mL of raw tg-FIX milk, significant amounts of both plasma-borne antigen and active FIX were observed in three of four mice (Table 4.1). The average plasma antigen level detected in these mice at 1 hour post-administration was 5.5 μg/mL, which corresponds to 13.8 μg of circulating FIX antigen (Table 4.2). This circulating antigen estimate is equivalent to 1.1% of the total tg-FIX antigen fed in the raw milk. The level of plasma coagulation activity detected in these mice at 1 hour post-administration corresponds to 0.04 IU/mL and a minimum bioavailability of 0.2 % of the tg-FIX activity from raw milk (Table 4.3). At this level, the ratio of activity to antigen rise is estimated

to be 6.9 IU/mg tg-FIX, which is about 25 to 30-fold lower than the specific activity of the most native and biologically active species that was purified from the milk.

Table 4.1. FIX levels one hour after oral delivery of 0.5 mL raw tg-FIX Milk into four CRM- mice.

Mouse	Total FIX Antigen* (µg/mL)	aPTT (sec)	% FIX activity in Plasma†	Effective concentration of functional transgenic factor IX (µg/mL plasma)
1	2.3	73.6	2.7%	0.14
2	7.8	68.4	4.2%	0.21
3	6.4	67.3	4.6%	0.23
4	ND‡	-	-	-

*Determined by ELISA

†100% FIX activity is set to be equivalent to 1 IU/mL.

‡Not detected.

Table 4.2. Estimated plasma levels of FIX antigen and coagulation activity. Total FIX levels based on 10% plasma volume in 25 g mice and 20 kg normal dog.

	Total FIX Administered		**Change in FIX Level from Baseline**		**Net FIX delivered to Plasma**	
Trial	**Activity (IU)**	**Antigen (µg)**	**Activity (IU/mL)**	**Antigen (µg/mL)**	**Activity (IU)**	**Antigen (µg)**
Oral Delivery of Milk						
CRM- Mice fed raw tg-FIX milk	50	1250	0.04	5.5	0.1	13.8
Normal dog fed raw tg-FIX milk*	5100	40000	0.19	0.9	124	588
Buccal Delivery of CaP:FIX						
Normal Mice fed CaP:pd-FIX	49	245	ND†	0.15	ND†	0.4
CRM+ Mice fed 2000 U/kg CaP:tg-FIX	40	200	ND†	0.48	ND†	1.2

*Median change over 10 hours

†Not Detected. Limit of detection of assay: 0.01 IU/mL

Table 4.3. Bioavailability of FIX after oral delivery of raw tg-FIX milk and buccal delivery of CaP:pd-FIX and CaP:tg-FIX.

Trial	Bioavailability (%)		
	Single Stage Coagulation Assay	ELISA	Ratio of delivered activity to antigen delivered rise in plasma (IU/mg)
Oral Delivery of Milk			
2000 U/kg CRM- Mice	0.2	1.1	6.9
250 U/kg Dog	2.4	1.5	210
Buccal Delivery of Cap:FIX			
2000 U/kg Mice (pd-FIX)	ND*	0.2	
2000 U/kg CRM+ Mice (tg-FIX)	ND*	0.6	

*Not Detected. Limit of detection of assay: 0.01 IU/mL

To further investigate the potential of oral delivery of tg-FIX into a more preclinically relevant animal model, we fed raw tg-FIX pig milk to two normal adult dogs at 250 IU/kg body weight. Similarly to the CRM- mice, both antigen and activity levels were found to rise 1 hour after feeding the tg-FIX milk in one of the two dogs (Fig. 4.1). In the responding dog, a rise in plasma FIX antigen (Fig. 4.1A) of 13% and a coagulation activity (Fig. 4.1B) of 33% was observed one hour after feeding. A relatively steady level of 13% to 18% antigen and 15 % coagulation activity above baseline was observed from 1 to 10 hours post milk administration by feeding.

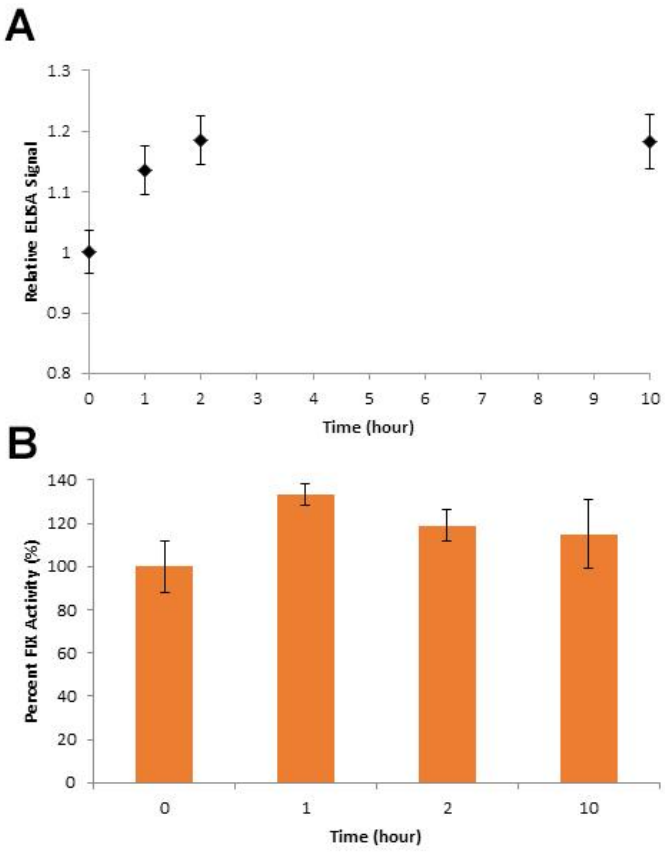

Figure 4.1. FIX levels after oral delivery of raw tg-FIX milk into normal dog. The animal was treated with 250 IU FIX/kg. (A) FIX plasma level determined by ELISA (B) FIX plasma activity determined by one stage coagulation assay and error bars indicate the range of for the assay for their respective sample.

CaP formulation for buccal delivery

We endeavored to administer FIX using a formulation and method of delivery that was more defined than feeding raw tg-FIX milk. CaP precipitation of FIX and its spray delivery was chosen to coat the interior surfaces of the mouth of the mice [29, 32]. Both pd-FIX and tg-FIX preparations were precipitated by CaP, which resulted in the formation of particles with sizes predominately in the range of 500 to 1800 nm (Figure 4.2).

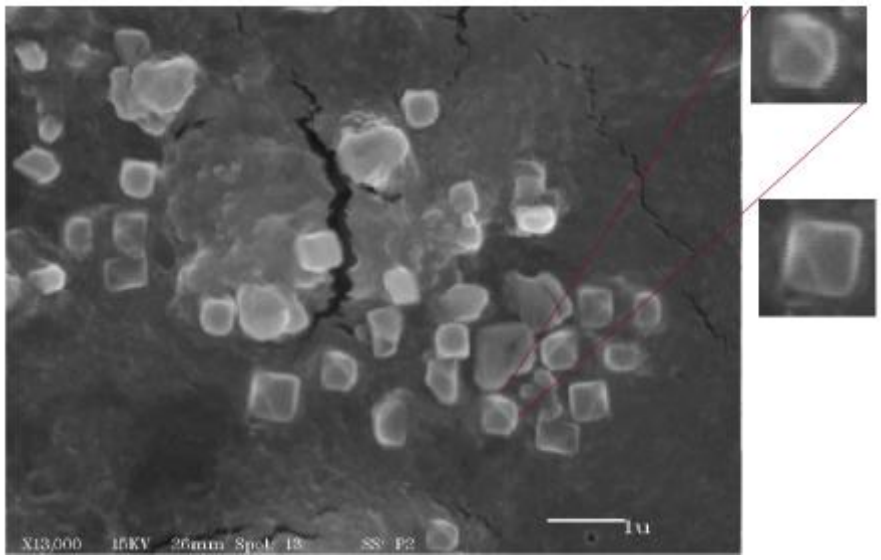

Figure 4.2. CaP:pd-FIX particles used in buccal administration to normal male CD-1 mice. CaP:pd-FIX was imaged by scanning electron microscope.

FIX plasma levels after buccal administration of CaP:pd-FIX and CaP:tg-FIX

We probed the buccal delivery efficiency of the CaP formulations of pd-FIX and purified tg-FIX using both normal and hemophilic CRM+ mice. The use of CRM+ enabled indirect detection of endothelial reservoir delivery which might occur during buccal delivery. The antigen levels in 3 of 4 normal CD-1 mice that were buccally administered CaP:pd-FIX at 2000 IU/kg gave an average maximal rise above baseline of 250 ng/mL (Fig. 4.3). The average baseline antigen levels ranged from 15 to 25 ng/mL. The maximum levels of FIX antigen occurred at 4 to 6 hours post-administration and values above baseline were detected at up to 72 hours. All mice showed a < 1% rise in coagulation activity.

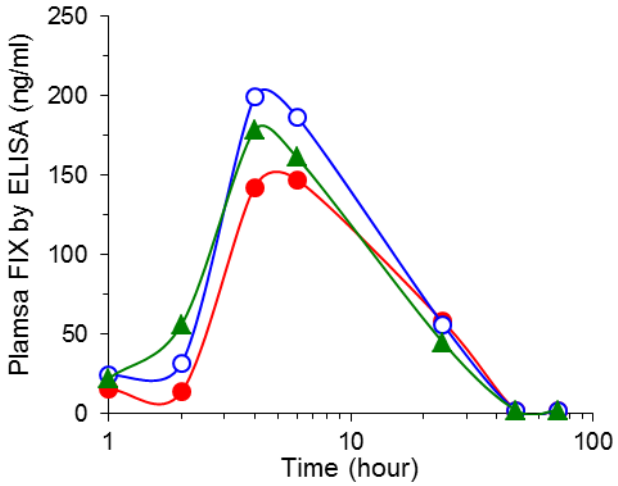

Figure 4.3. FIX plasma levels after buccal delivery of CaP:pd-FIX into CD-1 normal mice. FIX plasma levels after buccal delivery of CaP:pd-FIX into CD-1 normal mice. The animal was treated with 49 IU of FIX (n=4). (●) Mouse 1 (○) Mouse 2 (▲) Mouse 4.

When CaP:tg-FIX was administered at 2000 IU FIX/kg to CRM+ hemophilic mice (n=7), an increase in antigen level was observed in all mice (Fig. 4.4). These mice reached a maximum change in FIX antigen level of >400 ng/mL in 15 minutes and maintained a FIX antigen level of >300 ng/mL for ten hours. In contrast, CRM- hemophilic mice fed CaP alone (Fig. 4.5A) showed a decrease in FIX antigen. The CaP:tg-FIX administration of 2000 IU/kg was also repeated in a new set of CRM+ mice alongside a 6000 IU/kg administration. CaP delivery to CRM+ mice was used as a negative control group to determine the effect of buccally administered CaP alone (Fig. 4.5A).

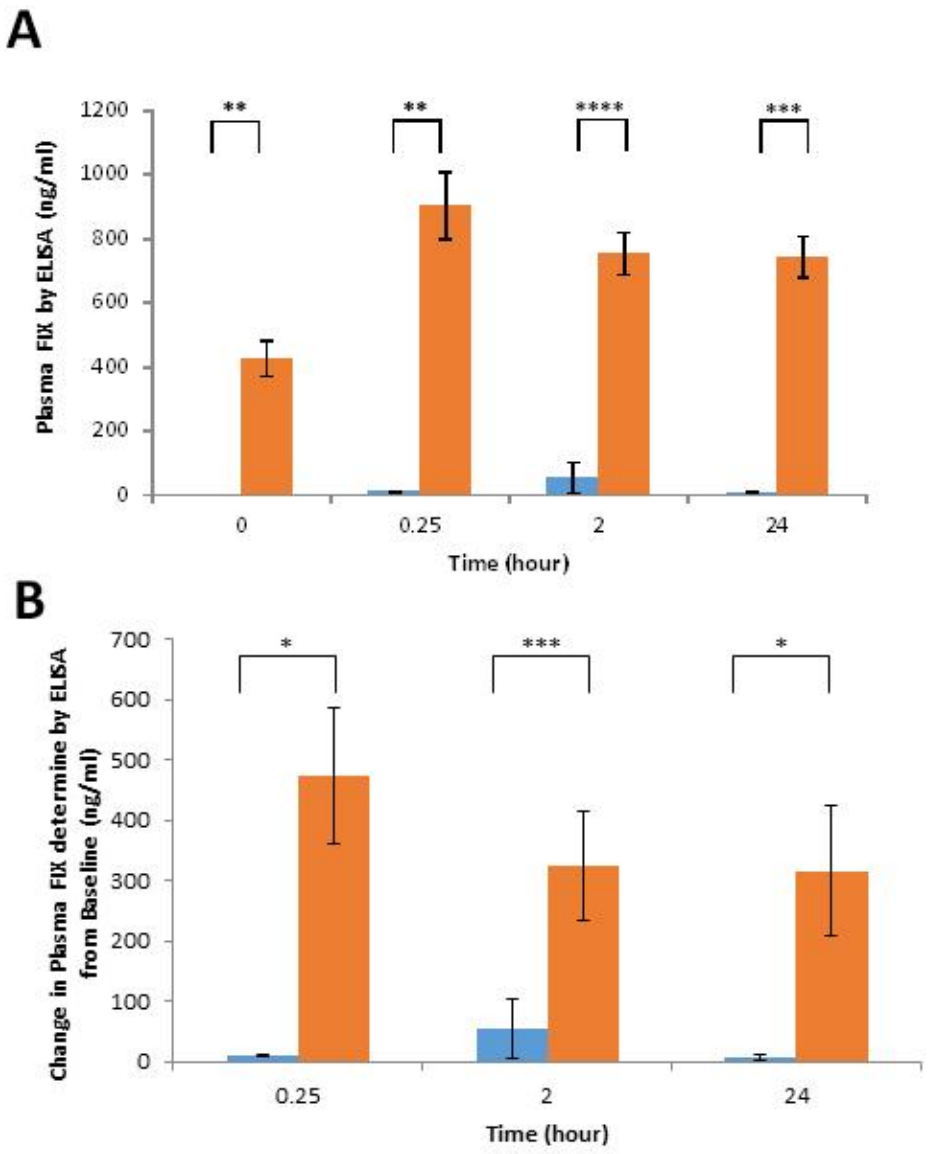

Figure 4.4. FIX plasma levels after buccal delivery of CaP:tg-FIX into KI-CRM+ R333Q (n=7) and CaP into CRM- mice (n=5). Each R333Q animal was treated with 2000 IU FIX/kg. Both plots were determined by ELISA. (A) FIX levels in plasma (B) Net change in FIX levels in plasma. ( ) FIXKO ( ) R333Q (*) P<0.05 (**) P<0.01 (***) P<0.001 (****) P<.0001.

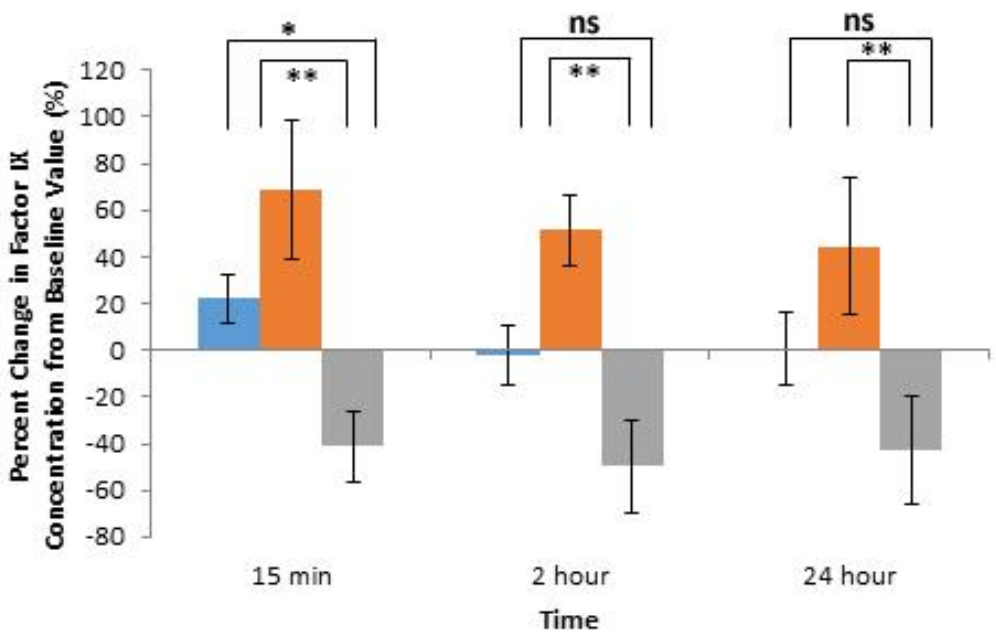

Figure 4.5. FIX levels after buccal delivery of CaP:tg-FIX into KI-CRM+ R333Q mice (n=8). Activity determined by ELISA. (■) 2000 U/kg (■) 6000 U/kg (■) Placebo. (*) P<0.05 (**) P<0.01 (ns) not significant.

We used the CRM+ mice to detect displacement phenomena of the inactive R333Q FIX from endogenous endothelial reservoirs that might be caused by buccal delivery of tg-FIX. Importantly, these ELISA measurements were used specifically to detect the threonine 148 natural variant present in the tg-FIX, but not in the R333Q inactive variant present in the CRM+ mice. These tg-FIX specific measurements showed no signal in any of treatment groups of CRM+ mice while nonspecific antibody indicated elevated levels.

The tail transection performed at 24 hours after feeding also detected no activity, potentially due to endothelial reservoir loading by the tg-FIX . During the first tail cut a significant reduction in bleeding time was observed in mice given 6000 IU/kg (Fig 6A).

Twenty minutes after the cessation of bleeding from the first tail-cut, the second tail transection was performed. The second-tail cut produced no significant reduction in bleeding (Fig 6B).

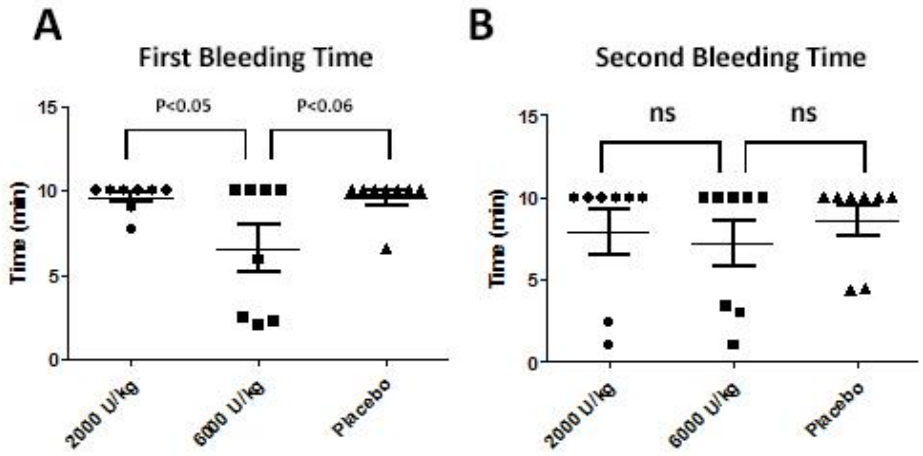

Figure 4.6. Bleeding Time after Tail Transection. Hemostatic effect in vivo of tg-FIX in infused R333Q CRM+ mice (n=8). Bleeding time caused by tail transection until bleeding termination. (A) Time from tail transection to bleeding termination. After 10 minutes, bleeding was ended by application of firm pressure. (B) After 30 minutes from time of bleeding termination, the clot was removed and secondary bleeding was recorded until bleeding termination. (ns) not significant.

4.5 Discussion

We previously reported the production of >100 IU/mL of tg-FIX activity in the milk of transgenic pigs [22, 23]. The antigen content of the pooled milk collected over a 40 day lactation was reliably detected at 1-1.5 g/l while the coagulation activity varied from 40-300 IU/mL, which is 40-300 fold higher activity than is found in human plasma. The tg-FIX in the milk was estimated to be about 10-15% biologically active and the average specific activity was about 40 IU/mg tg-FIX for all species in the milk. The most biologically active and highly purified tg-FIX preparations were similar in specific

activity to pd-FIX at >200 IU/mg [22, 23]. The variability of the activity in raw milk is due in part to the proteolytic nature of milk and due to broad distribution of tg-FIX with different post-translational modification. This is especially important with respect to sufficient levels of gamma-carboxylation of glutamic acid contained in the Gla domain which is required for coagulation activity. Importantly, pig milk is a lipophilic, micellular mixture containing 6-8% fat membrane globules that could facilitate oral delivery [21, 33] and that both mice and dogs readily ingested. Thus, the raw milk was used both as an abundant source and delivery vehicle of FIX activity for probing the possibility of the oral delivery of FIX.

We have used several different animal models to assess the potential for the delivery of tg-FIX by oral and buccal administration. Buccal delivery was explored due to the potential for decreased transport limitations that might be present in the mucosal tissue of the mouth and also due to its less proteolytic environment relative to the gut. However, the decision to predominately use mice despite the more keratinized and likely limiting nature of the mouse mouth relative to that of dogs [32] was due to low body weight and access to statistically significant numbers of mice. In addition, the (CRM+) R333Q mice have the human factor IX R333Q gene expressed with the alanine form of the Ala148Thr dimorphism, allowing for selective antibody detection between multiple variants of FIX [34]. These mice also have less than 1% clotting activity while having normal levels of FIX. Antibodies have been developed to detect both the infused FIX while ignoring endogenous R333Q-FIX and the total of all FIX in the sample, allowing for independent detection of the various FIX species in a given sample [34, 35] which allows for detection of the potential endothelial reservoir effects.

The majority of CRM- mice and 1 of 2 dogs exhibited increased coagulation and activity levels detectable one hour after feeding of raw tg-FIX pig milk. The bioavailability of the biologically active tg-FIX was >10-fold higher in the single responding dog than any of the responding mice. Interestingly, the bioavailability of tg-FIX antigen into plasma circulation was similar for mice and dogs. While a lipemic effect from the fat-rich pig milk might be increased in dogs over mice, the non-responding dog had no increase in plasma coagulation activity after ingesting the same amount of pig milk. Another explanation is the more selective absorption of biologically active tg-FIX from the milk, which contained only 10 to 15% biologically active tg-FIX. Indeed the specific activity of this additional circulating FIX was estimated to be 211 IU/mg, which corresponds to that typically found for tg-FIX that is highly purified from the same raw milk [22, 23]. Thus, unlike the mice, the tg-FIX delivered into circulation is primarily selective for biologically active tg-FIX. The dog antigen and coagulation activities were expressed as relative increases as both assays contained relatively high background levels. Thus, the amount of dog FIX displaced from the endothelial reservoirs was not able to be determined.

Because of the crude, less defined nature of tg-FIX when delivered from milk, we explored the use of highly purified CaP:tg-FIX and CaP:pd-FIX for use via buccal delivery. The formulation of CaP:FIX microparticles proved to be highly efficient. While the dose of 2000 IU/kg body weight was exceedingly high, the majority of normal mice studied (n=5) responded with easily observable and similar rises in the levels of FIX antigens after delivery of CaP:pd-FIX. The clearance of antigen lasted over 72 hours with a mean residence time of 17 hours, indicating that the mouse developed no negative

reaction to treatment and that the clearance phenomenon was not unlike that of endogenous FIX.

This led us to examine similar dosing in CRM+ mice using the CaP:tg-FIX which resulted in similar response to buccal delivery of pd-FIX by the normal mice treatment study. There was <1% activity in the coagulation assays of all treatment groups in the CRM+ mice, but the presence of antigen rise similar to buccal delivery of pd-FIX in normal mice indicates that a large amount of inactive FIX is stored in the endothelial reservoir and that the inactive FIX is displaced by the buccally delivered FIX, albeit by a small total rise in the levels of R333Q. A significantly decrease in amount of bleeding occurring at 24 hours post-administration was observed only in the 6000 IU/kg mice indicating that only a very small amount of tg-FIX was present in the reservoir at 24 hours.

Thus, this study showed that buccal and oral administration of FIX significantly increases FIX concentration in the plasma during animal studies. The >1% bioavailability of tg-FIX in oral delivery to a normal dog using crude milk as a formulation vehicle, shows a potential to utilize the >100 fold abundance of FIX that transgenic livestock production can provide. However, purified and well defined preparations of tg-FIX back-formulated into a defined, pasteurized milk vehicle would likely be necessary for the reproducibility needed for safe and efficacious biopharmaceutical use.

4.6 Acknowledgements

I would like to thank Tülin Morcöl and Captivate Pharmaceutical for the use of their bioencapsulation techniques.

4.7 References

1 Furie B, Furie BC. The molecular basis of blood coagulation. *Cell*. 1988; 53: 505-18.
2 Kurachi K, Kurachi S, Furukawa M, Yao S. Biology of factor IX. *Blood coagulation & fibrinolysis*. 1993; 4: 953-73.
3 Gui T, Reheman A, Funkhouser WK, Bellinger DA, Hagaman JR, Stafford DW, Monahan PE, Ni H. In vivo response to vascular injury in the absence of factor IX: examination in factor IX knockout mice. *Thrombosis Research*. 2007; 121: 225-34.
4 Thompson AR, Chen S-H. Characterization of factor IX defects in hemophilia B patients. *Methods in enzymology*. 1993; 222: 143-69.
5 Berntorp E, Astermark J, Baghaei F, Bergqvist D, Holmström M, Ljungberg B, Norlund A, Palmblad J, Petrini P, Stigendal L. Treatment of haemophilia A and B and von Willebrand's disease: summary and conclusions of a systematic review as part of a Swedish health-technology assessment. *Haemophilia*. 2012; 18: 158-65.
6 Ewenstein BM, Joist JH, Shapiro AD, Hofstra TC, Leissinger CA, Seremetis SV, Broder M, Mueller-Velten G, Schwartz BA. Pharmacokinetic analysis of plasma-derived and recombinant F IX concentrates in previously treated patients with moderate or severe hemophilia B. *Transfusion*. 2002; 42: 190-7.
7 Björkman S. A commentary on the differences in pharmacokinetics between recombinant and plasma-derived factor IX and their implications for dosing. *Haemophilia*. 2011; 17: 179-84.
8 White GC, 2nd, Beebe A, Nielsen B. Recombinant factor IX. *Thromb Haemost*. 1997; 78: 261-5.
9 Collins P, Fischer K, Morfini M, Blanchette V, Björkman S. Implications of coagulation factor VIII and IX pharmacokinetics in the prophylactic treatment of haemophilia. *Haemophilia*. 2011; 17: 2-10.
10 Berntorp E, Astermark J, Björkman S, Blanchette V, Fischer K, Giangrande P, Gringeri A, Ljung R, Manco-Johnson M, Morfini M. Consensus perspectives on prophylactic therapy for haemophilia: summary statement. *Haemophilia*. 2003; 9: 1-4.
11 Stonebraker JS, BOLTON-MAGGS PH, Brooker M, Farrugia A, Srivastava A. A study of reported factor IX use around the world. *Haemophilia*. 2011; 17: 446-55.
12 Journeycake JM, Quinn CT, Miller KL, Zajac JL, Buchanan GR. Catheter-related deep venous thrombosis in children with hemophilia. *Blood*. 2001; 98: 1727-31.

13 Izzi G, Franchini M, Bonetti L, Tagliaferri A. The use of central venous catheters in haemophilia patients. *Haemophilia*. 2010; 16: 29-31.
14 Verma D, Moghimi B, LoDuca PA, Singh HD, Hoffman BE, Herzog RW, Daniell H. Oral delivery of bioencapsulated coagulation factor IX prevents inhibitor formation and fatal anaphylaxis in hemophilia B mice. *Proceedings of the National Academy of Sciences*. 2010; 107: 7101-6. 10.1073/pnas.0912181107.
15 DiMichele D. Inhibitor development in haemophilia B: an orphan disease in need of attention. *British journal of haematology*. 2007; 138: 305-15.
16 Gouw SC, van der Bom JG, van den Berg HM. Treatment-related risk factors of inhibitor development in previously untreated patients with hemophilia A: the CANAL cohort study. *Blood*. 2007; 109: 4648-54.
17 Cheung W-F, Van Den Born J, Kühn K, Kjellen L, Hudson BG, Stafford DW. Identification of the endothelial cell binding site for factor IX. *Proceedings of the National Academy of Sciences*. 1996; 93: 11068-73.
18 Gailani D. Factor IX binding to collagen. *Journal of Thrombosis and Haemostasis*. 2009; 7: 1840-2.
19 Østergaard H, Bjelke JR, Hansen L, Petersen LC, Pedersen AA, Elm T, Møller F, Hermit MB, Holm PK, Krogh TN, Petersen JM, Ezban M, Sørensen BB, Andersen MD, Agersø H, Ahmadian H, Balling KW, Christiansen MLS, Knobe K, Nichols TC, Bjørn SE, Tranholm M. Prolonged half-life and preserved enzymatic properties of factor IX selectively PEGylated on native N-glycans in the activation peptide. *Blood*. 2011; 118: 2333-41. 10.1182/blood-2011-02-336172.
20 Gui T, Reheman A, Ni H, Gross P, Yin F, Monroe D, Monahan P, Stafford D. Abnormal hemostasis in a knock-in mouse carrying a variant of factor IX with impaired binding to collagen type IV. *Journal of Thrombosis and Haemostasis*. 2009; 7: 1843-51.
21 Hemker H, Muller A, Hermens WT, Zwaal R. Oral treatment of haemophilia A by gastrointestinal absorption of factor VIII entrapped in liposomes. *The Lancet*. 1980; 315: 70-1.
22 Van Cott KE, Butler SP, Russell CG, Subramanian A, Lubon H, Gwazdauskas F, Knight J, Drohan WN, Velander WH. Transgenic pigs as bioreactors: a comparison of gamma-carboxylation of glutamic acid in recombinant human protein C and factor IX by the mammary gland. *Genetic analysis: biomolecular engineering*. 1999; 15: 155-60.
23 Lindsay M, Gil G-C, Cadiz A, Velander WH, Zhang C, Van Cott KE. Purification of recombinant DNA-derived factor IX produced in transgenic pig milk and fractionation of active and inactive subpopulations. *Journal of Chromatography A*. 2004; 1026: 149-57.
24 Chang C-H, Chow T-K, Yang C-Y, Chang T-J, Wu Y-H, Lee T-W. Biodistribution and Pharmacokinetics of Transgenic Pig-produced Recombinant Human Factor IX (rhFIX) in Rats. *In Vivo*. 2008; 22: 693-7.
25 Chang L-C, Yang C-Y, Chua ACN, Lin Y-J, Lai S-M. Sustained Release of Transgenic Human Factor IX: Preparation, Characterization, and in Vivo Efficacy. *Molecular Pharmaceutics*. 2011; 8: 1767-74. 10.1021/mp200133s.
26 Takagi H, Hiroi T, Yang L, Tada Y, Yuki Y, Takamura K, Ishimitsu R, Kawauchi H, Kiyono H, Takaiwa F. A rice-based edible vaccine expressing multiple

T cell epitopes induces oral tolerance for inhibition of Th2-mediated IgE responses. *Proceedings of the National Academy of Sciences of the United States of America*. 2005; 102: 17525-30.

27 Gui T, Lin H-F, Jin D-Y, Hoffman M, Straight DL, Roberts HR, Stafford DW. Circulating and binding characteristics of wild-type factor IX and certain Gla domain mutants in vivo. *Blood*. 2002; 100: 153-8. 10.1182/blood.V100.1.153.

28 Arruda VR, Hagstrom JN, Deitch J, Heiman-Patterson T, Camire RM, Chu K, Fields PA, Herzog RW, Couto LB, Larson PJ. Posttranslational modifications of recombinant myotube-synthesized human factor IX. *Blood*. 2001; 97: 130-8.

29 He Q, Mitchell AR, Johnson SL, Wagner-Bartak C, Morcol T, Bell SJ. Calcium phosphate nanoparticle adjuvant. *Clinical and diagnostic laboratory immunology*. 2000; 7: 899-903.

30 Lin H-F, Maeda N, Smithies O, Straight DL, Stafford DW. A coagulation factor IX-deficient mouse model for human hemophilia B. *Blood*. 1997; 90: 3962-6.

31 Motulsky H. Prism 5 Statistics Guide, 2007. *GraphPad Software*. 2007.

32 Shojaei AH. Buccal mucosa as a route for systemic drug delivery: a review. *J Pharm Pharm Sci*. 1998; 1: 15-30.

33 O'brien J. The effect of some fatty acids and phospholipids on blood coagulation. *British journal of experimental pathology*. 1957; 38: 529.

34 Jin D-Y, Zhang T-P, Gui T, Stafford DW, Monahan PE. Creation of a mouse expressing defective human factor IX. *Blood*. 2004; 104: 1733-9. 10.1182/blood-2004-01-0138.

35 Monahan PE. Factor IX: Insights from knock-out and genetically engineered mice. *Thromb Haemost*. 2008; 100: 563-75.

Chapter 5:

Quantitative Measurements of Factor IX Metal Dependent Compaction

Nicholas C. Vanderslice[a] , Amanda S. Messer[a,b], Kanagasabai Vadivel[b], S. Paul Bajaj[b], Martin Phillips[c], Mostafa Fatemi[a], Kevin E. Van Cott[a], and William H. Velander[a]

[a]Protein Purification and Characterization Laboratories, Department of Chemical and Biomolecular Engineering, 207 Othmer Hall, University of Nebraska, Lincoln 68588, USA

[b]Protein Science Laboratory, UCLA/Orthopaedic Hospital, Department of Orthopaedic Surgery and Molecular Biology Institute, 615 Charles E. Young Dr South, University of California, Los Angeles 90095, USA

[c]UCLA-DOE Biochemistry Instrumentation Facility, Department of Chemistry and Biochemistry, 607 Charles E. Young Drive East, UCLA, Los Angeles, CA 90095, USA

5.1 Abstract

Background: Factor IX (FIX) is a member of the vitamin K-dependent (VKD) family of plasma glycoproteins which have a conserved γ-carboxyglutamic acid (Gla) domain that contains four Ca^{2+}, three Mg^{2+}, and one interchangeable divalent-metal binding sites. FIX also contains a Ca^{2+} binding site in both the EGF-1 like and catalytic domains. In contrast to previous studies using protein fragments, this study quantifies the compaction of factor IX (FIX) holoprotein by Ca^{2+} and Mg^{2+}.

Methods: A novel application of high pressure size exclusion chromatography (HPSEC) taken together with analytical ultracentrifugation (AUC) and molecular modeling were

used to quantify overall compaction in the FIX holoprotein caused by divalent metal binding.

Results: Over the range of sub- to physiologic levels of Ca^{2+}, we observed a stark compaction of FIX associated with Ca^{2+} and Mg^{2+} binding. The holoprotein compaction caused by the filling of Ca^{2+} sites was equivalent to a change in the radius of hydration by 5-6% and similar to the changes in radius of gyration predicted by molecular modeling of the holoprotein. The compaction induced by physiologic levels of Ca^{2+} alone is greater than for Mg^{2+} alone and the presence of both divalent metals provided a cooperative increase in compaction.

Conclusion: The divalent metal-induced compaction phenomenon primarily arises from conformational changes in the core Gla domain and secondarily in the EGF1-like domain that is directly observable in the holoprotein by HPSEC.

General Significance: This study provides a quantitative solution phase perspective to the metal dependent conformational attributes of the VKD holoproteins.

5.2 Introduction

The Vitamin K-dependent (VKD) family of plasma proteins are key participants in the coagulation cascade of hemostasis[1, 2]. The first nine amino terminal glutamic acids of these glycoproteins are well conserved and are γ-carboxylated to form "Gla residues". These residues are part of the "Gla domain" that is essential to the function of VKD proteins. This family includes the anticoagulant proteins C, S and Z, and the procoagulant factors (F) VII, IX, X and prothrombin [3]. The core Gla domain contains seven to eight total divalent metal binding sites [4-11]: in the absence of Mg^{2+} all of these

sites could be occupied by Ca^{2+}. However, higher than physiologic Ca^{2+} concentrations are needed for full occupancy of these sites. In the presence of physiologic Ca^{2+} (~1.1 mM) and Mg^{2+} (~0.6 mM), four sites (numbered 2, 3, 5 and 6) are occupied by Ca^{2+} and three (numbered 1, 4, and 7) by Mg^{2+} [4, 10]. It is important to note that all metal sites in the Gla domain will be filled by Ca^{2+} at greater than 2 mM in the absence of Mg^{2+}. The Mg^{2+}-site 4 is predicted to switch to Ca^{2+} upon binding of the Gla domain to phospholipid (PL) [11]. The conformational attributes of the isolated Gla domains have been well studied using NMR and x-ray crystallography [4, 5, 7-9, 12]. The Gla domain has also been studied using divalent metal, conformational-dependent monoclonal antibodies [13-16]. Collectively, these previous studies have observed the localized and cooperative folding of the Gla domain with respect to the filling of Ca^{2+}- and Mg^{2+}-binding sites [17].

FIX is a key VKD protein that consists of an N-terminal Gla domain followed by two epidermal growth factor-like domains and a C-terminal serine protease domain [1, 2]. It uniquely possesses a total of 12 Gla residues, but has a core Gla domain behavior typical of VKD coagulation proteins [18, 19]. With respect to other VKD coagulation proteins, FIX contains an additional divalent metal binding site that occurs outside of the core Gla domain; two additional Gla residues occur at amino acid positions 36 and 40 and participate in the formation of an eighth Mg^{2+} site [9, 19]. The absence of these Gla residues in under-carboxylated recombinant versions of FIX has indicated that the number eight metal binding site occupied either by Ca^{2+} or Mg^{2+} does not contribute to FIX biological activity associated with PL binding [19]. FIX also contains two additional Ca^{2+}-binding sites, one in the EGF1-like domain [20, 21] and the other in the protease domain [22, 23]. These two non-Gla divalent metal sites are specific for Ca^{2+} and

contribute to the structural and functional integrity of the molecule [21, 23]. During blood coagulation, FIX is converted to FIXa by FXIa as well as by the complex of FVIIa and cell surface tissue factor [1, 2]; both of these reactions require the divalent metal-dependent folded structure of the Gla domain of FIX [24, 25]. FIXa thus formed activates FX to FXa; for a biologically significant rate, this reaction requires Ca^{2+}/Mg^{2+} [26], PL (provided by platelets and the damaged endothelium) and FVIIIa [2]. These studies point out the role of individual domains in FIX and their importance in biologic function.

The solution phase transitions of VKD coagulation proteins which are divalent metal dependent have been detailed for FII and FIX using spectroscopic and fluorometric measurements [27-29]. However, these transitions have not been well detailed using molecular size measurements of the whole protein. Previous studies were not designed to quantify compaction of FIX in solution due to Ca^{2+} and Mg^{2+}. Studies of this type have typically been attempted using circular dichroism [30, 31], light scattering [30], and/or analytical ultracentrifugation (AUC) [31-34]. Molecular size studies of PC [35], FVIIa [34], FIX [30, 32], FIXa [33], and fragments of FII [31] were limited and frequently complicated by the tendency to form aggregates when studied by AUC [31]. In the present study, we use HPSEC, AUC and molecular modeling to elucidate changes in molecular size that are induced in FIX by the filling of Ca^{2+}- and Mg^{2+} -specific sites while in solution.

5.3 Materials and Methods

Reagents

All buffer components were purchased from VWR International LLC (Radnor, PA, USA) or Thermo Fisher Scientific (Waltham, MA, USA) or Sigma (St. Louis, MO, USA) unless otherwise stated. In order to minimize degradation, purification processes were performed at 4^0C. The stocks of plasma-derived, therapeutic grade FIX (Mononine, CSL Behring, USA) were expired for clinical use, but when used in experiments, exhibited full procoagulant activity by one stage clotting assay.

Size Exclusion Chromatography (SEC)

The FIX product was concentrated and exchanged into 20 mM Tris, 200 mM NaCl, pH 7.0 (SEC/Injection running buffer) using an Amicon Ultra 10 kDa molecular cut-off centrifugal filter (Millipore, Billerica, MA, USA). Both the SEC/Injection running buffer was treated with the sodium form of Analytical Grade Chelex 100 resin (Bio-Rad Laboratories, Hercules, CA USA) to remove any divalent metal contamination. Some running buffer studies contained $CaCl_2$ and or $MgCl_2$ that was added after Chelex 100 resin treatment while all injection samples contained divalent metal-free buffer. The FIX was loaded onto a 60 cm X 2.15 cm I.D. TSK gel G3000SW column (Tosoh Bioscience, King of Prussia, PA, USA) equipped with a guard column and a pre-filter.

Briefly, the chromatography was performed on the Knauer (Berlin, Germany) Smartline chromatography station described above. The flow rate was set at 0.5 mL/min and the run length was 45 minutes. Effluent's absorbance was measured at an absorbance of 280 nm. Samples were run in triplicate and the centers of the elution peaks were used to calculate residence time (with standard deviation <0.016).

Sodium Dodecylsulfate-Polyacrylamide Gel Electrophoresis (SDS-PAGE)

Samples were analyzed by SDS-PAGE stained with colloidal blue gel stain (Invitrogen, Carlsbad, CA, USA) using Invitrogen Novex precast gels and the Invitrogen Surelock XL apparatus. All gels were NuPage 12% Bis-Tris run with 2-(N-morpholino) ethanesulfonic acid (MES) running buffer (Invitrogen). Briefly, samples were mixed with 4x LDS sample buffer (Invitrogen) and deionized water followed by heating at 75 ◦C for 10 min. For reduced gels, samples were mixed with 10x reducing agent (Invitrogen) prior to heating.

Analytical Ultracentrifuge

FIX in 0.15 M NaCl, 50 mM Tris, pH 7.5 with either 10mM EDTA or $CaCl_2$ and/or $MgCl_2$ was examined by sedimentation velocity in a Beckman Optima XL-A analytical ultracentrifuge at 52,000 or 55,000 rpm and 20 ^{o}C in 12 mm path length double sector cells using absorption optics at 280 nm. All samples were at the same protein concentration, 0.3 mg/mL. Apparent sedimentation coefficient distributions, uncorrected for diffusion, were determined as g(s) plots using the Beckman Origin based software (Version 3.01). These plots display a function proportional to the weight fraction of material with a given sedimentation coefficient, s. The function g(s) was calculated as:

$$g(s) = (dc/dt)(1/c_o)(\omega^2 t^2/\ln(r_m/r))(r^2/r_m^2);$$

where s is the sedimentation coefficient, ω is the angular velocity of the rotor, c_o is the initial concentration, r is the radius, r_m is the radius of the meniscus, and t is time. The x-axis is converted to sedimentation coefficient by:

$s = (1/\omega^2 t)(\ln(r/r_m))$

These plots display a function proportional to the weight fraction of material with a given sedimentation coefficient, S [36]. The peak sedimentation coefficients were corrected for density and viscosity of the solution to $S_{20,w}$ values. To perform this correction, a value of 0.708 for the partial specific volume calculated from the amino acid and carbohydrate composition was used [37, 38]. This correction is quite insensitive to the value for the partial specific volume in this range. The Stokes radius was calculated using a molecular weight of 62,800 and a partial specific volume of 0.708.

Modeling of Divalent Metal-Free and Bound FIX

The equilibrated solution structures of the zymogen form of metal bound FIX were obtained from Perera [39]. The MODELLER program [40] was employed to model the metal-free FIX zymogen structures utilizing the metal bound zymogen structures and the NMR structure of metal-free FIX Gla domain (pdbid 1CFX,[12]) as templates. The built models were further refined by energy minimization using the CHARMM program with CHARMM19 force field [41] consisting of 50 steps of Steepest Descent, followed by 500 steps of Adopted Basis Newton-Raphson. Harmonic restraints of 10 kcal/mol/$Å^2$ were applied on the C^α atoms of the protein during the entire minimization.

5.4 Results and Discussion

FIX compaction induced by divalent metals predicted by molecular modeling

We first used molecular modeling to predict the nature and magnitude of the size change that would be induced by the filling of divalent metal binding sites within the FIX holoprotein structure. The modeled structures of the zymogen form of divalent metal-free and metal bound FIX are shown in Fig 5.1. This modeling effort employs no assumptions of shape, but a linear molecule is predicted for both divalent metal containing and under metal-free conditions. Thus, we use the model to predict a radius of gyration rather than a Stokes Radius (R) from the spherical assumption used to estimate changes in compaction using AUC. The radius of gyration values for the modeled structures of metal-free FIX is 34.46 Å while the radius of gyration value for the metal bound FIX is 32.75 Å. The change in radius of gyration between the metal bound and metal-free states of FIX is ~5%. As expected, the major transitions in structure arise from the Ca^{2+}/Mg^{2+} binding to the Gla domain of FIX (Fig 5.1A, 5.1B). Furthermore, the Ca^{2+} binding sites exterior to the Gla domain that occur in the EGF-1 [20] and protease domains [22, 23] are predicted to give much smaller contributions to compaction due to occupation of Ca^{2+} at those sites. It is known that the folding of the Gla domain is both Ca^{2+}/Mg^{2+} dependent [10, 12, 16, 42-44] and without these divalent ions, the Gla domain is in a completely unfolded state [12]. General conformation changes have been observed in all the coagulation proteins earlier in fluorescence quenching and metal binding studies [12, 30, 42].

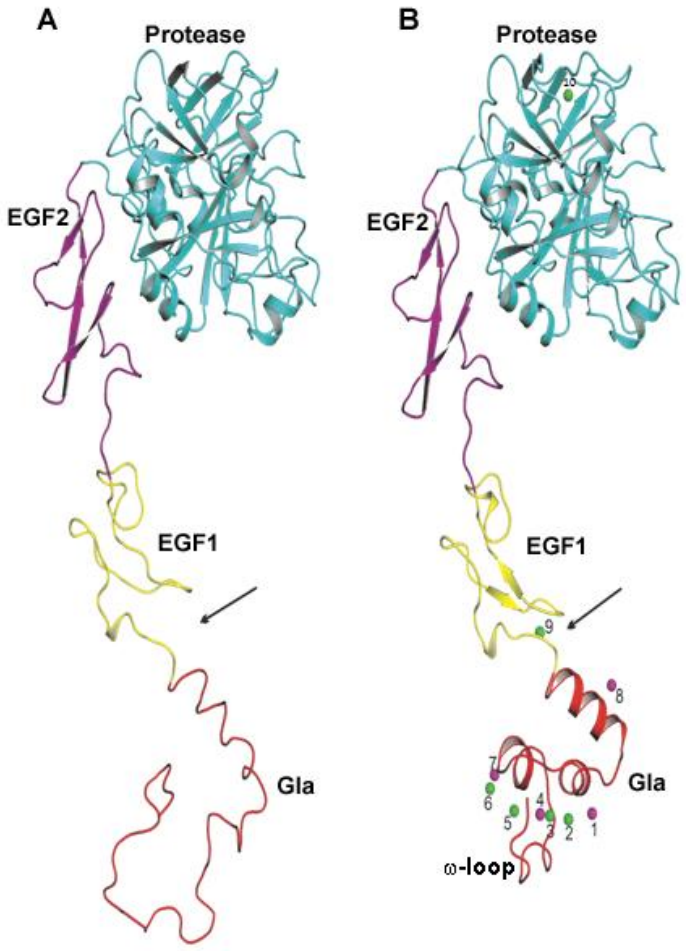

Figure 5.1. Modeled structures of intact FIX without (A) and with (B) divalent metal ions predicted from the crystallographic data. The Gla, EGF1-like, EGF2-like and the protease domain in FIX are colored red, yellow, purple and cyan, respectively. FIX contains 10 Ca^{2+}/Mg^{2+} binding sites, which are numbered 1 through 10; eight of these are in the Gla domain (number 1-8), one in the EGF1-like domain (number 9) and one in the protease domain (number 10). The Ca^{2+}-specific sites are shown as green spheres, whereas the sites 1, 4, 7 and 8 could be occupied by either Ca^{2+} or Mg^{2+} are shown as magenta spheres. As a result of divalent metal binding, a major structural change occurs in the Gla domain and a minor change in the EGF1-like domain of FIX. The properly formed ω-loop is clearly visible and positioned below metal sites 3, 4 and 5.

Homogeneity and extent of aggregation of the plasma derived FIX studied

We assessed both the homogeneity of the FIX and extent of protein aggregation that potentially could occur in the range of metal and protein concentrations studied here. Previous studies have reported protein aggregation in FIX in the presence of divalent metals observed by AUC at concentrations of >0.3 mg FIX/mL [30]. Fig. 5.2A shows analysis by SDS-PAGE under non-reducing conditions of immunoaffinity purified, therapeutic grade FIX. As has been well documented for preparations of plasma-derived FIX, the FIX studied here contained a proteolyzed FIX species of the Mr 47 kDa having a 10 kDa fragment removed from its carboxy-terminus known as FIXγ[45]. We estimated the FIX to be >95% zymogen having a Mr of 57 kDa and contained <5% proteolyzed FIX. Fig. 2B and 2C show the typical HPSEC chromatographic profiles for injections of 25 and 50 μg FIX that was obtained at physiologic pH in the presence of 1.1 mM Ca^{2+} alone and of 0.6 mM Mg^{2+} alone, respectively. Fig. 5.3-5.5 present the HPSEC chromatographic behavior for analysis of 100 μg injections. In all cases studied, the HPSEC behavior possessed a single predominant and symmetrical peak. In the case of the 100 μg injection, a peak height signal was observed, which was about 4- and 2-fold larger than those observed for the 25 μg and 50 μg injections. Furthermore, other than the main peak only a few peaks of less than 15% intensity of the main peak were observed. Taken together, these studies show that these samples predominately contained intact FIX zymogen and that there was no appreciable tendency of the FIX to form aggregates at any of the divalent metal or protein concentrations examined here by HPSEC or AUC.

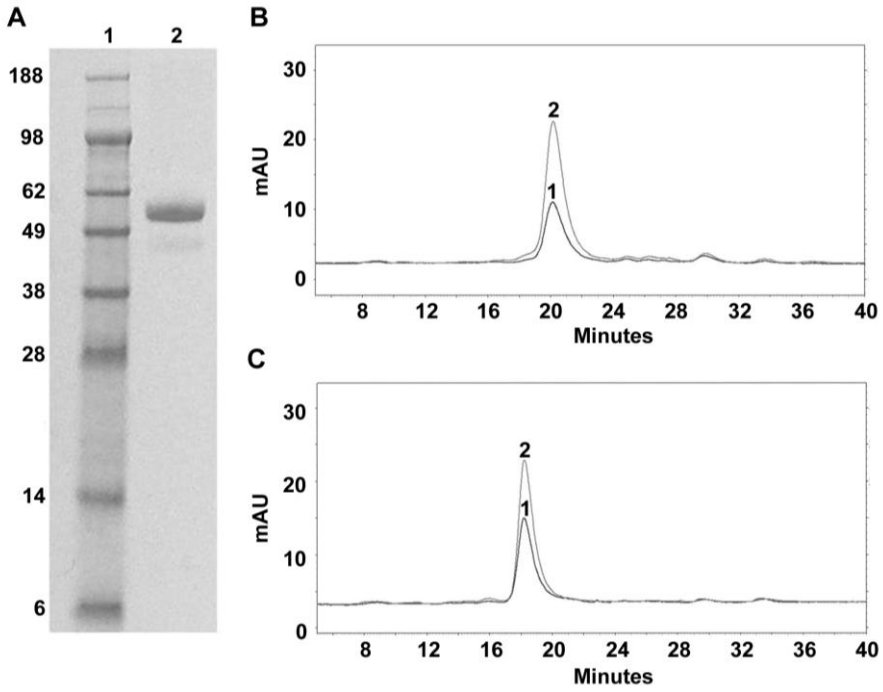

Figure 5.2. Homogeneity and extent of aggregation of starting samples of purified FIX. SDS-PAGE and HPSEC as a function of the injection amount was studied: A) Non-reducing SDS-PAGE of purified FIX: Lane 1. Molecular weight markers; Lane 2. FIX (2 μg). B) HPSEC chromatographic profiles of FIX at 25 μg (curve 1) and at 50 μg injected (curve 2) at physiologic 1.1 mM Ca2+ and C) HPSEC chromatographic profiles of FIX at 25 μg (curve 1) and at 50 μg injected (curve 2) at physiologic 0.6 mM Mg2+.

Ca^{2+}-specific compaction of FIX observed by HPSEC

We investigated the effect on FIX macromolecular size caused by the filling of divalent metal specific sites when chromatographed at physiologic pH and various levels of Ca^{2+} alone using HPSEC. While in the absence of Mg^{2+}, all sites in FIX Gla domain can be occupied by Ca^{2+}, positions 1, 4, 7 and 8 are occupied by Mg^{2+} at physiologic levels of Ca^{2+} and Mg^{2+}. However, at supraphysiologic levels of Ca^{2+} *in vitro*, Mg^{2+} at site 4 is displaced by Ca^{2+} [11]. Fig. 5.3A shows the HPSEC chromatographic profiles for

FIX collected over a range of sub- to supra-physiologic Ca^{2+} levels in the absence of Mg^{2+}. Under this condition, each divalent metal binding sites has the potential to be occupied by Ca^{2+}. A baseline residence time of about 17.1 minutes was obtained for the elution peak of FIX in a chelated environment (Fig. 5.3A: curve 1). When chromatographed at a subphysiologic level of 0.5 mM Ca^{2+}, the residence time shifted markedly to a longer time of 17.9 minutes (Fig. 5.3A: curve 2). Importantly, this signifies a compaction response at a Ca^{2+} level that completely fills each of the single Ca^{2+} specific sites that occurs within the EGF1-like and the catalytic domain. At the physiologic concentration of 1.1 mM Ca^{2+} (Fig. 5.3A: curve 3), the residence time of FIX was markedly shifted to 18.2 minutes. This correlates with the near half maximal filling that is known to occur within the four to five Ca^{2+} sites of the Gla domain [43]. A further and substantial shift was observed at the supra-physiologic level of 5 mM Ca^{2+} (Fig. 5.3A: curve 4) resulting in a longer residence time of 18.6 minutes. When FIX was chromatographed at 10 and 15 mM Ca^{2+}, similar residence time shifts of about 19 and 19.05 minutes were obtained (Fig. 5.3A: curves 5 and 6, respectively).

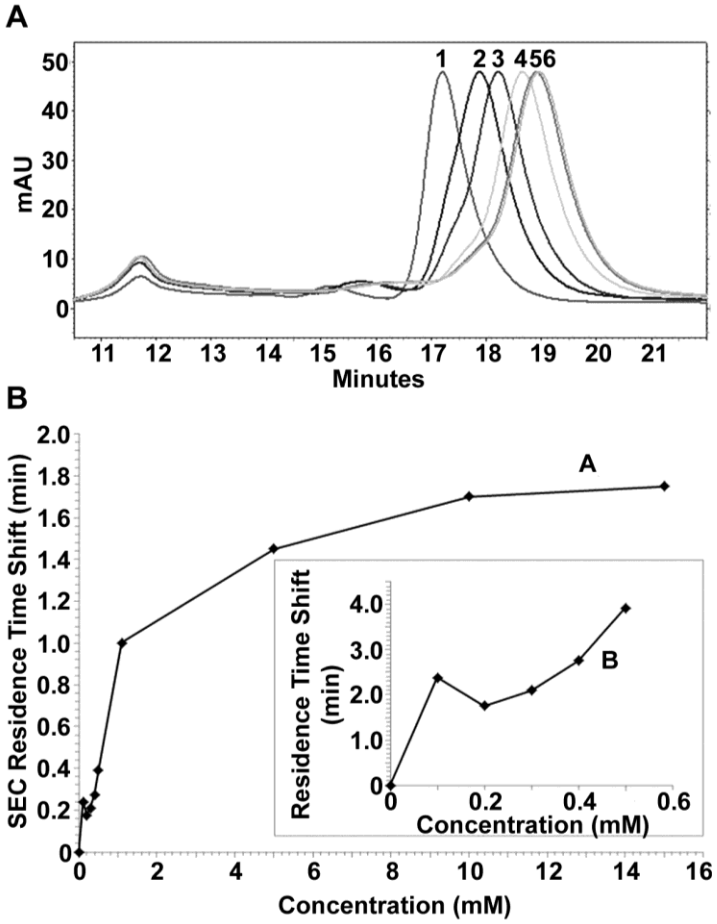

Figure 5.3 HPSEC residence time behavior of FIX in the presence of $CaCl_2$ only. In each case, amount of FIX injected was 100 µg. A) Curve 1: no divalent metal, Curve 2: 0.5 mM $CaCl_2$, Curve 3: 1.1 mM $CaCl_2$, Curve 4: 5 mM $CaCl_2$, Curve 5: 10 mM $CaCl_2$, Curve 6: 15 mM $CaCl_2$. B) Net residence time shift in the HPSEC residence time by FIX with change in $CaCl_2$ concentration in the range from 0 - 15 mM; *inset*, magnified view of residence time shift induced in the range from 0 – 0.5 mM $CaCl_2$. Each data point condition was performed in triplicate with a standard deviation <0.016 minutes.

Relative to that of a chelated environment, two distinct Ca^{2+}-specific compaction regimes are apparent in a plot of the net residence time shift versus Ca^{2+} concentration (Fig. 5.3B). A compaction regime reflecting interactions with higher affinity Ca^{2+} sites is seen spanning the range of about 0.1 to 0.3 mM Ca^{2+} (Fig. 5.3B: inset plot**).** Thereafter, a

shift occurs at about 0.3 to 5 mM which is consistent with the past reported filling of divalent metal sites within the Gla domain. The Gla sites have lower avidity for Ca^{2+} than each of the individual sites occurring within the catalytic [22, 43] and EGF1-like domains [21]. Thus, the compaction behavior of FIX observed at supra-physiologic levels of Ca^{2+} is likely the combined filling of both high avidity Ca^{2+}-specific sites in the EGF-like and protease domains along with the lower avidity Ca^{2+} sites of the Gla domain. It must be noted that in the absence of Mg^{2+}, all sites are occupied by Ca^{2+} at ≥2 mM [11].

Mg^{2+}-specific compaction of FIX observed by HPSEC

We investigated the effect on FIX macromolecular size caused by the filling of divalent metal specific sites when chromatographed at physiologic pH and various levels of Mg^{2+} alone using HPSEC. Based upon our molecular modeling and structure of FXa in the presence of Mg^{2+} only, the effect on molecular size is expected to be less for Mg^{2+} than Ca^{2+} both due to the positioning [9-11] and the presence of only four (number 1,4,7, and 8) Mg^{2+}-sites in the Gla domain of FIX [46]. The HPSEC chromatographic profiles of FIX in the presence of Mg^{2+} alone are shown in Fig. 5.4A. In these experiments, a baseline residence time of about 17.0 minutes was obtained for the elution peak of FIX under chelating conditions (Fig. 5.4A: curve 1). The presence of the physiologic level of 0.6 mM Mg^{2+} resulted in a small but significant residence time shift to a longer time of 17.3 minutes (Fig. 5.4A: curve 2). Past studies have shown that all four Mg^{2+}-specific sites within the core Gla domain of FIX (three in other VKD coagulation proteins and Protein C) are at least half maximally filled at physiologic levels of Mg^{2+} [47]. At supra-physiologic Mg^{2+} concentrations of 5, 10 and 15 mM Mg^{2+} the residence time further shifted to 17.6, 17.7, and 17.7 minutes, respectively (Fig. 5.4A: curves 3, 4, and 5

respectively). The asymptotic behavior of the response to supra-physiologic levels of Mg^{2+} is easily seen in a plot of the net residence time shift versus Mg^{2+} concentration (Fig. 5.4B). A much smaller compaction resulted when FIX was chromatographed in the presence of Mg^{2+} versus Ca^{2+} alone. This reduction in compaction response is consistent with the peripheral position and lesser number of Mg^{2+} sites within the core Gla domain (Fig. 5.1B).

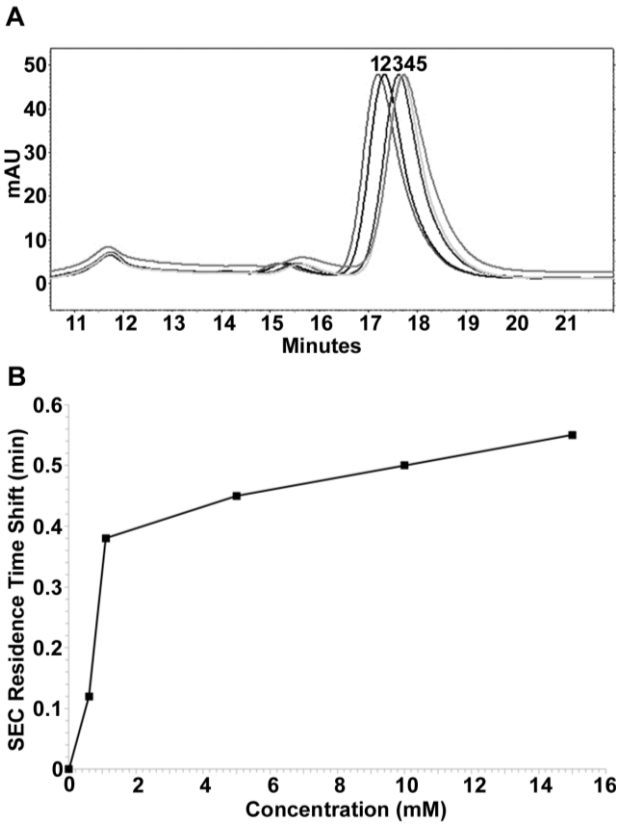

Figure 5.4. HPSEC residence time behavior of FIX in the presence of $MgCl_2$ only. In each case, the amount of FIX injected was 100 µg. A) Curve 1: no divalent metal, Curve 2: 0.6 mM $MgCl_2$, Curve 3: 5 mM $MgCl_2$, Curve 4: 10 mM $MgCl_2$, Curve 5: 15 mM $MgCl_2$. B) Net residence time shift in the HPSEC residence time by FIX with change in $MgCl_2$ concentration in the range from 0 - 15 mM. Each data point condition was performed in triplicate with a standard deviation <0.016 minutes.

FIX compaction resulting from presence of both Mg^{2+} and Ca^{2+} observed by HPSEC

The chromatographic data obtained in the presence of Ca^{2+} or Mg^{2+} alone showed that two different extents of compaction exist that are consistent with the highly Ca^{2+}- or Mg^{2+}-specific nature of the divalent metal binding sites within FIX. We investigated the interdependence of the compacted conformation resulting from the presence of both divalent metals: Fig. 5.5 shows the HPSEC chromatographic profile of FIX in the presence and absence of both physiologic levels Ca^{2+} and Mg^{2+} as well as presence of Ca^{2+} or Mg^{2+} alone at physiologic levels. We observed that the FIX residence time in the presence of both Mg^{2+} and Ca^{2+} at physiologic conditions (Fig. 5.5: Curve 4) was longer than that obtained in the presence of no divalent metal (Fig. 5.5: curve 1), 0.5 mM Mg^{2+} alone FIX (Fig. 5.5: curve 2) and 1.1 mM Ca^{2+} alone (Fig. 5.5: curve 3). While the residence time for Mg^{2+} is much smaller than for Ca^{2+} alone, the SEC residence time shift resulting from the simultaneous presence of both divalent metals is essentially additive. With respect to the Gla domain, this indicates that at physiologic levels of Mg^{2+} and Ca^{2+}, there is little competition between divalent metal ions for sites that induce compaction. This is consistent with the compaction predicted by our molecular modeling (Fig. 5.1) where the divalent metal sites 2, 3, 5, and 6 of FIX of the Gla domain are occupied by Ca^{2+} while sites 1, 4, 7 and 8 are occupied by Mg^{2+} [6, 9-11]. In contrast, the additive effect on compaction in the presence of physiological levels of both Ca^{2+} and Mg^{2+} was not detected by AUC. Previous literature on the effect of calcium on factor IX detected an expansion in FIX when calcium concentration was raised [30] By removing the effects of increased concentration and the corresponding aggregation, this new data reveals the compaction of FIX due to the filling of metal binding sites.

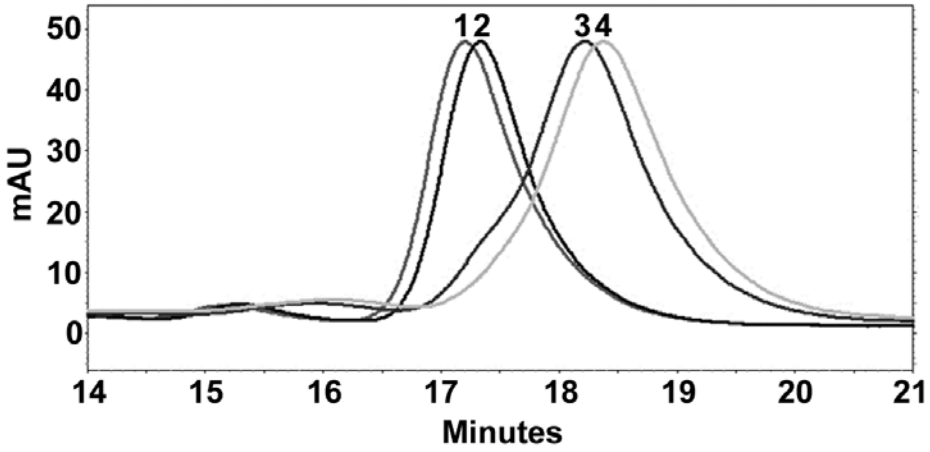

Figure 5.5. HPSEC residence time behavior of FIX in the presence of physiologic levels of both $CaCl_2$ and $MgCl_2$. Curve 1: no divalent metal, Curve 2: 0.6 mM $MgCl_2$, Curve 3: 1.1 mM $CaCl_2$, Curve 4: 1.1 mM $CaCl_2$ & 0.6 mM $MgCl_2$. Each data point condition was performed in triplicates with a standard deviation <0.016.

It is noted that the physiologic significance of the compaction of FIX resulting from the filling of the divalent metal binding sites within the Gla domain is profoundly embodied by the organization and formation of the ω-loop. The ω-loop is clearly seen in Fig. 5.1B. Divalent metal sites 2 to 6 strongly affect the positioning of the ω-loop which spans amino acids 1-14 and is central to phospholipid binding. Upon binding of phospholipid, site 4 is converted from a Mg^{2+} to a Ca^{2+} site, which results in profound repositioning of the ω-loop to the interior of the Gla domain [6, 9-11]. Supra-physiologic concentrations of Ca^{2+} can also result in the filling of site 4 by Ca^{2+} and a repositioning of the ω-loop.

Analytical ultracentrifuge studies of the compaction of pd-FIX induced by divalent metals

The HPSEC results presented above indicate a divalent cation induced compaction of FIX. We use AUC to both confirm the general compaction phenomena

and to calibrate the observed HPSEC chromatographic behavior for the correlative estimation [48-50] of the Stokes hydrodynamic radius (R) at the divalent metal ion concentrations studied here. It is important to note that past AUC studies of VKD coagulation proteins in the presence and absence of divalent metal did not statistically evaluate compaction phenomena, but were specifically used for the purpose of examining the presence or absence of aggregation. Table 5.1 provides the sedimentation coefficient (s) and calculated R values which were obtained by AUC for FIX in the absence and presence of physiologic levels of Ca^{2+} and Mg^{2+}. R is inversely proportional to the sedimentation coefficient, $S_{20,w}$, where compaction of the FIX increases the sedimentation coefficient. Specifically, the sedimentation coefficient s was used to calculate the Stokes Radius defined by the relationship:

$$s = [(M)(1-\tilde{v})(\rho)] / [(N)(6\pi)(\eta)(R)]$$

where M is the molecular weight, $\tilde{v}$ is the partial specific volume, ρ is the solvent density, N is Avagadro's Number and η is the viscosity [51].

Table 5.1. Sedimentation coefficients and estimated Stokes radii from analytical centrifugation of FIX. The sedimentation coefficient S is given for FIX centrifuged in the presence of EDTA, Ca^{2+} and/or Mg^{2+}.

Solvent[1]	$S_{20,w}$ (Svedberg)	Stokes Radius (nm)
10 mM EDTA[2]	3.71	4.36[a]
10 mM EDTA	3.72	4.35[a]
10 mM EDTA	3.72	4.35[a]
0.6 mM $MgCl_2$	3.82	4.24
0.6 mM $MgCl_2$ + 1.1 mM $CaCl_2$	3.83	4.23
0.3 mM $CaCl_2$	3.82	4.24
1.1 mM $CaCl_2$	3.85	4.21[a]
3.0 mM $CaCl_2$	3.89	4.16

[a]Used to determine coefficient of the SEC correlation by methods developed in Laurent and Killander (1964).

[1] The buffer contained 50 mM Tris, 0.15 M NaCl, pH 7.5 and the indicated reagent.

[2] Molecular weight of 62,800 Da and a partial specific volume of 0.708 for FIX were used in these calculations.

We observed an $S_{20,w}$ of 3.72 ± 0.006 Svedburgs (n=3) by AUC in 10 mM EDTA at 0.3 mg FIX/mL and this translates to an estimated R= 4.35 nm ± 0.006. Previously reported $S_{20,w}$ values were 4.17 Svedburgs for FIX measured in the presence of 2 mM EDTA and also for 2.5 mM Ca^{2+} [30]. Thus the value was larger than those reported here and the previous studies made no conclusions concerning the compaction induced by the presence of Ca^{2+}. Since Ca^{2+} was a predominant and largely independent variable associated with the observed compaction by HPSEC, we used the AUC observations obtained for 1.1 mm Ca^{2+} with or without Mg^{2+} as a statistical group for estimating its impact of the presence of Ca^{2+} on $S_{20,w}$**:** we obtained a value $S_{20,w}$ = 3.84 ± 0.014 Svedburgs (n=2) corresponding to R= 4.22 nm ± 0.014. Thus, the sedimentation obtained

by AUC supports a predominant and stark compaction effect by Ca^{2+} both observed by HPSEC and predicted by molecular modeling.

Estimation of the amount of compaction observed by SEC

We further used the values of R obtained by AUC for metal-free FIX (in EDTA) and the data point at presence of 1.1 mm Ca^{2+} to estimate column parameters needed to predict the change in R from all other HPSEC data. The correlation of Fish et al. [50] has been used to efficiently predict the R value behavior of many different proteins using size exclusion chromatographic behavior found in agarose [49] and Sepharose [48, 49] packings as well as the TSK 3000SW used in this study [52]. Fig. 5.6 shows a strong interpolative consistency for the R vs. Ca^{2+} concentration behavior using HPSEC values in the range of 0 to 1.1 mM Ca^{2+}. These values were very consistent with our experimental values obtained by AUC that were not used to predict column parameters. At a physiologic level of Ca^{2+} which is equal to or greater than that needed for half maximal filling of Ca^{2+} specific sites in the Gla domain, the overall change in R of FIX is about 2.7 % relative to the metal-free FIX. Furthermore, the HPSEC behavior that results from the complete filling of Ca^{2+} sites at supraphysiologic levels predicted an asymptotic compaction of about 5.6% change in R. The change in the radius of gyration predicted by our modeling was similar at about 5%. In summary, the quantitative compaction phenomena in the range of 0 to 15 mM Ca^{2+} measured by both AUC, HPSEC and the modeling of this work with consistent with each other and also the complete Ca^{2+} site filling within the Gla domain from equilibrium dialysis [43].

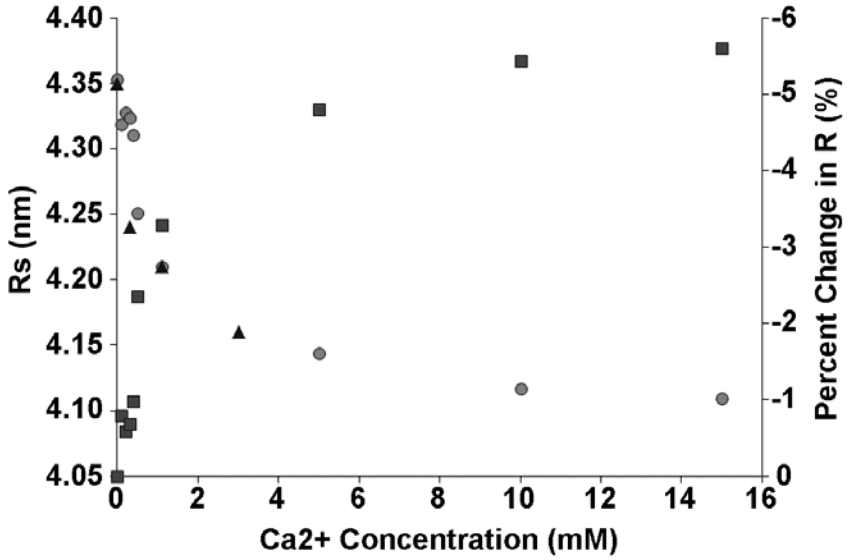

Figure 5.6. Estimated $CaCl_2$-dependent change in Stokes radius of FIX as measured by HPSEC. R values by HPSEC made by the correlation method of Laurent and Killander [33], Acker [34], and Fish and Reynolds et al. [35]. Circled data points at 1.1 mM $CaCl_2$ and 0 mM divalent metal indicates the experimental SEC and AUC values, which were used to calibrate column parameters. ● SEC Value; ▲ AUC Value; ■ Percent change in R estimated by SEC (%).

5.5 Conclusion

This is first direct observation of the VKD coagulation protein compaction. HPSEC was used to obtain a quantitative, solution phase assessment of the conformational effects on the overall macromolecular size of FIX that can be attributed to the independent filling of the high affinity Ca^{2+} specific sites of the EGF1-like and protease domains along with the Ca^{2+} and Mg^{2+} sites of the Gla domain. Molecular modeling indicates that the predominant source of compaction results from the change in conformation for the Gla domain and secondarily from the EGF1-like domain due to site filling by Ca^{2+}. A similar compaction likely occurs with other VKD coagulation proteins due to the well conserved core Gla domain of this family.

5.6 Acknowledgements

I would like to thank Dr. Messer, Dr. Vadivel, Dr. Philips, and Dr. Bajaj for their work on molecular modeling.

5.7 References

1 Furie B, Furie BC. The molecular basis of blood coagulation. *Cell*. 1988; 53: 505-18.

2 Davie EW, Fujikawa K, Kisiel W. The coagulation cascade: initiation, maintenance, and regulation. *Biochemistry*. 1991; 30: 10363-70.

3 Vadivel K, Schmidt AE, Marder VJ, Krishnaswamy S, Bajaj SP. Structure and function of vitamin K-dependent coagulant and anticoagulants proteins. In: Marder VJ, Aird WC, Bennett HS, Schulman S, White II GC, eds. *Hemostasis and Thrombosis*. Philadelphia, PA: Lippincott Williams and Willkins, 2013.

4 Soriano-Garcia M, Padmanabhan K, De Vos A, Tulinsky A. The calcium ion and membrane binding structure of the Gla domain of calcium-prothrombin fragment 1. *Biochemistry*. 1992; 31: 2554-66.

5 Freedman SJ, Furie BC, Furie B, Baleja JD. Structure of the calcium ion-bound gamma-carboxyglutamic acid-rich domain of factor IX. *Biochemistry*. 1995; 34: 12126-37.

6 Banner DW, D'Arcy A, Chene C, Winkler FK, Guha A, Konigsberg WH, Nemerson Y, Kirchhofer D. The crystal structure of the complex of blood coagulation factor VIIa with soluble tissue factor. *Nature*. 1996; 380: 41-6.

7 Mizuno H, Fujimoto Z, Atoda H, Morita T. Crystal structure of an anticoagulant protein in complex with the Gla domain of factor X. *Proceedings of the National Academy of Sciences*. 2001; 98: 7230-4.

8 Huang M, Rigby AC, Morelli X, Grant MA, Huang G, Furie B, Seaton B, Furie BC. Structural basis of membrane binding by Gla domains of vitamin K–dependent proteins. *Nature Structural & Molecular Biology*. 2003; 10: 751-6.

9 Shikamoto Y, Morita T, Fujimoto Z, Mizuno H. Crystal structure of Mg2+- and Ca2+-bound Gla domain of factor IX complexed with binding protein. *Journal of Biological Chemistry*. 2003; 278: 24090-4.

10 Bajaj SP, Schmidt AE, Agah S, Bajaj MS, Padmanabhan K. High resolution structures of p-aminobenzamidine- and benzamidine-VIIa/soluble tissue factor: unpredicted conformation of the 192-193 peptide bond and mapping of Ca2+, Mg2+, Na+, and Zn2+ sites in factor VIIa. *J Biol Chem*. 2006; 281: 24873-88. 10.1074/jbc.M509971200.

11 Vadivel K, Agah S, Messer AS, Cascio D, Bajaj MS, Krishnaswamy S, Esmon CT, Padmanabhan K, Bajaj SP. Structural and Functional Studies of γ-Carboxyglutamic Acid Domains of Factor VIIa and Activated Protein C: Role of Magnesium at Physiological Calcium. *Journal of molecular biology*. 2013.

12 Freedman SJ, Furie BC, Furie B, Baleja JD. Structure of the metal-free gamma-carboxyglutamic acid-rich membrane binding region of factor IX by two-dimensional NMR spectroscopy. *J Biol Chem*. 1995; 270: 7980-7.

13 Lewis RM, Furie BC, Furie B. Conformation-specific monoclonal antibodies directed against the calcium-stabilized structure of human prothrombin. *Biochemistry*. 1983; 22: 948-54.

14 Wakabayashi K, Sakata Y, Aoki N. Conformation-specific monoclonal antibodies to the calcium-induced structure of protein C. *Journal of Biological Chemistry*. 1986; 261: 11097-105.

15 Orthner C, Madurawe RD, Velander WH, Drohan WN, Battey F, Strickland D. Conformational changes in an epitope localized to the NH2-terminal region of protein C. Evidence for interaction of protein C domains. *Journal of Biological Chemistry*. 1989; 264: 18781-8.

16 Huang M, Furie BC, Furie B. Crystal structure of the calcium-stabilized human factor IX Gla domain bound to a conformation-specific anti-factor IX antibody. *J Biol Chem*. 2004; 279: 14338-46. 10.1074/jbc.M314011200.

17 de Courcy B, Pedersen L, Parisel O, Gresh N, Silvi B, Pilmé J, Piquemal J-P. Understanding Selectivity of Hard and Soft Metal Cations within Biological Systems Using the Subvalence Concept. 1. Application to Blood Coagulation: Direct Cation− Protein Electronic Effects versus Indirect Interactions through Water Networks. *Journal of chemical theory and computation*. 2010; 6: 1048-63.

18 Wolberg AS, Li L, Cheung WF, Hamaguchi N, Pedersen LG, Stafford DW. Characterization of gamma-carboxyglutamic acid residue 21 of human factor IX. *Biochemistry*. 1996; 35: 10321-7. 10.1021/bi960502i.

19 Gillis S, Furie BC, Furie B, Patel H, Huberty MC, Switzer M, Barry Foster W, Scoble HA, Bond MD. γ-Carboxyglutamic acids 36 and 40 do not contribute to human factor IX function. *Protein science*. 1997; 6: 185-96.

20 Handford PA, Baron M, Mayhew M, Willis A, Beesley T, Brownlee GG, Campbell ID. The first EGF-like domain from human factor IX contains a high-affinity calcium binding site. *EMBO J*. 1990; 9: 475-80.

21 Rao Z, Handford P, Mayhew M, Knott V, Brownlee GG, StuartZ D. The structure of a Ca< sup> 2+</sup>-binding epidermal growth factor-like domain: Its role in protein-protein interactions. *Cell*. 1995; 82: 131-41.

22 Bajaj SP, Sabharwal AK, Gorka J, Birktoft JJ. Antibody-probed conformational transitions in the protease domain of human factor IX upon calcium binding and zymogen activation: putative high-affinity Ca(2+)-binding site in the protease domain. *Proc Natl Acad Sci U S A*. 1992; 89: 152-6.

23 Zögg T, Brandstetter H. Structural basis of the cofactor-and substrate-assisted activation of human coagulation factor IXa. *Structure*. 2009; 17: 1669-78.

24 Aktimur A, Gabriel MA, Gailani D, Toomey JR. The factor IX γ-carboxyglutamic acid (Gla) domain is involved in interactions between factor IX and factor XIa. *Journal of Biological Chemistry*. 2003; 278: 7981-7.

25 Ndonwi M, Broze GJ, Agah S, Schmidt AE, Bajaj SP. Substitution of the Gla Domain in Factor X with That of Protein C Impairs Its Interaction with Factor VIIa/Tissue Factor Lack Of Comparable Effect By Similiar Substitution In Factor IX. *Journal of Biological Chemistry*. 2007; 282: 15632-44.

26 Sekiya F, Yamashita T, Atoda H, Komiyama Y, Morita T. Regulation of the tertiary structure and function of coagulation factor IX by magnesium (II) ions. *Journal of Biological Chemistry*. 1995; 270: 14325-31.

27 Nelsestuen G. Role of gamma-carboxyglutamic acid. An unusual protein transition required for the calcium-dependent binding of prothrombin to phospholipid. *Journal of Biological Chemistry*. 1976; 251: 5648-56.

28 Prendergast FG, Mann K. Differentiation of metal ion-induced transitions of prothrombin fragment 1. *Journal of Biological Chemistry*. 1977; 252: 840-50.

29 Bajaj SP. Cooperative Ca2+ binding to human factor IX. Effects of Ca2+ on the kinetic parameters of the activation of factor IX by factor XIa. *J Biol Chem*. 1982; 257: 4127-32.

30 Amphlett GW, Kisiel W, Castellino FJ. The interaction of Ca2+ with human Factor IX. *Archives of biochemistry and biophysics*. 1981; 208: 576-85.

31 Nelsestuen GL, Resnick RM, Wei GJ, Pletcher CH, Bloomfield VA. Metal ion interactions with bovine prothrombin and prothrombin fragment 1. Stoichiometry of binding, protein self-association, and conformational change induced by a variety of metal ions. *Biochemistry*. 1981; 20: 351-8.

32 Amphlett GW, Byrne R, Castellino FJ. The binding of metal ions to bovine factor IX. *J Biol Chem*. 1978; 253: 6774-9.

33 Amphlett GW, Byrne R, Castellino FJ. The binding of calcium to the activation products of bovine factor IX. *J Biol Chem*. 1979; 254: 6333-6.

34 Butenas S, Lawson JH, Kalafatis M, Mann KG. Cooperative interaction of divalent metal ions, substrate, and tissue factor with factor VIIa. *Biochemistry*. 1994; 33: 3449-56.

35 Amphlett GW, Kisiel W, Castellino FJ. Interaction of calcium with bovine plasma protein C. *Biochemistry*. 1981; 20: 2156-61.

36 Stafford WF, 3rd. Boundary analysis in sedimentation transport experiments: a procedure for obtaining sedimentation coefficient distributions using the time derivative of the concentration profile. *Analytical biochemistry*. 1992; 203: 295-301.

37 Cohn EJaE, J.T. Density and apparent specific volume of proteins. In: Edsall EJCaJT, ed. *Proteins, Amino Acids and Peptides as Ions and Dipolar Ions*. New York: Reinhold Publishing Corporation, 1943, 370-81.

38 Durschschlag H. Specific volumes of biological macromolecules and some other molecules of biological interest. . In: Hinz HJ, ed. *Thermodynamic Data for Biochemistry and Biotechnology*. Berlin: Springer-Verlag, 1986, 45-128.

39 Perera L, Darden TA, Pedersen LG. Modeling human zymogen factor IX. *Thromb Haemost*. 2001; 85: 596-603.

40 Eswar N, Webb B, Marti-Renom MA, Madhusudhan MS, Eramian D, Shen MY, Pieper U, Sali A. Comparative protein structure modeling using Modeller. *Current protocols in bioinformatics / editoral board, Andreas D Baxevanis [et al]*. 2006; Chapter 5: Unit 5 6. 10.1002/0471250953.bi0506s15.

41 Brooks BR, Bruccoleri RE, Olafson BD, States DJ, Swaminathan S, Karplus M. Charmm - a Program for Macromolecular Energy, Minimization, and Dynamics Calculations. *J Comput Chem*. 1983; 4: 187-217. DOI 10.1002/jcc.540040211.

42 Li L, Darden TA, Freedman SJ, Furie BC, Furie B, Baleja JD, Smith H, Hiskey RG, Pedersen LG. Refinement of the NMR solution structure of the gamma-carboxyglutamic acid domain of coagulation factor IX using molecular dynamics simulation with initial Ca2+ positions determined by a genetic algorithm. *Biochemistry*. 1997; 36: 2132-8. 10.1021/bi962250r.

43 Agah S, Bajaj SP. Role of magnesium in factor XIa catalyzed activation of factor IX: calcium binding to factor IX under physiologic magnesium. *Journal of thrombosis and haemostasis : JTH*. 2009; 7: 1426-8. 10.1111/j.1538-7836.2009.03506.x.

44 Messer A, Velander W, Bajaj S. Contribution of magnesium in binding of factor IXa to the phospholipid surface: implications for vitamin K-dependent coagulation proteins. *Journal of Thrombosis and Haemostasis*. 2009; 7: 2151-3.

45 Samis JA, Ramsey GD, Walker JB, Nesheim ME, Giles AR. Proteolytic processing of human coagulation factor IX by plasmin. *Blood*. 2000; 95: 943-51.

46 Wang SX, Hur E, Sousa CA, Brinen L, Slivka EJ, Fletterick RJ. The extended interactions and Gla domain of blood coagulation factor Xa. *Biochemistry*. 2003; 42: 7959-66.

47 Deerfield D, Olson D, Berkowitz P, Byrd P, Koehler K, Pedersen L, Hiskey R. Mg (II) binding by bovine prothrombin fragment 1 via equilibrium dialysis and the relative roles of Mg (II) and Ca (II) in blood coagulation. *Journal of Biological Chemistry*. 1987; 262: 4017-23.

48 Laurent TC, Killander J. A theory of gel filtration and its exeperimental verification. *Journal of Chromatography A*. 1964; 14: 317-30.

49 Ackers G. A new calibration procedure for gel filtration columns. *Journal of Biological Chemistry*. 1967; 242: 3237-8.

50 Fish WW, Reynolds JA, Tanford C. Gel Chromatography Of Proteins In Denaturing Solvents Comparison Between Sodium Dodecyl Sulfate and Guanidine Hydrochloride as Denaturants. *Journal of Biological Chemistry*. 1970; 245: 5166-8.

51 Cole JL, Lary JW, P Moody T, Laue TM. Analytical ultracentrifugation: sedimentation velocity and sedimentation equilibrium. *Methods in cell biology*. 2008; 84: 143-79.

52 Corbett RJ, Roche RS. Use of high-speed size-exclusion chromatography for the study of protein folding and stability. *Biochemistry*. 1984; 23: 1888-94.

Chapter 6:

A Novel High Specific Activity, Monomeric, Recombinant Factor XIIIA1 with Improved Crosslinking and Thromboelastic Kinetics

Nicholas Vanderslice,[*] Jennifer Calcaterra,[*] Mehmet Inan,[*] Vijay P. Jain,[*] William H.Velander[*]

[*] Department of Chemical & Biomolecular Engineering, University of Nebraska, Lincoln, NE 68588-0643

6.1 Abstract

Human factor XIII (FXIII) is activated by thrombin during fibrin formation, releasing a dimeric, transglutaminase (FXIIIA2a) which both converts fibrin into a crosslinked, viscoelastic barrier and covalently anchors it to wound surfaces. Past examples of expression in yeast resulted in a secreted dimeric recombinant (r-) FXIIIA2 zymogen. An expression cassette using the cDNA for r-FXIII catalytic subunit A-chain (r-FXIIIA) with His-tag sequences at both amino- and carboxy-terminii was inserted into *Pichia pastoris*. The r-FXIIIA was recovered from cell lysate, purified by immobilized metal affinity chromatography (IMAC), and evaluated by SDS-PAGE, Western analysis, amino terminal sequencing, size exclusion chromatography (SEC), and a chromogenic assay for transglutaminase activity. We characterized the kinetic and crosslinking properties of monomeric, recombinant FXIII subunit A (r-FXIIIA1) for both plasma-derived fibrinogen and recombinant fibrinogen purified from the milk of transgenic cows. *Pichia pastoris* novelly formed an 81 kDa monomeric r-FXIIIA (r-FXIIIA1) while being expressed at >0.25 mg per gram of fermentation cell mass. SEC showed monomeric r-FXIIIA1 was the predominant purified species where SDS-PAGE, amino terminal sequencing, and anti-His-tag Western showed that the amino terminal His-tag activation peptide sequence was removed; however, the carboxy-terminal His- and myc-tags remained

in place, forming an artificial, kinetically-favorable thrombin-sensitive activation peptide. The r-FXIIIA1 had a ≥2-fold specific activity by chromogenic assay than plasma-derived (pd-) FXIIIA2, and thromboelastography determined that fibrin sealant formed with the r-FXIIIA1 reached the same maximum amplitude fibrin sealant without FXIII 15 minutes faster. The unique *in situ* processing of the r-FXIII catalytic subunit to form a fully functional r-FXIIIA1 by the *P. pastoris* production system can potentially provide a dose-dependent abundant source of transglutaminase with higher specific activity and kinetically enhanced crosslinking.

6.2 Introduction

Human factor XIII (FXIII) is a coagulation protein that circulates in plasma and is also displayed on the surface of platelets [1]. FXIII performs the essential hemostatic tasks of intrachain crosslinking needed to form insoluble fibrin and the concomitant anchoring of the fibrin hemostatic plug to wound surfaces. The transglutaminase activity of enzymatically activated FXIII (FXIIIa) serves to crosslink other proteins to fibrinogen (FI) or fibrin. Some of these proteins are necessary for clot stabilization and adherence of the clot to the lesions in blood vessel walls [2] and include: α2-antiplasmin and fibrinogen to confer resistance to fibrin clot lysis by plasmin [3], fibronectin and fibrin for cell recruitment during wound healing [4-6], fibrin and extracellular matrix collagen [4, 7], von Willebrand factor and fibrin and/or collagen [8, 9] associated with activated platelet wound adhesion.

Plasma-derived (pd-) FXIII is a 326 kDa tetrameric, non-covalent complex consisting of a homodimer of two identical catalytic A-chains (FXIIIA2) that is packaged by two identical B-chains [2, 10-12]. The A2 subunit alone is displayed on the surface of platelets as part of the mechanism to incorporate both fibrin and activated platelets into primary hemostatic plug. The 82 kDa A-chain [13-15] is hydrophobic and synthesized by hepatocytes, monocytes and megakaryocytes [13-15]. In the case of plasma-borne tetrameric FXIII, the B-chains are secreted into plasma by hepatocytes as single chains, where some form complexes with the A-chain [15]

and others circulate freely [2]. Each chain in the A2 subunit of plasma or platelet FXIII can be activated by thrombin to form activated FXIIIA2 (FXIIIA2a) [1, 16-18]. The enzymatic activation of the A2 by thrombin releases a 4.5 kDa activation peptide [19] after cleavage at Arg37-Gly38 [20, 21]. The A2 of tetrameric FXIII is stabilized by the B-chains and therefore are more slowly activated by thrombin than that of A2 displayed on platelet surfaces [22-26]. Specifically, the interactions of the B-chains with fibrin and calcium ions cause the dissociation of the B-chain to form free A2 prior to its activation [17, 21, 22, 27-29]. Feedback control over FXIIIA2a activity is made by further proteolysis by thrombin which cleaves the A-chain at Lys513 resulting in two fragments of 25 and 54 kDa [12], resulting in FXIIIA2a inactivation. Human recombinant (r-) FXIIIA2 has been produced in *Saccharomyces cerevisiae* [30-32] for use in FXIII deficiency replacement therapy. It has also been produced in *Pichia pastoris* [33] and in transgenic plants [34] using the cDNA of FXIIIA. The purified r-FXIIIA2 obtained from both plant and *S. cerevisiae* cell lysates were confirmed to be dimeric assemblies by measurements using analytical ultracentrifugation. The FXIIIA cDNA expressed in *P. pastori*s was secreted but the extent of assembly into a dimer was not reported. In each case, the activation of the r-FXIIIA2 to form r-FXIIIA2a by human thrombin and then subsequent transglutaminase activity was demonstrated. The *S. cerevisae* derived zymogen r-FXIIIA2 was shown to restore clot strength and provide lysis resistance *in vivo* [35]. This past study demonstrated that parenterally administered, therapeutic grade r-FXIII could be produced using intracellular expression in yeast fermentation. However, r-FXIIIa has uses in recombinant fibrin sealants [36, 37]. We report on the production of monomeric, r-FXIIIA1 (r-FXIIIA1) containing an artificial activation peptide using intracellular expression in Pichia pastoris.

6.3 Materials and Methods

Materials

Plasma-derived human FXIII (pd-FXIII), human thrombin (pd-FIIa), and plasma-derived fibrinogen (pd-FI) were bought from Enzyme Research Labs (South Bend, IN). Recombinant human thrombin (r-FIIa) was purchased from ZymoGenetics (Seattle, WA). Apolipoprotein E (APOE) recombinant human protein was purchased from Life Technologies (Grand Island, NY). Purified recombinant fibrinogen (r-FI), expressed in the milk of transgenic cows, and was obtained from Pharming Group NV (Leiden, Netherlands). PPACK was purchased from Haematologic Technologies (Essex Junction, VT).

Expression vector construction and expression

The human Ultimate ORF clone containing the human coagulation FXIIIA1 cDNA in the pENTR^{TM}221 vector was purchased from Invitrogen (Clone ID: IOH11901, Carlsbad CA). The following primers were used to subclone the FXIIIA1 cDNA into the pPICZA extracellular Pichia expression vector containing the α-secretion signal sequence:

Forward, 5'-
CCAATTGATGCATCATCATCATCATCATTCAGAAACTTCCAGGACCGC-3'
Reverse, 5'-GCGGCCGCTCACATGGAAGGTCGTCTTTGAATC-3'.

The forward primer introduced a methionine and six histidine amino acids (His-tag) at the N-terminal of mature FXIIIA1 peptide. The PCR product was digested with MfeI and NotI and subcloned into pPICZA, which was digested with the same enzymes (Fig. 6.1A). The 3'-His-tag encoding site within the pPICZA expression vector was retained

after insertion of the FXIIIA1 cDNA (Fig. 6.1). The sequence of the PCR amplified DNA of the yeast insertion indicated that the full and native FXIIIA1 cDNA was present with both 5' and 3' His-tag sequences in place. One of the confirming plasmid pPICZA-FXIIIA1 was linearized with PmeI and transformed into Pichia pastoris X-33 host strain and copy number of the clones was determined. Varying copy number clones were screened in a shake flask culture to confirm intracellular production of FXIIIA protein. The highest-producing clone was scaled up to 5 L bench scale. A fed-batch fermentation protocol was followed to optimize FXIIIA1 production as described by Zhang et al. [38]. At the end of the fermentation process the cells were separated by centrifugation (6,000xg) and the pellet was stored at -80^{o}C.

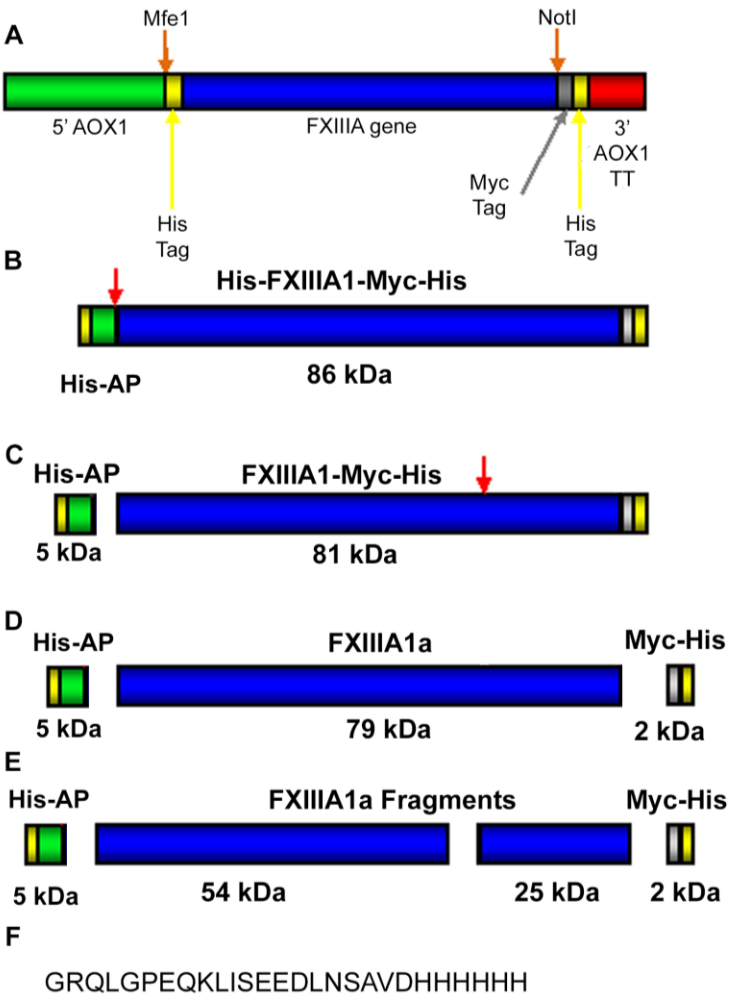

Figure 6.1. Schematic description of parent r-FXIIIIA1 and observed cleavage products with the molecular weights of observed cleavage products. (A) Schematic of vector pPICZA-FXIIIA. FXIIIA cDNA (2199 bases) with a His-tag (17 bases) on the N-terminal was inserted into the pPICZA vector containing a 5' AOX1 promoter (941 bases), multiple cloning site (79 bases), Myc-tag (32 bases), His-tag (17 bases) and 3' AOX1 transcription termination region (341 bases). The restriction enzyme sites utilized are shown with orange arrows. (B) Schematic of the expected r-FXIIIA expressed by yeast, (C) r-FXIIIA1 molecule purified from yeast cell lysate by IMAC, (D) cleavage products of r-FXIIIA1 when exposed to thrombin, and (E) degradation products of FXIIIA1 when exposed to r-FIIa. FXIIIA is composed of a His-tagged activation peptide (His-AP) (green, ~5.3 kDa) and the FXIIIa catalytic domain (blue, ~79 kDa). His-tags are designated in yellow (~0.8 kDa) and the Myc-tag in grey (~1.2 kDa). The known thrombin cleavage sites are indicated by red arrows. (F) Sequence of the C-terminal of r-FXIIIIA1a.

r-FXIIIA1 purification

Frozen cell paste was processed in 300 gram batches. Cells were lysed in three sets of 100 gram batches. 100 grams of cell paste were resuspended in 100 mL of cold lysis buffer (50 mM Tris-HCL, 10 mM $MgSO_4$, 1 mM EDTA, 10 mM potassium acetate, 1 mM DTT (DL-Dithiothreitol), 2 mM PMSF (phenylmethanesulphonylfluoride) in methanol, pH 9.5). 100 mL (250 g) of 0.5 mm glass beads (Biospec, Bartlesville, OK) were added. Surrounded by an ice bath, cells were lysed using a BeadBeater Blender (Biospec, Bartlesville, OK) with twenty 20-second on/off cycles. The cell lysate mixture was then centrifuged to remove cellular debris. The lysate from 300 grams of cell paste was combined and purified using the HisBind Purification Kit (EMD Chemicals, Inc., San Diego, CA) with 40 mL of resin slurry. Following purification by immobilized metal-chelate affinity chromatography (IMAC), the r-FXIIIA1 was diluted 2-fold in order to minimize aggregation and then dialyzed in 10 mM Tris-HCl, 0.1 mM EDTA, 60 μM polysorbate-20, pH 8.0 in snake-like dialysis membranes and the protein samples were filter-sterilized and concentrated using the Amicon tubes (Millipore, Billerica, MA). The purity of the sample was tested by SDS-PAGE (NuPAGE 12% Bis-Tris) (Life Technologies, Carlsbad, CA) and immunoblot. The concentration of r-FXIIIA1 was determined by standard Bicinconic Acid (BCA) methods [39].

Comparison of r-FXIIIA1 with pd-FXIII by SDS-PAGE and Western blot

Non-reduced and reduced FXIII samples (pd-FXIII and r-FXIIIA1) were evaluated by sodium dodecylsulfate-polyacrylamide gel electrophoresis (SDS-PAGE) on 4-12% NuPage® Bis-Tris gels (Life Technologies, Carlsbad, CA). Gels were then stained

with Colloidal Blue (Life Technologies) or electroblotted onto Immun-Blot™ polyvinylidene fluoride (PVDF) membranes (BioRad, Hercules, CA) for immunoblotting. Blots were probed with an anti-His-tag monoclonal antibody (Invitrogen, Carlsbad CA) and anti-human FXIII Subunit A polyclonal antibody (US Biological, Swampscott, MA).

Size exclusion chromatography

Size exclusion chromatography (SEC) was used to characterize the extent of aggregation of the affinity purified r-FXIIIA1 though estimation of the Stokes radius (R_s) and the molecular weight [40]. Reference proteins of known R_s were used: Bovine serum albumin (Sigma, St. Louis, MO), human plasma-derived prothrombin, immunoglobulin A (IgA) (Sigma, St. Louis, MO) and immunoglobulin G (IgG) (Green Mountain Antibodies, Burlington, VT) were exchanged into 20 mM Tris-HCl, 200 mM NaCl, 60 μM Tween 20, pH 7.0. After being passed through a 0.20 μm nylon filter (Millipore, Billerica, MA), 0.5 mL of each sample were chromatographed through a TSK-G3000SW_{xL} (Tosoh Biosciences, South San Francisco, CA) column (14 mL, 30 cm length, 7.8 mm ID) attached to a Knauer HPLC System at 0.5 mL/min for 45 minutes and data were collected by a photodiode array (PDA) with a 1 mm flow cell and analyzed by EZChrom Elite software. The affinity purified r-FXIIIA1 (0.5 mL at 1.94 mg/mL) in 20 mM Tris-HCl, 200 mM NaCl, 60 μM Tween 20, pH 7.0 was also chromatographed using the same method. The EZChrom Elite software was used to overlay the tracings and match the heights of the primary peaks. The R_s and relative molecular weight (M_r) of affinity purified r-FXIIIA1 was estimated using the method of Laurent and Killander [40] using SEC retention times of reference proteins with known R_s values.

Amino acid Sequencing and Activation and inactivation of pd-FXIII and r-FXIIIA1 by r-FIIa

The activation and inactivation the r-FXIIIA1 by r-FIIa was evaluated by SDS-PAGE by a similar procedure previously described [30]. Reference pd-FXIII (final concentration: 0.31 mg/mL) was incubated with r-FIIa (0.03 U/mL) in Ringer's solution (155 mM NaCl, 5 mM KCl, 2 mM $CaCl_2$, 1 mM $MgCl_2$) at 37°C. Activation samples were incubated for 0, 0.5, 1.0, 1.5, 2, 3, 4 and 5 minutes. Inactivation samples were incubated for 2 seconds, 5, 15, 30, 60, 120, 240 and 360 minutes. Reactions were halted by the addition of NuPage® LDS sample buffer and NuPage® Sample Reducing buffer (β-mercaptoethanol) (Life Technologies, Carlsbad, CA). For the zero time point for the activation samples, FXIII and r-FIIa were added directly into sample buffer and reducing agent. Samples were evaluated by sodium dodecylsulfate-polyacrylamide (SDS-PAGE) gel electrophoresis on 4-12% NuPage® Bis-Tris gels. Gels were stained with Colloidal Blue or electroblotted onto PVDF membrane and stained with Colloidal Blue. Bands were excised and the first ten amino acids in the N-terminal were sequenced by Edman degradation with an Applied Biosystems 494 Procise automated sequencer. N-terminal sequencing was performed by the University of Nebraska Medical Center's Protein Structure Core Facility.

Chromogenic activity assay

The chromogenic activity assay was performed using a modified version of the procedure described in Ariëns et al. [39]. A 96-well polystyrene plate (Fisher, Pittsburgh, PA) was coated with pd-FI purified by EtOH precipitation (0.04 mg/mL) and then blocked with bovine serum albumin (10 mg/mL). Dilutions of pooled plasma from 10

donors (0, 0.0002, 0.0004, 0.0006, 0.0008 and 0.001) were added to some wells and used to create a standard curve assuming pd-FXIII content is 1 U/mL. Six dilutions of pure pd-FXIII (Enzyme Research Labs) and r-FXIIIA1 samples were added to the wells. Biotin-pentylamine (Life Technologies) (0.27 μM), dithiothreitol (0.10 mM), $CaCl_2$ (1 mM) and r-FIIa (1 U/mL) were added to the wells and incubated at room temperature for 25 min. Streptavidin-alkaline phosphatase (Sigma, St. Louis, MO) (2 μg/mL) was added and incubated at 37^{o}C for 60 min. Finally, p-nitrophenyl phosphate (1 mg/mL) in diethanolamine (1 M) was added and incubated at room temperature for 2 min. p-nitrophenol was detected at 405 nm. All samples were run in triplicate. Multiple dilutions of pd-FXIII and r-FXIIIA1 that fell within the standard curve range created with the plasma dilutions were used to estimate activity. The mean and standard deviation of activity estimates from multiple dilutions are reported.

FXIIIa catalyzed crosslinking of fibrin

Crosslinking of pd-FI purified by EtOH precipitation by r-FXIIIA1 was analyzed as previously described [41]. pd-FI (0.38 mg/mL) was incubated with and without r-FIIa (1 U/mL) and without added FXIII or with pd-FXIII, pd-FXIIIa, or r-FXIIIA1 (1.1 U/mL) in Ringer's solution for 0, 1, 2.5, 5, 10 and 15 minutes. pd-FXIIIa for the trial without thrombin was created by treating pd-FXIII with thrombin for 2.5 minutes and then inactivating the thrombin in a solution containing 0.02 mM PPACK. Crosslinking was examined by reducing SDS-PAGE gel electrophoresis (4-12% Bis-Tris NuPAGE) stained with Colloidal Blue (Life Technologies, Carlsbad, CA). The bands at approximately 130 and 150 kDa were excised and the first ten amino acids in the N-

terminal of each were sequenced by Edman degradation with an Applied Biosystems 494 Procise automated sequencer [36].

Dose Response

The crosslinking due to dosing of r-FXIIIA1 on r-FI and pd-FI by was analyzed as previously described [41]. pd-FI (9mg/mL) and r-FI (9 mg/mL) were incubated in Ringer's solution with FIIa (0.2 mg/mL) and with 0, 0.18, 0.36, and 0.53 mg/mL r-FXIIIa to initiate fibrin formation. The reaction was quenched with LDS and reducing buffer after 2.5 minutes. Crosslinking was examined by reducing SDS-PAGE gel electrophoresis (4-12% Bis-Tris NuPAGE) stained with Colloidal Blue (Life Technologies, Carlsbad, CA).

Viscoelastic characterization of fibrin crosslinking

Clot stiffness resulting from fibrin cross-linking of pd-FI by affinity purified r-FXIIIA1 was evaluated by thromboelastography (TEG) using a Thromboelastograph® (TEG®) Hemostasis System 5000 series (Haemoscope Corp., Niles, IL). Biotherapeutic grade fibrin sealant (Tisseel, Baxter) was formulated according label instructions. Fibrin sealant was transferred at 34 mg/mL FI and 9 mg/mL FI, based on a final volume of 360 µl, into a single-use TEG cup maintained at 37 ^{o}C by the instrument. r-FXIIIA1 at a final concentration of 2,500 U/mL (0.36 mg/mL) was added to the 9 mg/mL FI samples. $CaCl_2$ (final concentration: 12 mM) and Ringer's solution (155 mM NaCl, 5 mM KCl, 2 mM $CaCl_2$, 1 mM $MgCl_2$, added to standardize volume in cup) were added followed quickly by rFIIa (final concentration: 106 U/mL) to initiate fibrin clot formation. Data were collected every five seconds for 30 minutes by the TEG interfaced with a computer. The TEG Analytical Software (version 4.2.2, Haemoscope, Niles, IL) collected the time to

clot initiation (R), the time to achieve a clot firmness of 20mm (K) and the maximum clot strength (MA). The instrument was calibrated each day of use. Each sample was run in triplicate so means and standard deviations could be calculated. The data was exported and analyzed in Microsoft® Excel.

6.4 Results

Transgene integration, purification and confirmation of r-FXIIIA1 primary structure PCR screening of selected clones of Pichia pastoris were shown to contain between one and five gene copies of the expression cassette, containing the dual amino and carboxy-terminal His and Myc-tagged r-FXIIIA-chains (Fig. 6.1). In spite of the presence of α-secretion signal sequence in cassette, protein was observed to accumulate in cell inclusion bodies and not in the culture media after induction of expression. This intracellular protein was extracted and then purified from the cell mass lysate by IMAC. The average final yield following the sequence of affinity IMAC purification and post-elution imidazole elution buffer dilution, dialysis and concentration steps was approximately 0.24 mg r-FXIIIA1 antigen per gram cell paste as detected by Western analysis. The majority species appearing in the affinity purified product was confirmed to be r-FXIIIA1 by comparing Western analysis with stained SDS-PAGE (Fig. 6.2) and estimated to be greater than 98% pure. The non-reducing SDS-PAGE analysis of the expressed r-FXIIIA1 (Fig. 2A) exhibited an M_r of ~81 kDa and similar to the A-chain of reference plasma-derived FXIII sample. Furthermore, this analysis showed that the SDS caused the disassembly of the tetrameric pd-FXIIIA reference sample and any multimeric structures present in the r-FXIIIA1 preparation.

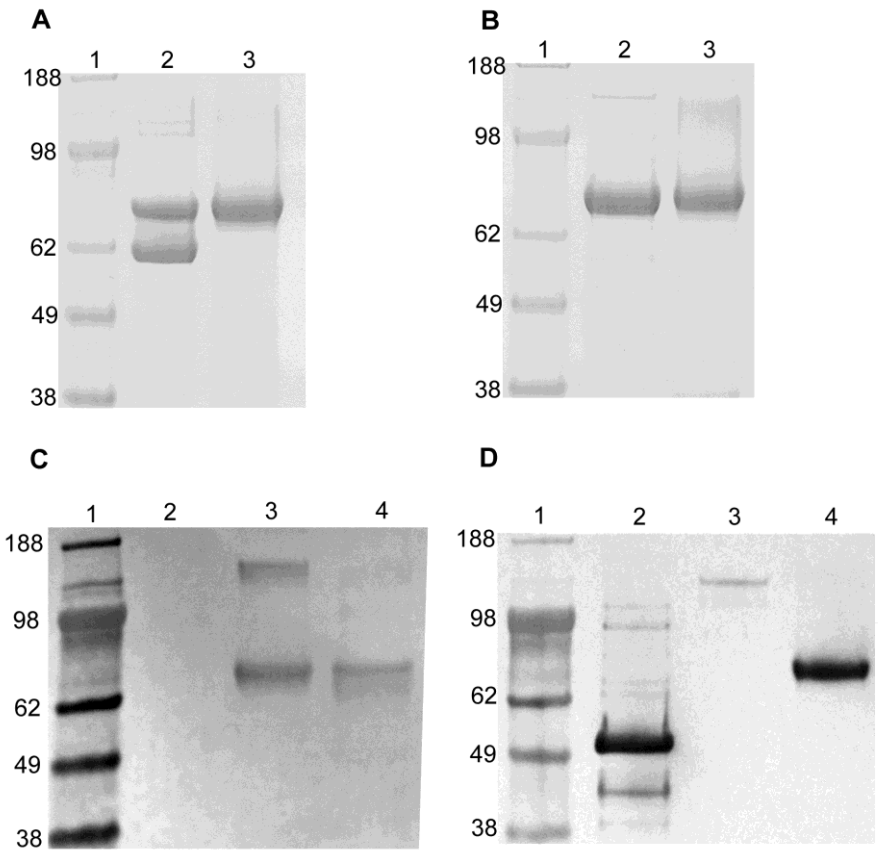

Figure 6.2. Comparison of pd-FXIII and IMAC purified r-FXIIIA1 by SDS-PAGE. Colloidal Blue stained SDS-PAGE under (A) non-reducing and (B) reducing conditions; Lane 1. M_r marker; Lane 2. pd-FXIII reference; Lane 3. r-FXIIIA1. Western analysis by (C) polyclonal anti-FXIIIA and (D) anti-His-tag Mab: Lane 1. M_r marker; Lane 2. His-tag labeled reference protein (APOE), Lane 3. pd-FXIII; Lane 4 r-FXIIIA1.

Surprisingly, amino acid sequencing showed that the N-terminal domain of the r-FXIIIA1 comprised of the 0.84 kDa His-tag and 1.03 kDa activation peptide was removed (Table I). Western analysis using an anti-His-tag monoclonal antibody indicated the presence of the remaining His-tag at the carboxy-terminus of the r-FXIIIA1 (Fig. 6.2D). Thus, the overall similarity of the M_r of the FXIIIA1 with the pd-FXIIIA-

chain was consistent with the removal of the activation peptide and remaining presence of the carboxy-terminal His-tag used in the IMAC purification. It is noted that under non-reducing conditions, the B-chain from the SDS disassembly of the tetrameric pd-FXIII reference protein was observed at M_r 60 kDa, which increased to approximately 81 kDa under non-reducing conditions (Fig. 6.2B) as previously reported [17].

Stokes Radius estimates using SEC

The R_s of r-FXIIIA1 in solution was estimated by SEC using a semi-empirical correlation [42, 43], originally developed by Laurent and Killander [40]. Four protein standards were used to calibrate the constants within the correlation: the R_s of 6.5 nm was used for IgA [44], 5.3 nm for IgG [44], 4.08 nm for coagulation factor IX [45], and 4.1 nm for Prothrombin [46] where these R_s were previously determined by analytical ultracentrifuge and gel filtration. The resulting linear form of the correlation gave an R^2 of 0.936 using the above reference proteins and the r-FXIIIA1's retention time yielded an R_s of 4.2 nm (Fig. 6.3C) and M_r of 72 kDa (Fig. 6.3D). The similarity of the R_s of the r-FXIIIA1 to prothrombin indicates that it predominately occurred as a monomeric form.

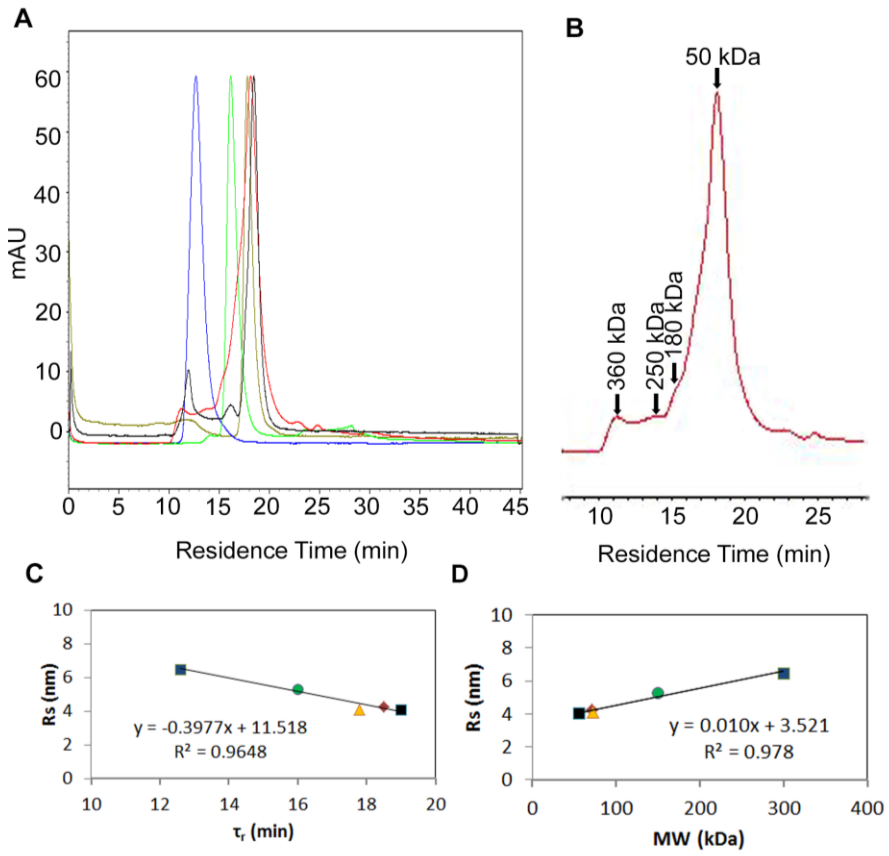

Figure 6.3. Molecular size and aggregation analysis of r-FXIIIA1 by SEC. (A) Reference protein residence time (t_r) profiles with MW: Coagulation factor IX (MW~56 kDa, R_s=4.08 nm, Black), IgG (MW~150 kDa, R_s=5.3 nm, green), Prothrombin (MW~72 kDa, R_s=4.1 nm, Gold), and IgA (MW~300 kDa, R_s=6.5 nm, blue) and r-FXIIIA1 (red). (B) Magnified SEC profile for r-FXIIIA1 for aggregate detection. (C) R_s prediction using residence time data of panel A and a semi-empirical correlation of Laurent and Killander [40] (D) MW prediction using residence time data of panel A. ♦r-FXIIIA1 ■ IgA ● IgG ▲ Prothrombin ■ factor IX**.**

Inactivation of pd-FXIII and r-FXIIIA1 by r-FIIa

The time course inactivation of pd-FXIIIA2 and r-FXIIIA1 by r-FIIa was evaluated by SDS-PAGE gel electrophoresis under reducing conditions (Fig. 6.4). The respective N-terminal sequences of the resulting proteolytic fragments were also

determined (Table 6.1). Prior to treatment with r-FIIa, the zymogen pd-FXIII and the r-FXIIIA1 consisted of single bands at an M_r of approximately 81 kDa (Fig. 4A and B, Lane 2). Within 0.5 min of incubation with r-FIIa, a second band appears for both pd-FXIII and r-FXIIIA1. A decrease in M_r of 3 kDa was seen for the pd-FXIII which is consistent with the removal of the activation peptide as detected by N-terminal amino acid sequencing. In contrast, the r-FXIIIA1 showed an M_r of >3 kDa cleavage where approximately half of the r-FXIIIA1 had been proteolyzed by 5 minutes. Western analysis using monoclonal anti-His-tag showed that this cleavage removed the remaining carboxy-terminal His-tag. The total decrease of M_r by >3 kDa indicates that the Myc-tag was likely also cleaved.

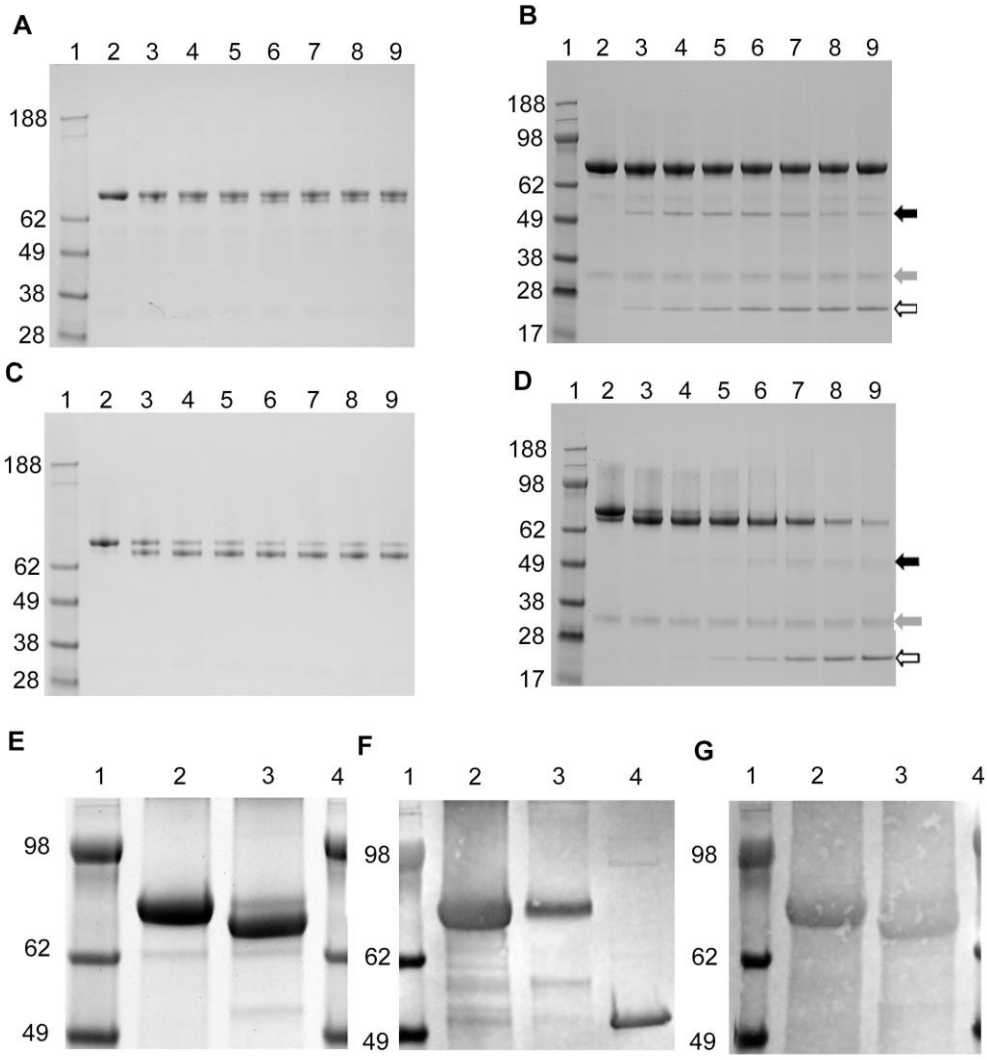

Figure 6.4. Time course r-FIIa proteolysis of pd-FXIII and r-FXIIIA1 by SDS PAGE. (A) pd-FXIII and (C) r-FXIIIA1l treated with r-FIIa for 0 to 5 minutes: Lane 1: molecular weight marker; Lanes 2 through 9: pd-FXIII or r-FXIIIA1 incubated with r-FIIa for 0, 0.5, 1.0, 1.5, 2, 3, 4 and 5 minutes. (B) pd-FXIII and (D) r-FXIIIA1 treated with r-FIIa for 0 to 360 minutes: Lane 1: molecular weight marker; Lanes 2 through 9: pd-FXIII or r-FXIIIA1 incubated with r-FIIa for 0, 5, 15, 30, 60, 120, 240 and 360 minutes. (E) SDS PAGE, (F) Western analysis by monoclonal anti-His-tag, and (G) Western analysis by polyclonal anti-FXIIIA of r-FXIIIA1 treated with r-FIIa at 0 and 5 minutes post exposure. Lane 1: molecular weight marker; Lanes 2: 0 minutes; Lane 3: 5 minutes; Lane 4: (E, G) molecular weight marker or (F) His-labeled

reference protein (APOE). The gray arrow indicates the band associated with r-FIIa. Open and closed arrows indicate degradation products at M_r ~25 kDa and ~54 kDa, respectively.

Table 6.1. N-terminal amino acid sequence of purified r-FXIIIA1 and furin cleavage products.

Approximate M_r by SDS-PAGE (kDa)	Amino Acid Sequence	r-FXIIIIA1 Species Description
~81	GVNLQEFLNV	r-FXIIIA1 + Myc-tag + His-tag
~79	GVNLQEFLNV	r-FXIIIA1
~54	GVNLQEFLNV	r-FXIIIA1 N-terminal-K513 cleavage product
~25	SRSNVDMXFE	r-FXIIIA1 S514-C-terminal cleavage product

While FIIa activates zymogen FXIII, it also further proteolysis FXIIIa to inactivate it. This inactivation of pd-FXIII and r-FXIIIA1 was evaluated by SDS-PAGE gel electrophoresis under reducing conditions for six hours (Fig. 4B and 4D). A-chain of the pd-FXIII was noticeably degraded into M_r 25 and M_r 54 kDa fragments by 15 minutes. The B-chain of pd-FXIII does not appear to be degraded by r-FIIa. Similarly, the r-FXIIIA1 band, which has no B-chain, also decreases gradually over the incubation period with an increase in the M_r 25 kDa band. In contrast, the appearance of the degradation in r-FXIIIA1 was delayed until 30 minutes. By the end of the 360 minutes, very little intact A1 chain remained in either pd-FXIIIA1 or r-FXIIIA1. The N-terminal amino acids of the bands at Mr ~81, ~79, ~54 and ~25 kDa of r-FXIIIA1 were sequenced (Table 6.1) and the bands at Mr ~81, ~79, and ~54 were consistent with that for FXIII activated A-chain. The first 10 residues of the 25 kDa band are consistent with the thrombin cleavage site at Lys513 [12].

Chromogenic activity assay

The activities of pd-FXIIIa and r-FXIIIA1 were estimated by comparison to plasma using a solid phase chromogenic activity assay. The linear trendline fit to the standard curve from plasma had an R^2 value of 0.95. Four dilutions of pd-FXIII fell within the standard curve yielding a specific activity estimate of 11 ± 6 IU/mg, with IU being defined as the amount of FXIII in 1 mL of plasma by Raut et al. [47]. The manufacturer provided specific activity of pd-FXIII as 18.9 IU/mg, while literature cites normal levels at 11-31 IU/mg in plasma based on a normal range of 10-30 μg FXIII per mL plasma [48, 49]. Two dilutions of r-FXIIIA1 were within the range of the standard curve yielding a specific activity estimate of 23 ± 3 U/mg. Post-hoc analysis (t-test) determined that r-FXIIIA1 had significantly greater activity than pd-FXIII ($p < 0.025$, $\alpha = 0.05$).

The γ-γ crosslinking of fibrin formed from pd-FI by FXIIIa was analyzed by SDS-PAGE gel electrophoresis as previously described [41] (Fig. 6.5). The pd-FXIIIa in the absences of r-FIIa began creating α and γ multimers within 5 minutes, which is confirmed by previous literature[50, 51], while the r-FXIIIA1 in the absences of r-FIIa did not catalyze the formation of a significant population until 60 minutes (Fig. 6.5A and 6.5B). As previously reported, a constitutive level of FXIII was present in pd-FI preparations and was observable by the appearance of γ-γ dimers after treatment by r-FIIa alone (Fig. 6.5C). The pd-FI samples containing no added FXIII (Fig. 6.5C) and the fibrinogen samples containing pd-FXIII (Fig. 6.5D) catalyzed the formation of γ-chain aggregates at similar rates as seen by the disappearance of the γ-chain monomer and appearance of the γ-γ dimer. The rates of γ-chain aggregates of samples containing pd-

FXIIIa (Fig. 6.5E) and r-FXIIIA1 (Fig. 6.5F) were similar but significantly faster than those containing pd-FXIII and no added FXIII. By the end of the 15-minute incubation period, a non-complexed γ-chain band is still visible for the no added FXIII and pd-FXIII samples. The γ-chain band for the pd-FXIIIa and r-FXIIIA1 samples is essentially gone. The α-chain monomer is also disappearing for all samples resulting in higher molecular weight bands. The α-chain of samples with no added FXIII, pd-FXIII and pd-FXIIIa decreases at a similar rate but a majority remains after 15 -minutes of incubation. However, the α-chain of the r-FXIIIA1 sample gradually decreased, leaving very little monomer remaining at the end of the 15-minute incubation period. N-terminal sequencing indicates the presence of both α- and γ-chain multimers in all samples.

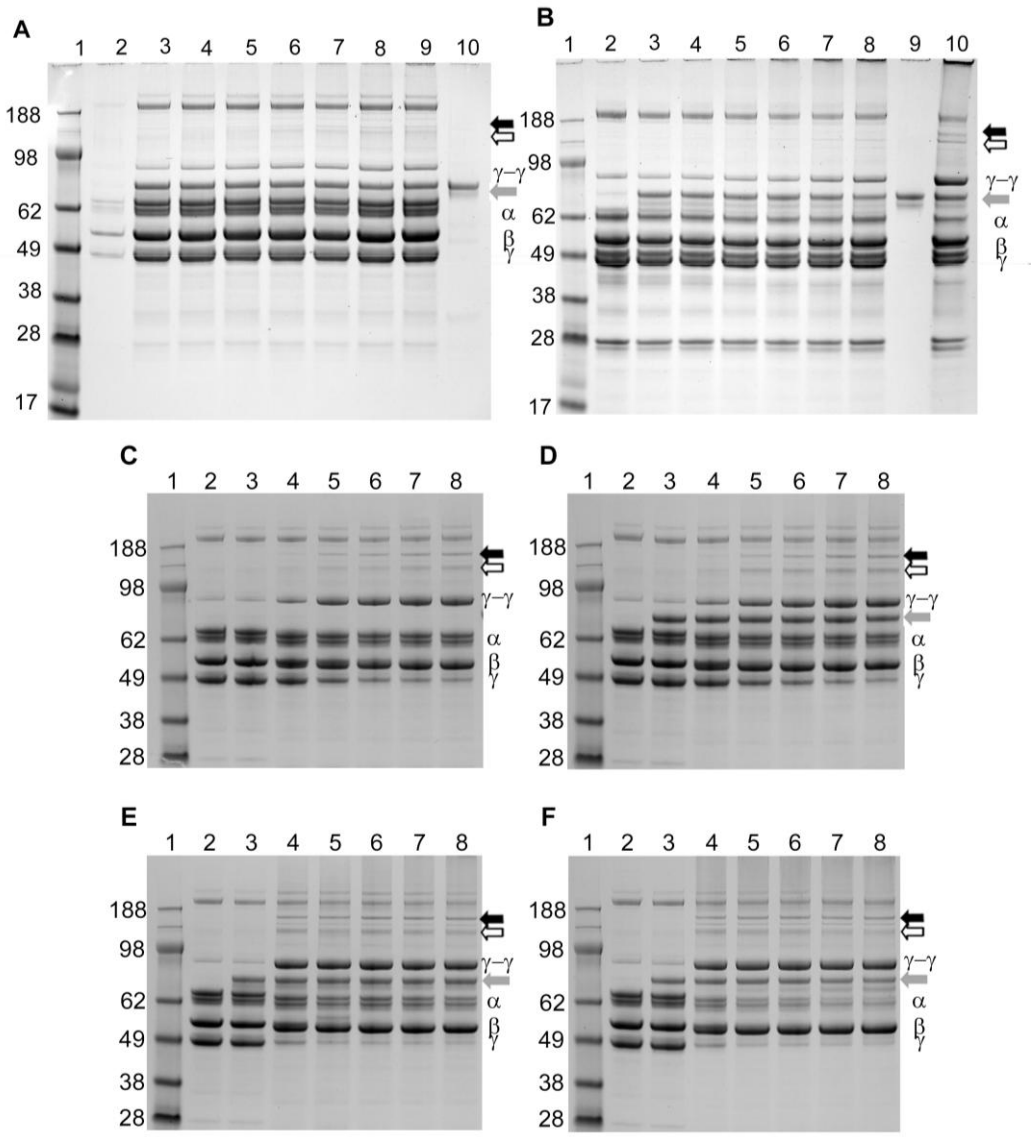

Figure 6.5. SDS-Page of fibrin crosslinking by r-FXIIIA1 versus zymogen pd-FXIII. Purified pd-FI (0.38 mg/mL) having a typical constitutive level of FXIII activity was treated with and without r-FIIa (1 U/mL) to initiate fibrin formation in the absence and presence of added zymogen pd-FXIII or pd-FXIIIa having prior activation by FIIa or r-FXIIIA1 (1.1 U/mL): (A) no r-FIIa with added pd-FXIIIa (B) no r-FIIa with added r-FXIIIA1; (C) r-FIIa alone; (D) r-FIIa with pd-FXIII; (E) r-FIIa with pd-FXIIIa; (F) r-FIIa with r-FXIIIA1. All samples run under reducing conditions. All panels Lane 1: molecular weight marker; Lane 2: pd-FI prior to r-FIIa and FXIII treatment; Lanes 3 through 8: pd- FI, r-FIIa and FXIII incubated for 0, 1,

2.5, 5, 10 and 15 minutes. Panel A only: Lane 9: pd-FI, r-FIIa and FXIII incubated for 60 minutes; Lane 9 r-FXIIIA1; Panel B only: Lane 9 r-FXIIIA1; Lane 10: pd-FI, r-FIIa and FXIII incubated for 60 minutes. The Aα-, Bβ- and γ-chains (66, 52 and 46 kDa, respectively) of FI are indicated by α, β, and γ, γ- γ indicates the cross-linked γ-chains. The gray arrow indicates the band associated with the added FXIII species. As detected by N-terminal sequencing, the open arrow indicates an α-chain multimer and the closed arrow indicates a γ-chain multimer.

Dose Response

The dose response crosslinking of both r-FI and pd-FI to r-FXIIIA1 and r-FIIa were evaluated by SDS-PAGE (Fig. 6.6). The reaction of r-FXIIIA1, FI, and r-FIIa was allowed to continue for 2.5 minutes before being quenched by LDS and reducing buffer. No γ-γ dimer was found in the r-FI sample in the absence of r-FXIIIa, while pd-FI produced a noticeable amount of γ-γ dimer in the absence of non-endogenous r-FXIIIA1. When dosed with r-FXIIIA1, both samples produced α- and γ-chain multimers in addition to γ-γ dimer in a dose-dependent manner.

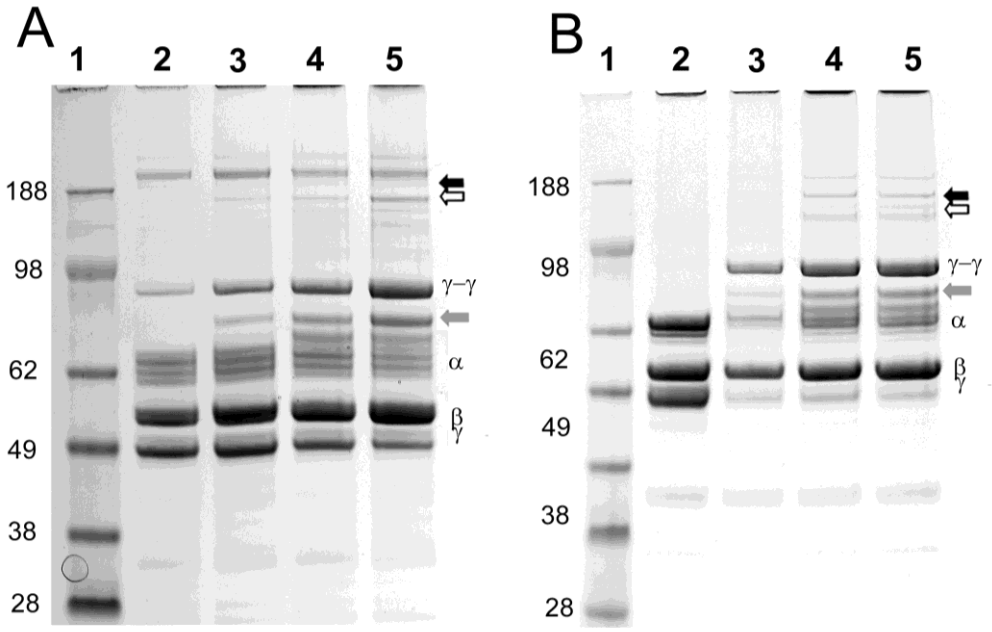

Figure 6.6. Dose-response SDS-Page of r-FXIIIA1 on r-FI with no endogenous FXIII and pd-FI containing endogenous FXIII. (A) pd-FI (9mg/mL) and (B) r-FI (9 mg/mL) were incubated with FIIa (0.2 mg/mL) and with and without r-FXIIIa to initiate fibrin formation. The reaction was quenched with LDS and reducing buffer after 2.5 minutes. Lane 1: Molecular weight marker; Lane 2: No added r-FXIIIA1; Lane 3: 0.18 mg/mL r-FXIII added; Lane 4: 0.36 mg/mL r-FXIII added; Lane 5: 0.53 mg/mL r-FXIII added. The Aα-, Bβ- and γ-chains (66, 52 and 46 kDa, respectively) of FI are indicated by α, β, and γ, γ-γ indicates the cross-linked γ-chains. The gray arrow indicates the band associated with the added FXIII species. As detected by N-terminal sequencing, the open arrow indicates an α-chain multimer and the closed arrow indicates a γ-chain multimer.

Viscoelastic properties

The effectiveness of r-FXIIIA1 in increasing clot strength of pd-FI was evaluated by thromboelastography (TEG) (Fig. 6.7). The evolution of viscoelasticity during the formation of a crosslinked fibrin clot from 34 mg/mL FI biotherapeutic fibrin sealant was measured against 9 mg/mL FI biotherapeutic fibrin sealant with 0.36 mg/mL r-FXIIIA1.

The lower concentration of fibrin sealant with r-FXIIIA1 was found to reach a maximum amplitude plateau over 6 minutes before higher concentration fibrin sealant without any added FXIII while maintaining significantly higher maximum amplitude for over 15 minutes.

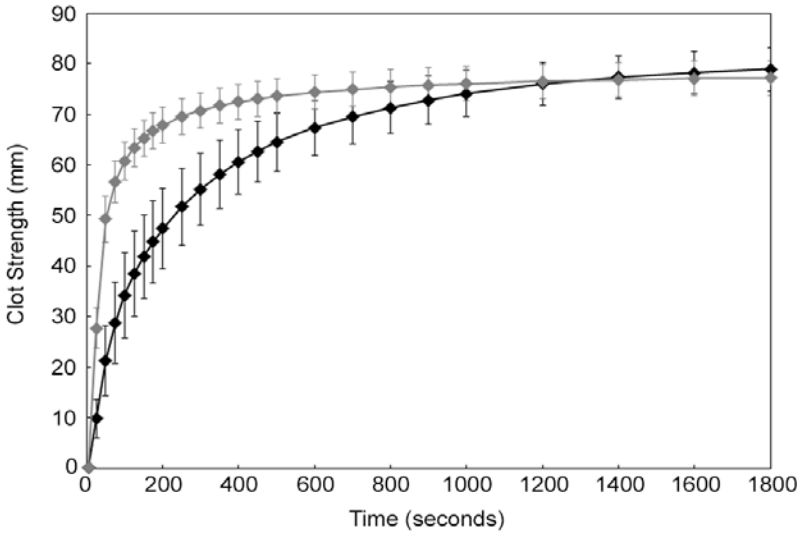

Figure 6.7. Thromboelastography acceleration and strengthening of plasma-derived biotherapeutic grade fibrin sealant by rFXIIIA1. TEG analysis of the kinetics of clot initiation and clot strength over time for biotherapeutic grade fibrin sealant at 33.5 mg/mL (◆) and biotherapeutic grade fibrin sealant formulated at 9 mg/mL FI and 0.36 mg/mL rFXIIIA1 (◆). Data are expressed as mean +/- standard deviation.

6.5 Discussion

The expression cassette used here to produce FXIIIA1 contained an alpha secretion signal as well as N- and COOH-terminal affinity tags that flanked the primary sequence of the A-chain. In spite of the secretion signal, the cell media showed almost undetectable levels of A-chain antigen while the FXIIIA-chain was easily purified by IMAC from cell lysates at 0.24 mg per gram cell paste. Surprisingly, it had been

converted into a FXIIIA1 without the amino-terminal activation peptide. This r-FXIIIA1 demonstrated high specific activity and contained no other degradation. While the activation resulted in the loss of the N-terminal His tag, it left the carboxy-terminal His tag still in place which enabled IMAC purification. In summary, a prodigious yield from cell lysates was obtained showing the capacity of the *P. pastoris* to intracellularly process r-FXIIIA1 into r-FXIIIA1 without an amino-terminal activation peptide.

While the specificity of the intracellular activation of the A-chain is indicative of a serine protease with thrombin-like activity, we found that further treatment with human thrombin resulted in the cleavage of the carboxy-terminal His affinity tag sequence. A time course loss of the anti-His Mab signal was observed over 5 minutes with a concomitant reduction in M_r of about 3 kDa while retaining the N-terminal sequencing FXIIIA1. We could not verify the carboxy-terminal removal of the Myc affinity tag that was juxtaposed between the FXIIIA1 and the carboxy terminal His tag, as we could not obtain a myc-tag antigen signal before or after thrombin treatment. At longer times, we observed further proteolysis by thrombin to inactivate the FXIIIA1 with similar cleavages than that observed with the activated A-chain of pdFXIIIA2 [17] yielding fragments of approximately 25 and 54 kDa. The physiologic feedback inactivation of FXIIIA2a by thrombin exerts an important control over fibrin cross-linking.

Although the primary structure of r-FXIIIA1 appears similar to pd-FXIIIA2a produced from activating pdFXIII, the quaternary structure is different. Past studies of zymogen pd-FXIIIA2 from platelets and r-FXIIIA2 from *S. cerevisiae* and also their respective thrombin activated products have been reported to be homodimeric structures [30]. In contrast, we observed by HPSEC analysis that the r-FXIIIA1 purified here from

P. pastoris primarily exists as a monomer with only small amounts of aggregates. It is possible that the intracellular activation and or carboxy-terminal His tag could prevent the dimer formation. We estimate the specific activity of the r-FXIIIA1 to be >2-fold higher than pd-FXIIIA2a. Despite possible differences in quaternary structure, inactivation of r-FXIIIA1 by thrombin was similar if not slightly slower than its plasma-derived counterpart. These results were similar to those seen with r-FXIIIA2 produced in *Saccharomyces cerevisiae* that has been advanced to human clinical study [52, 53].

We used r-FXIIIA1 to assess the nature and kinetic benefit of the cross-linking of fibrin made when augmenting the pd-FXIII activity that is constitutively present in most pd-FI preparations [54]. This constitutive activity arises from pd-FXIII that is associated with the γγ' heterodimer subpopulation, which is about 20% of the total pd-FI population [1, 35, 55]. The r-FXIIIA1 catalyzed a similar distribution of cross-linked fibrin products to that from pd-FXIII: both γ-γ chain cross-linked dimers and higher molecular weight fibrin cross-linking involving the α-chains were made from thrombin treated pd-FI (Fig. 6.5). The α-α fibrin crosslinking is especially important for overall clot strength [6]. With respect to crosslinking kinetics, we observed an appreciable lag in the onset of fibrin crosslinking kinetics of pd-FI having only constitutive pd-FXIII zymogen, relative to those when the fibrin formation was in the presence of augmented levels of r-FXIIIA1 or pd-FXIII2Aa. The pd-FI samples treated by pre-activated pd-FXIII and r-FXIIIA1 treatment groups yielded much faster γ-γ and α-α crosslinks. This relative lag is likely due to the activation step by thrombin on the constitutively present pd-FXIII.

Interestingly, the r-FXIIIA1 appears to have a longer crosslinking lag-time than pd-FXIIIa when there is no thrombin present. As Fig. 6.5B demonstrates, r-FXIIIA1 is

not sufficient to induce the creation of α and γ multimers in a kinetically favorable time. However, in the presence of r-FIIa, r-FXIIIA1 produces α and γ multimers in a kinetically favorable manner that is similar to pd-FXIIIa. The slower formation of α and γ multimers in the absence of thrombin and the kinetically favorable formation of these same multimers in the presence of thrombin indicates the creation of an artificial, kinetically favorable activation peptide in the form of the carboxy-terminal His- and myc-tag. The activation times for pd-FXIII and r-FXIIIA1 as seen in Fig. 4A and 4C correspond to the lag time in the creation of α and γ multimers in Fig. 5B and 5C.

Today's surgical sealants rely solely on the constitutively present FXIII for fibrin cross-linking and thus consist of only thrombin and pdF1 starting materials. The addition of rFXIIIA1 would eliminate the 2 minute lag in cross-linking and decrease the time for a clot to reach maximum strength by over 15 minutes. The r-FXIIIA1 could be added at an optimized dose to potentially improve topical fibrin sealants in treatment of acute hemorrhage. We have previously investigated the use of r-FXIIIA1 in recombinant sealants [37].

We have produced a functional r-FXIIIA1 in abundance in *Pichia pastoris*. The production of r-FXIIIA1 rather than FXIIIA2 may be beneficial for therapeutic uses. The use of rFXIIIA1 in topical sealants creates a kinetically favorable time-lag compared to the activation of tetrameric, BB/AA structure of the pd-FXIII zymogen, which proceeds through a step that dissociated of the B-chain [22-26] and also the removal of the activation peptide. Importantly, in the absence of thrombin, the rFXIIIA1 showed a greatly reduced cross-linking activity related to the removal of the His- and myc-tag artificial activation peptide.

6.6 Acknowledgements

I am grateful to Dr. Helen Philippou and Dr. Emma Smith for their FXIII chromogenic activity assay. I am also grateful to Weijie Xu and Ayman Ismail for assisting in r-FXIIIa purification and to University of Nebraska Medical Center's Protein Structure Core Facility for conducting the N-terminal sequencing.

6.7 References

1 McDonagh JM, McDonagh RP, Jr., Delage JM, Wagner RH. Factor XIII in human plasma and platelets. *Journal of Clinical Investigation*. 1969; 48: 940.
2 McDonagh J. Structure and function of Factor XIII. In: Colman RW, Hirsh J, Marder VJ, Salzman EW, eds. *Hemostasis and Thrombosis: Basic Principles and Clinical Practice*, Third Edition edn. Philadelphia: J.B. Lippincott Company, 1994.
3 Valnickova Z, Enghild JJ. Human procarboxypeptidase U, or thrombin-activable fibrinolysis inhibitor, is a substrate for transglutaminases. Evidence for transglutaminase-catalyzed cross-linking to fibrin. *J Biol Chem*. 1998; 273: 27220-4.
4 Mosher DF, Schad PE, Vann JM. Cross-linking of collagen and fibronectin by factor XIIIa. Localization of participating glutaminyl residues to a tryptic fragment of fibronectin. *J Biol Chem*. 1980; 255: 1181-8.
5 Procyk R, Adamson L, Block M, Blomback B. Factor XIII catalyzed formation of fibrinogen-fibronectin oligomers--a thiol enhanced process. *Thromb Res*. 1985; 40: 833-52. 0049-3848(85)90320-2 [pii].
6 Ariens RA, Lai TS, Weisel JW, Greenberg CS, Grant PJ. Role of factor XIII in fibrin clot formation and effects of genetic polymorphisms. *Blood*. 2002; 100: 743.
7 Mosher DF, Schad PE. Cross-linking of fibronectin to collagen by blood coagulation Factor XIIIa. *J Clin Invest*. 1979; 64: 781-7. 10.1172/JCI109524 [doi].
8 Hada M, Kaminski M, Bockenstedt P, McDonagh J. Covalent crosslinking of von Willebrand factor to fibrin. *Blood*. 1986; 68: 95-101.
9 Bockenstedt P, McDonagh J, Handin RI. Binding and covalent cross-linking of purified von Willebrand factor to native monomeric collagen. *J Clin Invest*. 1986; 78: 551-6. 10.1172/JCI112608 [doi].
10 Grundmann U, Amann E, Zettlmeissl G, Kupper HA. Characterization of cDNA coding for human factor XIIIa. *Proc Natl Acad Sci U S A*. 1986; 83: 8024-8.
11 Ichinose A, Hendrickson LE, Fujikawa K, Davie EW. Amino acid sequence of the a subunit of human factor XIII. *Biochemistry*. 1986; 25: 6900-6.
12 Takahashi N, Takahashi Y, Putnam FW. Primary structure of blood coagulation factor XIIIa (fibrinoligase, transglutaminase) from human placenta. *Proc Natl Acad Sci U S A*. 1986; 83: 8019-23.

13 Weisberg LJ, Shiu DT, Conkling PR, Shuman MA. Identification of normal human peripheral blood monocytes and liver as sites of synthesis of coagulation factor XIII a-chain. *Blood*. 1987; 70: 579-82.
14 Muszbek L, Adany R, Kavai M, Boda Z, Lopaciuk S. Monocytes of patients congenitally deficient in plasma factor XIII lack factor XIII subunit a antigen and transglutaminase activity. *Thromb Haemost*. 1988; 59: 231-5.
15 Nagy JA, Kradin RL, McDonagh J. Biosynthesis of factor XIII A and B subunits. *Adv Exp Med Biol*. 1988; 231: 29-49.
16 Kiesselbach TH, Wagner RH. Fibrin-stabilizing factor: a thrombin-labile platelet protein. *Am J Physiol*. 1966; 211: 1472-6.
17 Schwartz ML, Pizzo SV, Hill RL, McKee PA. Human Factor XIII from plasma and platelets. Molecular weights, subunit structures, proteolytic activation, and cross-linking of fibrinogen and fibrin. *J Biol Chem*. 1973; 248: 1395-407.
18 Folk JE, Finlayson JS. The epsilon-(gamma-glutamyl)lysine crosslink and the catalytic role of transglutaminases. *Adv Protein Chem*. 1977; 31: 1-133.
19 Freyssinet JM, Lewis BA, Holbrook JJ, Shore JD. Protein-protein interactions in blood clotting. The use of polarization of fluorescence to measure the dissociation of plasma factor XIIIa. *Biochem J*. 1978; 169: 403-10.
20 Takagi T, Doolittle RF. Amino acid sequence studies on factor XIII and the peptide released during its activation by thrombin. *Biochemistry*. 1974; 13: 750-6.
21 Lewis SD, Janus TJ, Lorand L, Shafer JA. Regulation of formation of factor XIIIa by its fibrin substrates. *Biochemistry*. 1985; 24: 6772-7.
22 Greenberg CS, Achyuthan KE, Fenton JW, II. Factor XIIIa formation promoted by complexing of a-thrombin, fibrin, and plasma factor XIII. *Blood*. 1987; 69: 867.
23 Lorand L, Gray AJ, Brown K, Credo RB, Curtis CG, Domanik RA, Stenberg P. Dissociation of the subunit structure of fibrin stabilizing factor during activation of the zymogen. *Biochem Biophys Res Commun*. 1974; 56: 914-22. S0006-291X(74)80275-5 [pii].
24 Chung SI, Folk JE. Kinetic studies with transglutaminases. The human blood enzymes (activated coagulation factor 13 and the guinea pig hair follicle enzyme. *J Biol Chem*. 1972; 247: 2798-807.
25 Chung SI, Lewis MS, Folk JE. Relationships of the catalytic properties of human plasma and platelet transglutaminases (activated blood coagulation factor XIII) to their subunit structures. *J Biol Chem*. 1974; 249: 940-50.
26 Hornyak TJ, Bishop PD, Shafer JA. Alpha-thrombin-catalyzed activation of human platelet factor XIII: relationship between proteolysis and factor XIIIa activity. *Biochemistry*. 1989; 28: 7326-32.
27 Janus TJ, Lewis SD, Lorand L, Shafer JA. Promotion of thrombin-catalyzed activation of factor XIII by fibrinogen. *Biochemistry*. 1983; 22: 6269-72.
28 Greenberg CS, Miraglia CC, Rickles FR, Shuman MA. Cleavage of blood coagulation factor XIII and fibrinogen by thrombin during in vitro clotting. *Journal of Clinical Investigation*. 1985; 75: 1463.
29 Credo RB, Curtis CG, Lorand L. Ca2+-related regulatory function of fibrinogen. *Proc Natl Acad Sci U S A*. 1978; 75: 4234-7.

30 Bishop PD, Teller DC, Smith RA, Lasser GW, Gilbert T, Seale RL. Expression, purification, and characterization of human factor XIII in Saccharomyces cerevisiae. *Biochemistry*. 1990; 29: 1861.
31 Bishop PD, Lasser GW, Le Trong I, Stenkamp RE, Teller DC. Human recombinant factor XIII from Saccharomyces cerevisiae. Crystallization and preliminary x-ray data. *Journal of Biological Chemistry*. 1990; 265: 13888.
32 Lewis KB, Teller DC, Fry J, Lasser GW, Bishop PD. Crosslinking kinetics of the human transglutaminase, factor XIII A2 , acting on fibrin gels and gamma-chain peptides. *Biochemistry*. 1997; 36: 995. 10.1021/bi961636z.
33 Park D-S, Kim J-H, Lee SW, Jeong J-M. Secretory expression of the α-subunit of human coagulation factor XIII in the yeast Pichia pastoris. *Biotechnology letters*. 2002; 24: 97-101.
34 Gao J, Hooker BS, Anderson DB. Expression of functional human coagulation factor XIII A-domain in plant cell suspensions and whole plants. *Protein expression and purification*. 2004; 37: 89-96.
35 Lovejoy AE, Reynolds TC, Visich JE, Butine MD, Young G, Belvedere MA, Blain RC, Pederson SM, Ishak LM, Nugent DJ. Safety and pharmacokinetics of recombinant factor XIII-A2 administration in patients with congenital factor XIII deficiency. *Blood*. 2006; 108: 57. 10.1182/blood-2005-02-0788.
36 Calcaterra J, Van Cott KE, Butler SP, Gil GC, Germano M, van Veen HA, Nelson K, Forsberg EJ, Carlson MA, Velander WH. Recombinant Human Fibrinogen That Produces Thick Fibrin Fibers with Increased Wound Adhesion and Clot Density. *Biomacromolecules*. 2013; 14: 169-78.
37 Carlson MA, Calcaterra J, Johanning JM, Pipinos II, Cordes CM, Velander WH. A totally recombinant human fibrin Sealant. *Journal of Surgical Research*. 2013.
38 Zhang W, Inan M, Meagher MM. Rational design and optimization of fed-batch and continuous fermentations. *Methods in Molecular Biology (Totowa, NJ, United States)*. 2007; 389: 43.
39 Ariëns RA, Philippou H, Nagaswami C, Weisel JW, Lane DA, Grant PJ. The factor XIII V34L polymorphism accelerates thrombin activation of factor XIII and affects cross-linked fibrin structure. *Blood*. 2000; 96: 988-95.
40 Laurent TC, Killander J. A theory of gel filtration and its exeperimental verification. *Journal of Chromatography A*. 1964; 14: 317-30.
41 Gorkun OV, Veklich YI, Weisel JW, Lord ST. The conversion of fibrinogen to fibrin: recombinant fibrinogen typifies plasma fibrinogen. *Blood*. 1997; 89: 4407.
42 Ackers G. A new calibration procedure for gel filtration columns. *Journal of Biological Chemistry*. 1967; 242: 3237-8.
43 Fish WW, Reynolds JA, Tanford C. Gel Chromatography Of Proteins In Denaturing Solvents Comparison Between Sodium Dodecyl Sulfate and Guanidine Hydrochloride as Denaturants. *Journal of Biological Chemistry*. 1970; 245: 5166-8.
44 Armstrong J, Wenby R, Meiselman H, Fisher T. The hydrodynamic radii of macromolecules and their effect on red blood cell aggregation. *Biophysical journal*. 2004; 87: 4259-70.
45 Suomela H. Human coagulation factor IX. *European Journal of Biochemistry*. 1976; 71: 145-54.

46 Tishkoff GH, Williams LC, Brown DM. Preparation of Highly Purified Prothrombin Complex I. CRYSTALIZATION, BIOLOGICAL ACTIVITY, AND MOLECULAR PROPERTIES. *Journal of Biological Chemistry*. 1968; 243: 4151-67.

47 Raut S, Merton R, Rigsby P, Muszbek L, Seitz R, AriENs R, Barrowcliffe T, Ichinose A. A collaborative study to establish the 1st International Standard for factor XIII plasma. *Journal of Thrombosis and Haemostasis*. 2007; 5: 1923-9.

48 Rea C, Foley J, Ingerslev J, Sørensen B. Factor XIII combined with recombinant factor VIIa: a new means of treating severe hemophilia A. *Journal of Thrombosis and Haemostasis*. 2011; 9: 510-6.

49 Hedner U, Henriksson P, Nilsson I. Factor XIII in a clinical material. *Scandinavian journal of haematology*. 1975; 14: 114-9.

50 Siebenlist KR, Meh DA, Mosesson MW. Protransglutaminase (factor XIII) mediated crosslinking of fibrinogen and fibrin. *Thrombosis and haemostasis*. 2001.

51 Siebenlist KR, Meh DA, Mosesson MW. Plasma factor XIII binds specifically to fibrinogen molecules containing gamma chains. *Biochemistry*. 1996; 35: 10448-53. 10.1021/bi9606206 [doi]
bi9606206 [pii].

52 Reynolds TC, Butine MD, Visich JE, Gunewardena KA, MacMahon M, Pederson S, Bishop PD, Morton KM. Safety, pharmacokinetics, and immunogenicity of single-dose rFXIII administration to healthy volunteers. *Journal of thrombosis and haemostasis : JTH*. 2005; 3: 922. 10.1111/j.1538-7836.2005.01224.x.

53 Visich JE, Zuckerman LA, Butine MD, Gunewardena KA, Wild R, Morton KM, Reynolds TC. Safety and pharmacokinetics of recombinant factor XIII in healthy volunteers: a randomized, placebo-controlled, double-blind, multi-dose study. *Thromb Haemost*. 2005; 94: 802.

54 Marx G, Mou X. Characterizing fibrin glue performance as modulated by heparin, aprotinin, and factor XIII. *Journal of Laboratory and Clinical Medicine*. 2002; 140: 152-60.

55 Hethershaw EL, Cilia La Corte AL, Duval C, Ali M, Grant PJ, Ariëns RA, Philippou H. The Effect of Blood Coagulation Factor XIII on Fibrin Clot Structure and Fibrinolysis. *Journal of Thrombosis and Haemostasis*. 2013.

Chapter 7:

Thromboelastic Kinetics are Increased by Recombinant Human Factor XIII

Nicholas Vanderslice*, Jennifer Calcaterra*, Ayman Ismail*, Mehmet Inan,[*] Vijay P. Jain,[*] William H.Velander[*]

[*] Department of Chemical & Biomolecular Engineering, University of Nebraska, Lincoln, NE 68588-0643

7.1 Abstract

Background*:* Factor XIII (FXIII) is activated by thrombin (IIa) during fibrin formation releasing a dimeric, transglutaminase which both converts fibrin into a crosslinked, viscoelastic barrier and also covalently anchors to wound surfaces. The dose-dependent clot kinetics of coagulation factors during fibrin clot formation and strengthening are not yet understood. Thromboelastography (TEG) is a common method for determining these initiation time and strength of a clot; however, the influence of the transport phenomena associated with TEG, especially in the case of fibrin sealants, is not well characterized in literature.

Methods: Normal human blood, platelet poor plasma, platelet rich plasma, and fibrin sealant were assayed by thromboelastography (TEG) to assess the effect of crosslinking on clot strength and initiation time. Fibrin sealant (FS) containing recombinant thrombin, recombinant fibrinogen, and recombinant FXIII was also doped into the human blood products to assess the effect of elevated clotting factors for potential topical use.

Results: Thromboelastic behavior of fibrin formation was assessed for pdF1 concentrations typical of plasma at 9 mg/mL to that of FS at 34 mg/mL. It took 1000 seconds for tissue sealant to reach an MA=75 mm without rFXIIIa1a treatment while a 0.16 molar ratio of rFXIIIA1a to pd-F1 took only 450 seconds to reach an MA=75 mm while at only 9 g/mL pd-F1. Thromboelastic behavior was found to exhibit vastly different transport models based on the concentration of platelets and coagulation factors. At low levels of platelets or fibrinogen, the volume of the clot is insufficient to establish the standard transport regime where the clot is in contact with both wall of the TEG cup. The inability of the clot to contact both walls of the TEG cup vastly changes the rheological properties measured by TEG.

Conclusions: The levels of coagulation factors and platelets have the potential to change rheological factors measured by TEG due to changes in the solid and liquid interfaces. These findings have a profound implications for the measurement of the effects of coagulation factors like factor XIII which crosslink and compact the clot.

7.2 Introduction

The coagulation cascade is responsible for restoring hemostasis in the event of an injury [1, 2]. This convoluted mechanism contains over 15 different proteins including serine proteases, transglutaminases, and glycoproteins. The end result of the coagulation cascade is a fibrin clot that holds together platelets in a mesh that prevents further blood loss [3]. However in many instances of traumatic hemorrhage, the rate of blood loss exceeds the capabilities of the body to both maintain levels of coagulation factors and/or form a clot with substantial strength to restore hemostasis [4]. In order to restore

hemostasis in these cases, liquid fibrin sealant (FS) containing fibrinogen (Fib), a 340 kDa glycoprotein responsible for holding a clot together, calcium, and thrombin (IIa), a serine protease responsible for activating Fib and several other coagulation factors [1, 5-7]. Factor XIII (FXIII), a transglutaminase responsible for crosslinking Fib, has also previously been looked at as an additional protein for its clot strengthening properties [8]. Traditionally plasma-derived proteins have been used in FS due to their availability, but the growing availability of recombinant proteins has allowed the creation of a wholly recombinant FS that is currently in preclinical trials [4].

The traditional assays for clot kinetics and strength are thromboelastography (TEG) and rotational thromboelastometry (ROTEM) [9]. These assays rely on perturbation of the clot to measure the adhesion and strength of the clot at 37° C, and have the advantage of being accurate enough for laboratory use while also swift enough to provide results in the surgical theater [10]. TEG functions by rotating a 360 µl TEG cup around a torsion wire connected to a pin suspended in a coagulating solution and measuring resistance as the clot forms around the pin [11]. ROTEM in contrast rotates the pin and measuring the resistance through either optical or torsion sensors. By measuring this increase in resistance, four clotting variables can be found: maximum amplitude (MA), a measure of the maximum resistance and clot strength reached; reaction time (R), the time until clotting is first detected; K value (K), the time from R until the clot is fully formed, indicated by an amplitude of 20 mm; and angle (α), the tangent of the K. Values for K and α are not considered valid unless the clot reaches a strength of 25 mm. These variables can be taken together to find information about clot kinetics and strength. This information is valuable to both scientists evaluating the

strength of FS and surgeons evaluating the presence of coagulation factors during a surgery. This chapter strives to characterize the effect of the components of FS both as an isolated combination of proteins and in the presence of blood products that would be seen in application.

7.3 Materials and Methods

Materials

Purified, plasma-derived prothrombin was bought from Enzyme Research Laboratories (South Bend, IN). Recombinant thrombin (Recothrom®) was purchased from Zymogenetics. Purified plasma-derived fibrinogen was purchased from Enzyme Research Laboratories or purified on-site from donated blood. Purified recombinant fibrinogen (rFib), expressed in the milk of transgenic Swiss Brown cows, was obtained from Pharming Group NV (Leiden, Netherlands). Thromboelastography materials were purchased from Haemoscope (Niles, IL). Recombinant FXIII was obtained from *Pichia pastoris* using methods described in Chapter 6. Unless otherwise specified, reagents were purchased from Sigma (St. Louis, MO).

Thrombin preparation

Frozen, plasma-derived human prothrombin (Enzyme Research Laboratories, South Bend, IN), was thawed at 37^{o}C. Plasma-derived thrombin (Enzyme Research Laboratories, South Bend, IN) was added at a 1/10 mass to mass thrombin/prothrombin ratio. 0.35 grams of sodium citrate per milliliter of solution was added (Lanchantin 1965). This solution was incubated at 37^{o}C on a rotating mixer for five hours. Sodium citrate was removed using PD-10 desalting columns (GE Healthcare, Giles, United Kingdom).

Activation of prothrombin to thrombin was confirmed by reducing and nonreducing SDS-PAGE (12% Bis-Tris NuPAGE) (Invitrogen, Carlsbad, CA) stained with Colloidal Blue (Invitrogen, Carlsbad, CA). The concentration of the thrombin solution was determined by standard Bicinconic Acid (BCA) methods. The specific activity was determined by one-stage coagulation assay.

Human blood sampling and processing

Fresh, normal whole human blood (NHB) from 20 healthy, medication-free individuals, collected in tubes containing 3.2% citrate, was obtained from Research Blood Components (Brighton, MA). Each individual NHB sample was divided into thirds. The NHB sample remained unprocessed while the other two were processed into platelet rich plasma (PRP) and platelet-poor plasma (PPP). PRP was prepared by centrifuging NHB at 160xg for 8 minutes at 22^{o}C. NHB was centrifuged at 2300xg for 15 minutes at 22^{o}C to obtain PPP. All blood fractions were used within 36 hours of being drawn and were stored at 0^{o}C until analyzed at which time the samples were warmed to 37^{o}C.

Thromboelastography analysis of fibrin clot formation

TEG analysis was conducted on individual fresh, citrated NHB, and respectively derived PRP and PPP samples from 20 individuals. Aliquots of each NHB, PRP and PPP sample were dosed with purified rFib, FXIII and/or IIa alone or in combination. All blood fractions were diluted to 1.3x to provide volume for addition of the biologics. Control samples were performed to determine the effects of diluting NHB, PRP and PPP based on time to clot initiation (R), coagulation time (K, time to reach clot firmness of 20 mm) and maximal clot strength (MA) as evaluated by TEG. Each NHB and respective plasma

sample (429.72 µl) was transferred to single-use TEG cups that had been enlarged by boring with a 0.406 inch bit (650 µl final volume). Combinations of solutions containing rFib (1.42 mg, 2.32 mg/mL rFib in cup), FXIII (0.11 mg, 0.18 mg/mL FXIIIa in cup, FXIII/rFib molar ratio = 0.16), IIa (0.08 mg, 0.13 mg/mL IIa in cup, IIa/rFib molar ratio = 0.25), and CaCl2 (11 mM) were added to the TEG cups. Ringer's solution was used to normalize mixture volumes.

The TEG Analytical Software (version 4.2.2, Haemoscope, Niles, IL) collected R, K, α, and MA for blood products collected from 20 donors. Samples were run until program termination. The instrument was calibrated each day of use. All tests described above include three replicate samples in each treatment group. All NHB and respective plasma samples were tested within 36 hours of the blood draw of each individual donor. NHB, PRP and PPP samples from 20 donors were tested untreated and treated with rFib alone, rFib and IIa together, rFib and FXIII together, rFib, FXIII and IIa together. NHB, PRP and PPP samples from 10 donors were tested when treated with IIa alone, FXIII alone and IIa and FXIII in combination.

Thromboelastography of Fibrin Sealant

Samples of FS were also analyzed using 360 µl TEG cups. All assays were carried out at 11 mM calcium and all assays with exogenous FXIII and IIa contained a FXIII to Fib molar ratio of 0.16 and a IIa to Fib molar ratio of 0.25. Biotherapeutic grade FS (Tisseel®, Baxter) was analyzed at 3 mg/mL without FXIII and IIa, formulation strength (minimum of 34 mg/mL Fib) without FXIII and IIa, 3 mg/mL Fib in the presence of FXIII, and IIa and at 9 mg/mL Fib in the presence of FXIII and IIa. Plasma-

derived fibrinogen (pdFib) and rFib were analyzed at 9 mg/mL with and without IIa and FXIII.

Optical Imaging

Images of NHB, PRP, PPP, and PS in TEG cups were obtained post-termination of the TEG run. Images of the TEG cup before, during, and after removal of the pin were taken using a Canon Powershot®. FS at 3, 4.35, and 9 mg/mL pdFib, a FXIII to Fib molar ratio of 0.16, and a IIa to Fib molar ratio of 0.25 were imaged. NHB was dosed to a final FS concentration of 3, 4.35, and 5 mg/mL pdFib, PPP was dosed to a final FS concentration of 3 and 5 mg/mL, and PRP was dosed to final FS concentration of 3 mg/mL, all at the same molar ratio of FXIII and IIa previously stated. Samples were qualitatively assessed for location of the clot and presence of liquid not suspended in the clot.

7.4 Results

Addition of Coagulation Factors to Normal Human Blood Products

Samples of NHB, PRP, and PPP exhibited a wide range of variance in both clot initiation time and overall clot strength (Fig 7.1). This variance is attributed to the difference between human donors' level of coagulation factors. Overall, NHB, PRP, and PPP exhibited similar clot initiation time medians and ranges, but exhibited stark differences in maximum amplitude. Due to the increased platelet count and coagulation factors found in the PRP fraction, PRP exhibited a marked increase in median clot strength while PPP exhibited a significant reduction. The addition of FXIII and IIa had either no effect on the median sample clot strengths or reduced the clot strength;

however, increased exogenous FXIII alone was able to decrease clot initiation time and the addition of IIa greatly reduced clot initiation time by over ten-fold. The addition of rFib to the human blood products and FXIII increased the median clot initiation time, but the addition of IIa brought the clot initiation time back to levels similar to samples with IIa and no rFib.

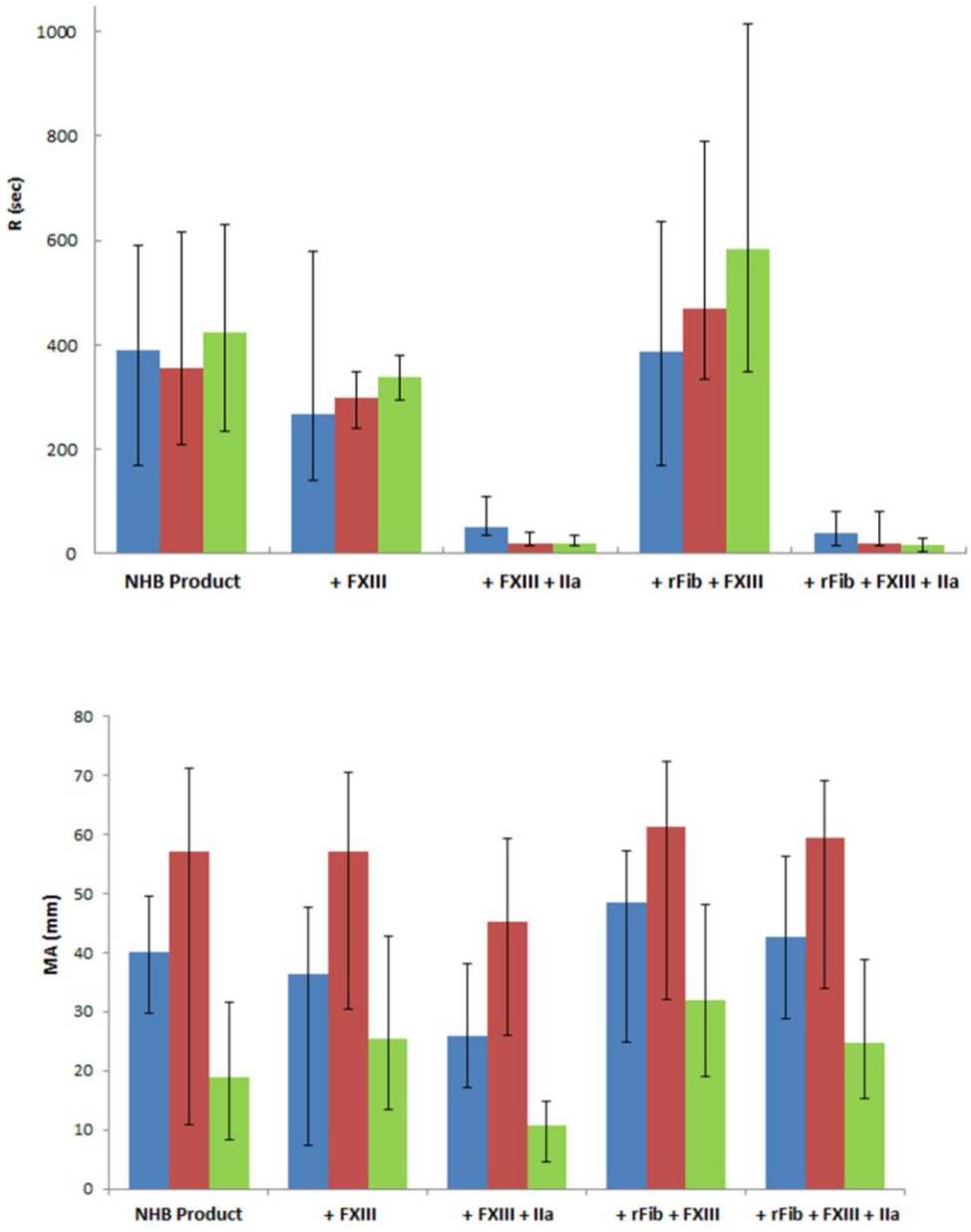

Figure 7.1. Median clot strength (MA) and clot formation time (R) as a function of FXIII, rFib, and IIa. Normal Human Blood (■) Platelet Rich Plasma (■) Platelet Poor Plasma (■). Data are plotted as median and the maximum and minimum detected values are indicated by the error bars (N=20).

The mean values of this same study with outliers removed reveal several additional pieces of information. The data shows an increase in clot strength in the presence of rFib for all human blood products. FXIII had no significant impact on the clot strength of NHB and PRP in the absence of IIa, but increased the average clot strength of PPP significantly. Interestingly, FXIII with IIa reduced overall clot strength and greatly reduced the clot initiation time in all human blood products. In contrast, the clot formation time for PRP and NHB appeared to increase in the presence of IIa. These results were analyzed again as total clot formation time, the sum of clot initiation time and clot formation time (Fig. 7.3). It was found that in NHB, a significant change in total clot formation time was not seen unless all three exogenous coagulation factors were increased, while in PRP, a decrease was seen with the addition of exogenous FXIII, FXIII and IIa, and when all three exogenous factors were present.

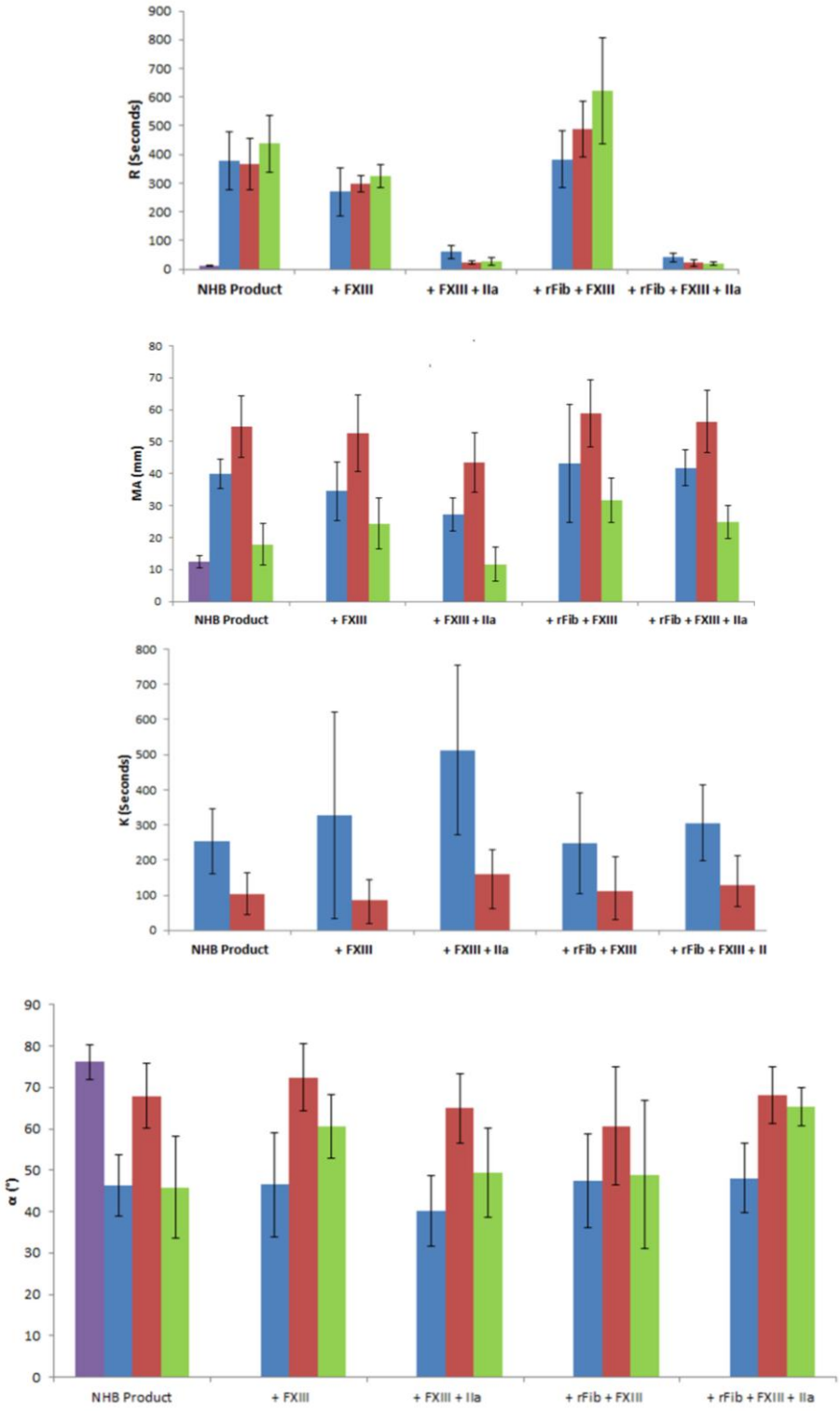

Figure 7.2. Mean clot strength (MA), clot formation time (R), and two TEG rheological variables (K and α) as a function of FXIII, rFib, and IIa. Normal Human Blood (■) Fibrin Sealant formulated at 4.35 mg/mL FI (■) Platelet Rich Plasma (■) Platelet Poor Plasma (■). Data are plotted as mean ± SEM (N=20).

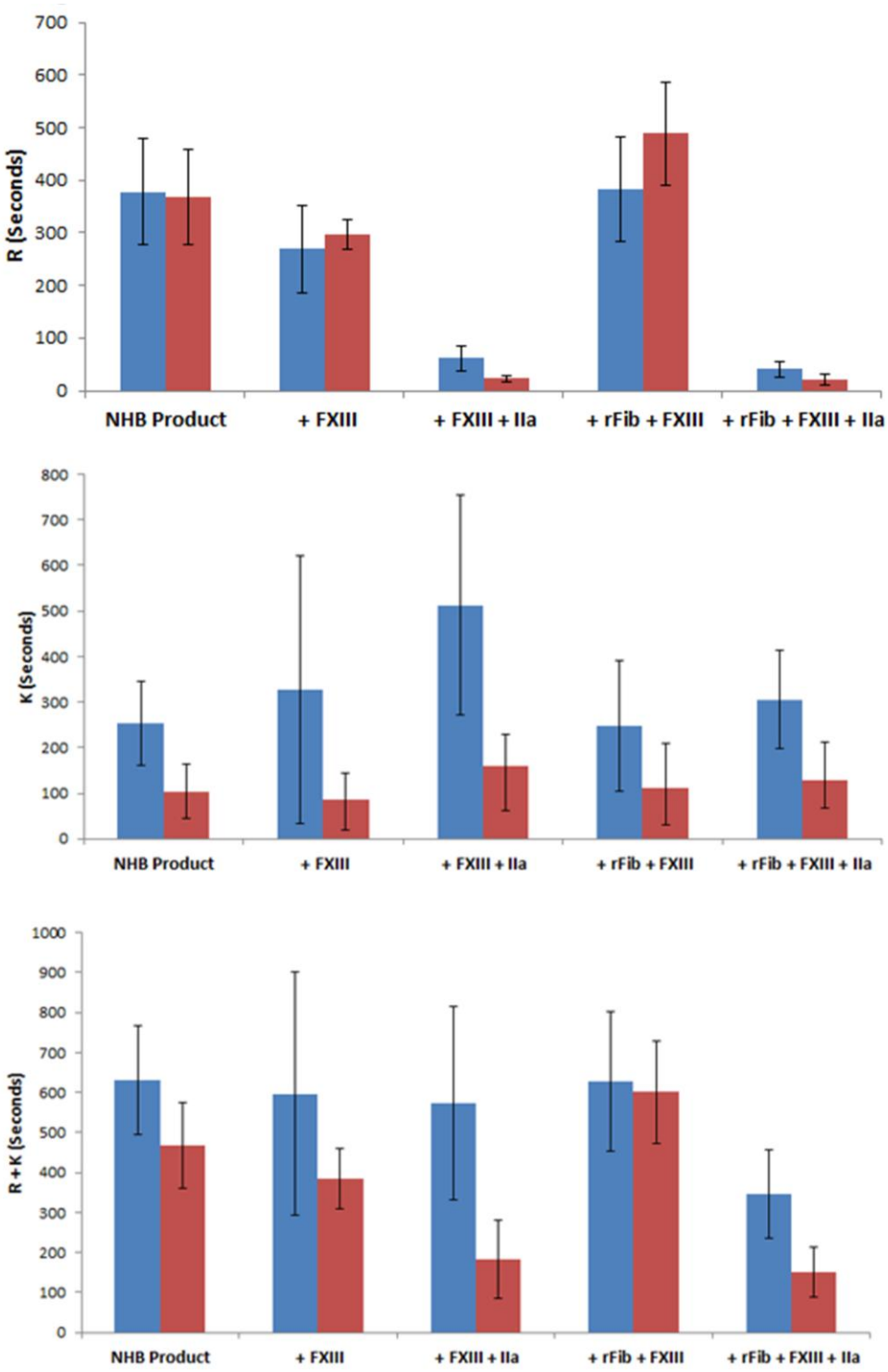

Figure 7.3. Time from assay initiation to clot firmness equaling an amplitude of 20 mm. Normal Human Blood (■) Platelet Rich Plasma (■) Platelet Poor Plasma (■). Data are plotted as mean ± SEM (N=20). Samples which did not reach a maximum amplitude of 25 mm were excluded from this analysis.

In contrast to the FS in the presence of human blood products, FS containing FXIII exhibited a significant increase in clotting strength for both rFib and pdFib (Fig. 7.4A). rFib exhibited a lower clot strength than pdFib; however, in the presence of FXIII nearly equaled the clot strength of pdFib. In the case of a commercial FS, the addition of FXIII at FXIII to Fib molar ratio of 0.16 to commercial biotherapeutic FS formulated 9 mg/mL resulted in the same maximum amplitude as commercial FS formulated at a minimum of 34 mg/mL Fib. In addition, the maximum amplitude of the sample containing 9 mg/mL Fib was reached in 450 seconds, significantly less than the label strength FS which took 1000 seconds to reach the same clot strength. However, when commercial biotherapeutic FS was formulated at 3 mg/mL, the addition of FXIII exhibited reduced clotting strength with identical clot kinetics, indicating a lower threshold for this effect.

Upon examining the TEG cups after successful completion of the experiments, several different morphologies were seen (Fig 7.5-7.8). All images without removed pins shown indicate that no clot was attached to the pin. The 3 mg/mL Fib FS and PPP exhibited limited solidification and almost no attachment to the pin. Higher concentrations of FS exhibited weak attachment to the pin and strong attachment to the outer wall. The gap between the clot attached to the outer wall of the TEG cup and the pin was reduced as FS concentration increased. In NHB dosed with FS, PRP with and without added FS, and PPP with 5 mg/mL FS added, the clot attached to the pin and could be removed from the TEG cup with the clot still attached. These samples had the smallest liquid gaps between the clot and the walls of the TEG cup and often demonstrated attachment to the outer wall upon removal of the pin.

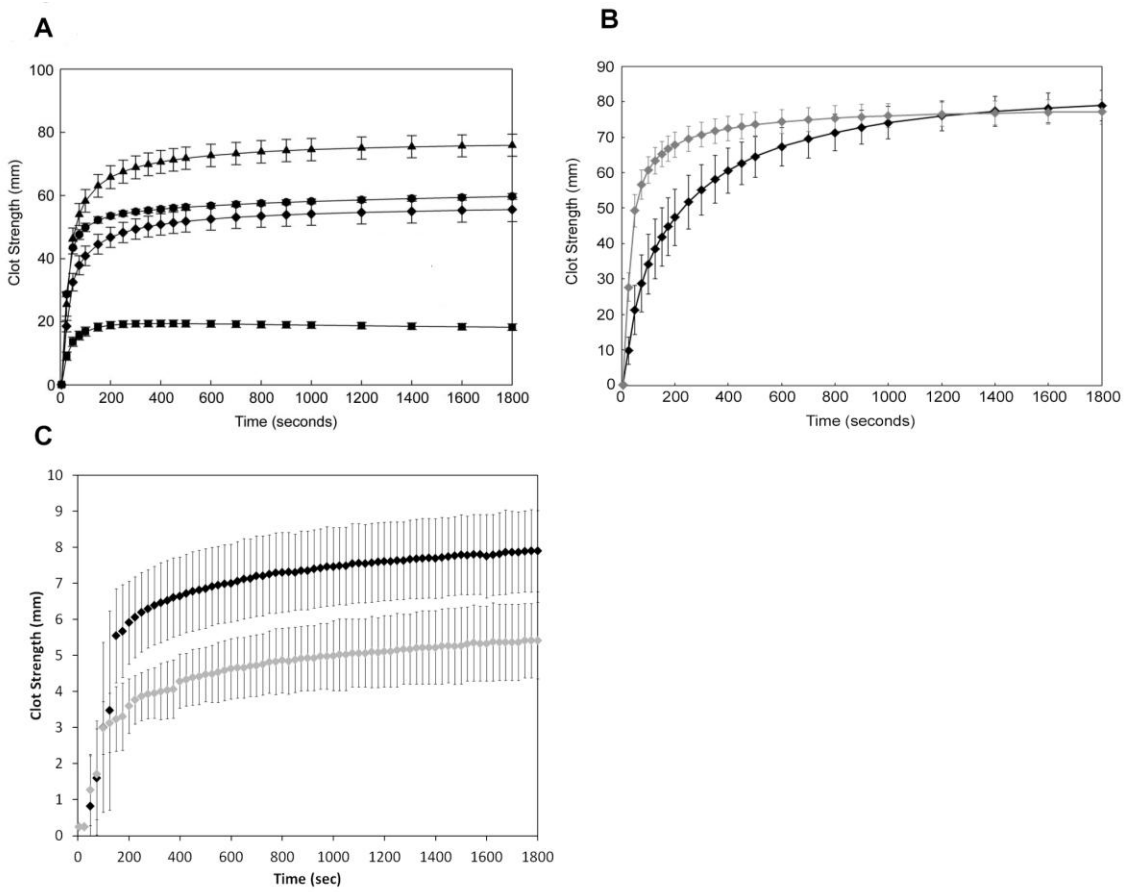

Figure 7.4.Viscoelastic characterization of pdFib and rFib treated with IIa with and without added FXIII. A) TEG analysis of the kinetics of clot initiation and clot strength over time for 9 mg/mL pdFI activated by rFIIa without added FXIII (●), 9 mg/mL pdFI activated by IIa with added FXIII (▲), 9 mg/mL rFib activated by IIa without added FXIII (■), and 9 mg/mL rFib activated by IIa with added FXIII (◆). Data are expressed as mean ± standard deviation. B) TEG analysis of the kinetics of clot initiation and clot strength over time for 34 mg/mL biotherapeutic grade FS without exogenous FXIII (◆) and 9 mg/mL biotherapeutic grade FS with added FXIII (◆). C) TEG analysis of the kinetics of clot initiation and clot strength over time for 3 mg/mL biotherapeutic grade FS without exogenous FXIII (◆) and 3 mg/mL biotherapeutic grade FS with added FXIII (◆).

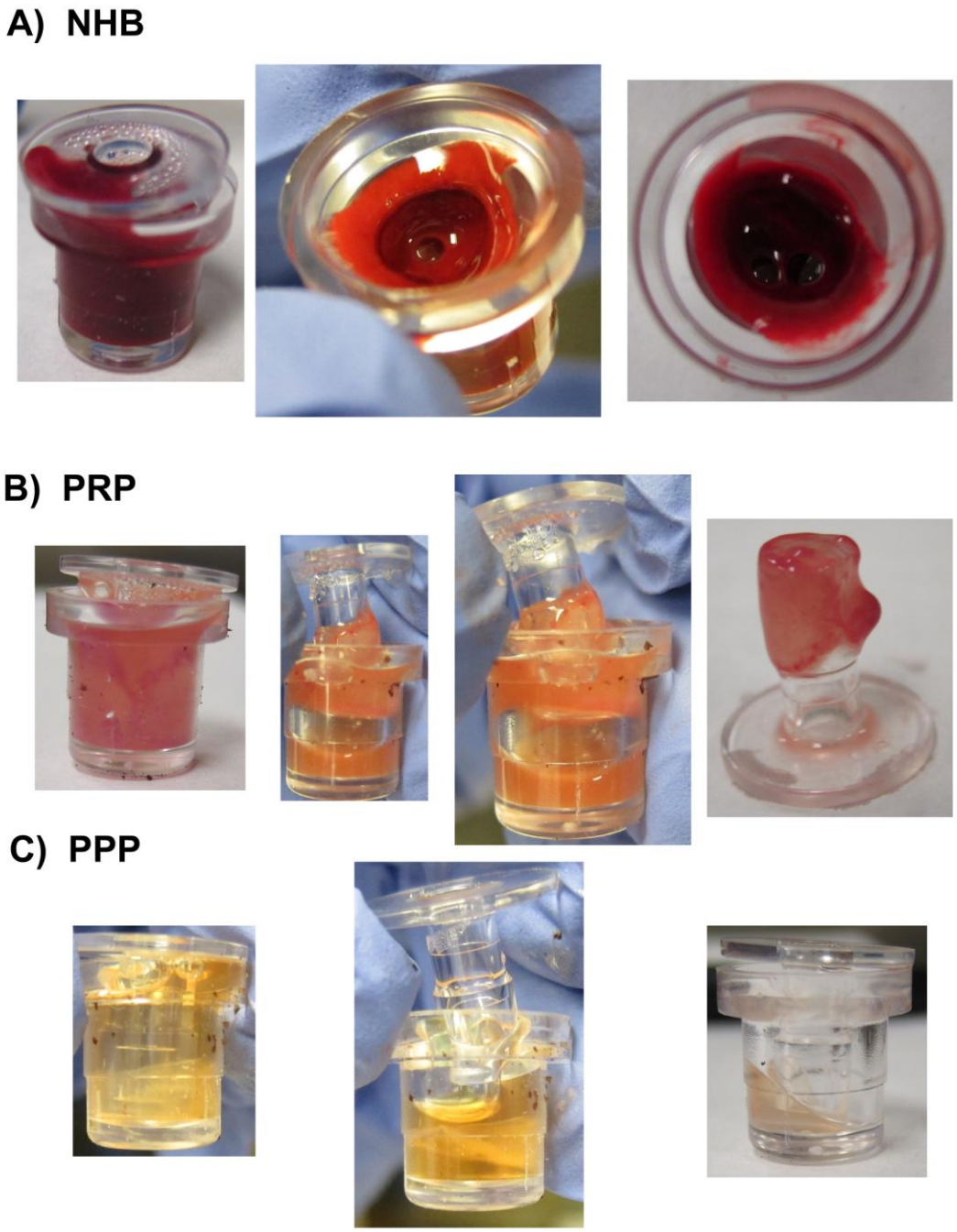

7.5 Normal TEG morphology for normal human blood products. A) In NHB, the clot formed alongside the outer wall with a small liquid gap between the clot and the pin; B) In PRP, the clot formed alongside the pin with a medium liquid gap between the outer wall and the clot; C) In PPP, the clot formed as a mixture that did not attach to the TEG cup.

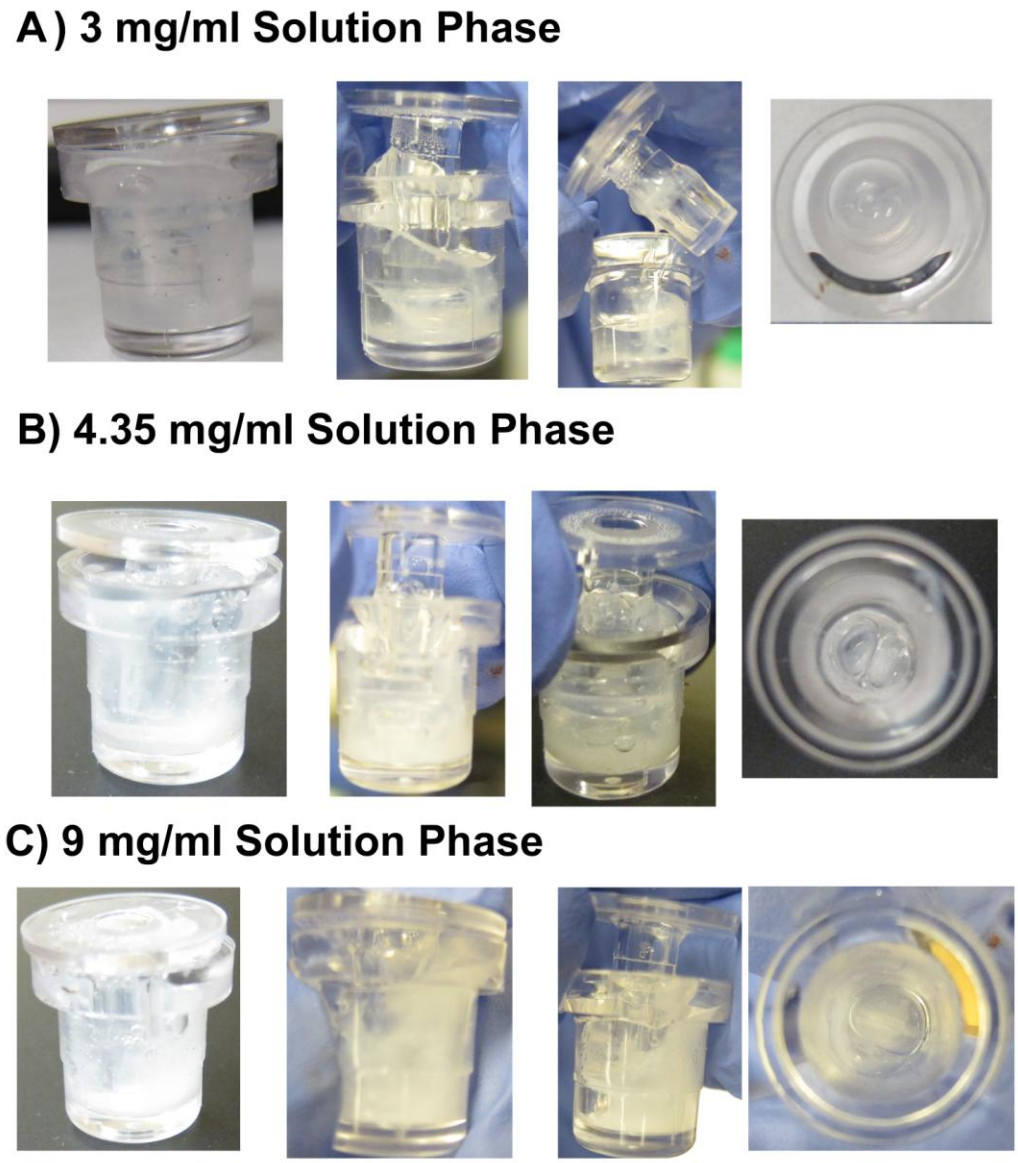

Figure 7.6. Changes in TEG transport model based on concentrations of fibrin sealant coagulation factors. A) At 3 mg/mL pdFib FS, a thin layer of sealant attached to the outer wall of TEG cup with a large liquid gap between the pin and the FS; B) At 4.35 mg/mL pdFib FS, a medium layer of sealant attached to the outer wall of TEG cup with a small liquid gap between the pin and the FS; C) At 9 mg/mL pdFib FS, a large layer of sealant attached to the outer wall with no liquid gap between the walls and the FS.

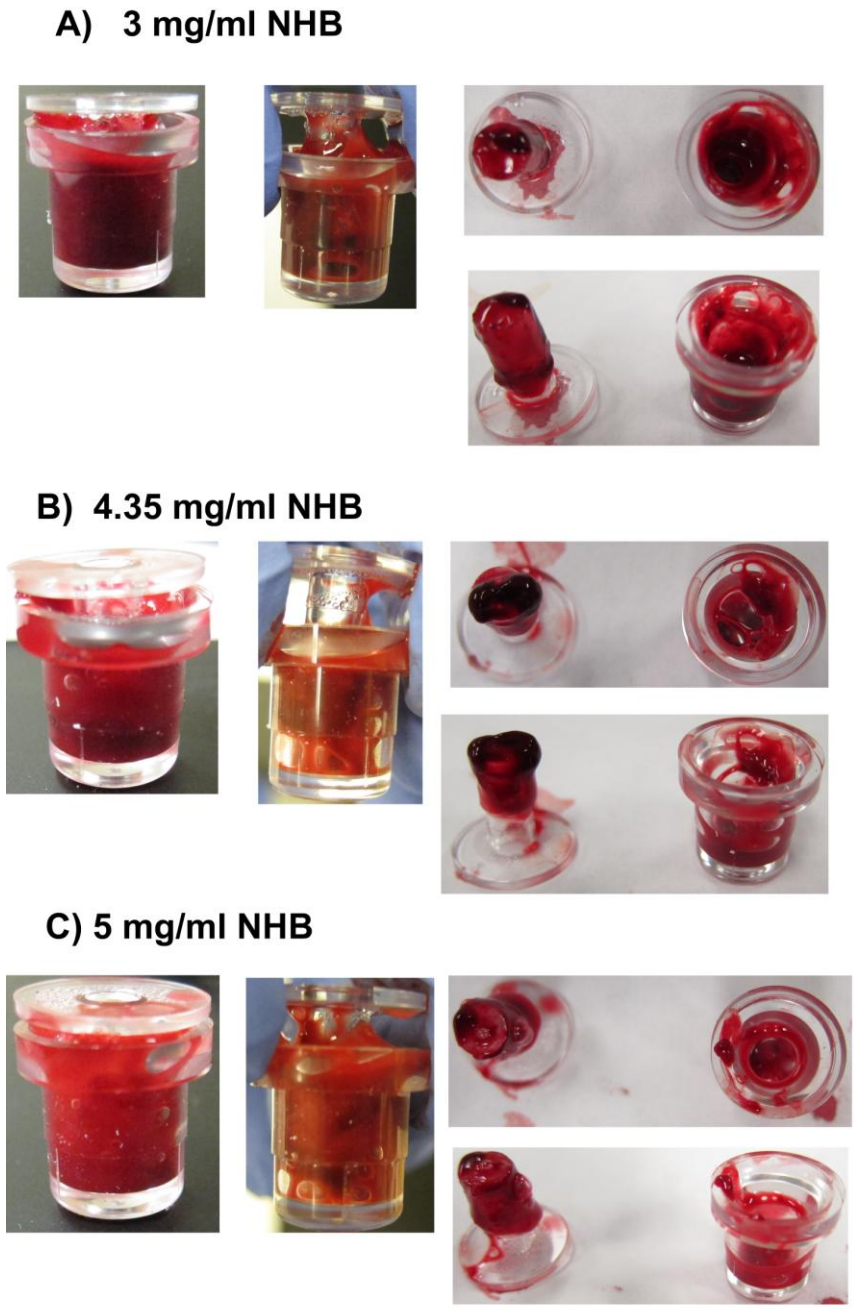

Figure 7.7. Changes in TEG transport model based on concentrations of fibrin sealant coagulation factors added to Normal Human Blood. A) In NHB with 3 mg/mL pdFib FS added, a medium layer of clot attached to the pin of TEG cup with a medium liquid gap between the outer wall and the clot; B) In NHB with 4.35 mg/mL pdFib FS added, a medium layer of clot attached to the pin of TEG cup with a small liquid gap between the outer wall and the clot; C) In NHB with 9 mg/mL pdFib FS added, a larger layer of clot attached to the outer wall with a minimal liquid gap between the walls and the clot.

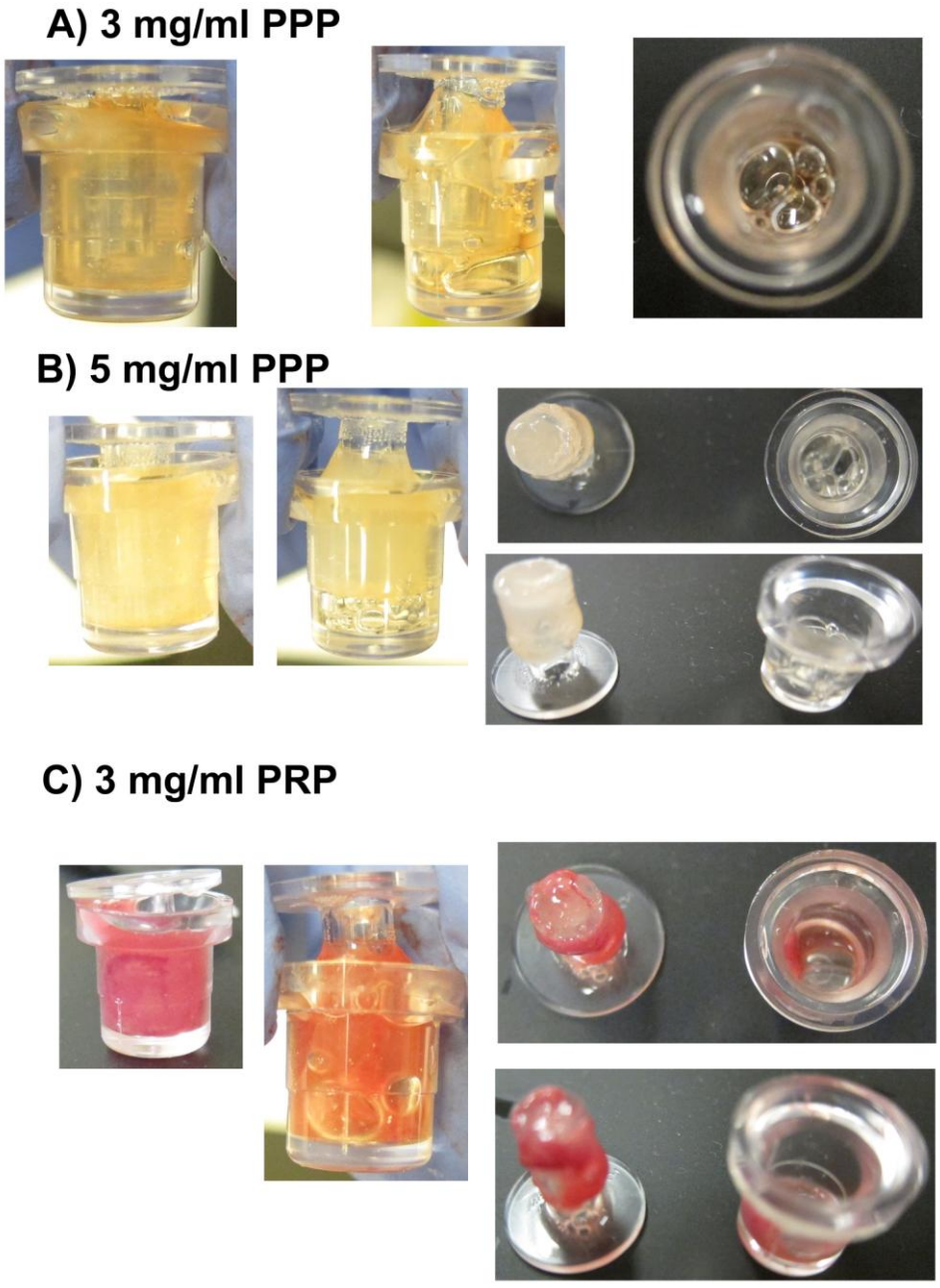

Figure 7.8. Changes in TEG transport model based on concentrations of fibrin sealant coagulation factors added to PRP and PPP. In PPP with 3 mg/mL pdFib FS added, a medium layer of clot attached to the outer wall of TEG cup with a medium liquid gap between the pin and the clot; B) In PPP with 5 mg/mL pdFib FS added, a larger layer of clot attached to the pin of TEG cup with a small liquid gap between the outer wall and the clot; C) In PRP with 3 mg/mL pdFib FS added, a larger layer of clot attached to the pin with a minimal liquid gap between clot and the walls of the TEG cup.

7.5 Discussion

We have demonstrated that at least four different morphologies can occur during TEG: a non-solidified clot which does not attach to the TEG cup, a clot which attaches to the outer wall of the TEG cup leaving a liquid gap between the clot and pin, a clot which attaches to the pin of the TEG cup leaving a liquid gap between the clot and outer wall, and a clot which attaches to both the pin and outer wall. While technical limitations prevent us from observing the TEG while running, these post-experimentation observation allow us to draw some qualitative conclusions. The location of the attachment of the clot plays a large role in the modeling of the strength and clot formation. If the clot attaches to the outer wall and is insufficient in size to attach to the pin, the TEG will measure a different phenomenon than a clot that attaches to a both walls. Transport phenomenon shows the profound differences in the cases of annulus where the inner and outer ring are rotating [12], and the addition of multiple, shearing layers of expanding and contracting clot only expands the complexity of modeling these scenarios. While TEG provides accurate and robust data for the cases of attachment of the clot to both walls, the accuracy of the device for low concentrations of platelets and fibrinogen must be re-evaluated.

The differences in impact of FXIII on maximum clot strength can be explained by the compaction of the clot by platelet borne and exogenous FXIII. Previous studies have shown both *ex vivo* and *in vivo* that blood without FXIII exhibits larger clots with lower strength [13-16]. From this it can be hypothesized that the reduced clot size of samples containing FXIII directly impacts the likelihood of attachment to both the pin and outer wall of the TEG cup. As resistance of the torsion wire used to detect increased clot

strength depends on attachment to both walls, the effect of FXIII on clot strength may need to be re-evaluated using a methodology that can account for decreased clot size.

The total clotting time also indicates a profound resiliency of coagulation cascade to modification. Samples of NHB with added coagulation factors exhibited largely unchanged total clotting time unless additional IIa, FXIII, and Fib were all present. In PRP, a subpopulation with increased concentration of coagulation factors bound to platelets [17, 18], the addition of FXIII and IIa appear to accelerate total clot formation. rFib and FXIII without additional IIa introduces new kinetic lag. While new experimental methodology is necessary to determine the exact kinetics of the human blood products with and without additional coagulation factors due to both clot compaction and the natural variance between humans, these results present preliminary indications of the effects of IIa, FXIII, pdFib, and rFib on clot kinetics and strength.

7.6 Acknowledgements

I would like to thank Jennifer Calcaterra, who in addition to laying the groundwork for this chapter and performing many of the initial experiments, taught me everything from FXIII purification to FS optimization. Leonard Akert also spent many hours modifying TEG cups for the initial experimentation. This work was supported by a grant from the Department of Defense titled “Production and Purification of Fibrinogen Components for the Production of a Fibrin Sealant Hemostatic Dressing.”

8.7 References

1 Furie B, Furie BC. The molecular basis of blood coagulation. *Cell*. 1988; **53**: 505-18.

2 Jackson CM, Nemerson Y. Blood coagulation. *Annual review of biochemistry*. 1980; **49**: 765-811.
3 Wolberg AS. Thrombin generation and fibrin clot structure. *Blood reviews*. 2007; **21**: 131-42.
4 Carlson MA, Calcaterra J, Johanning JM, Pipinos II, Cordes CM, Velander WH. A totally recombinant human fibrin Sealant. *Journal of Surgical Research*. 2013.
5 Radosevich M, Goubran H, Burnouf T. Fibrin sealant: scientific rationale, production methods, properties, and current clinical use. *Vox sanguinis*. 1997; **72**: 133-43.
6 Sierra DH. Fibrin sealant adhesive systems: a review of their chemistry, material properties and clinical applications. *Journal of Biomaterials Applications*. 1993; **7**: 309-52.
7 Jackson MR. Fibrin sealants in surgical practice: an overview. *The American journal of surgery*. 2001; **182**: S1-S7.
8 Hethershaw EL, Cilia La Corte AL, Duval C, Ali M, Grant PJ, Ariëns RA, Philippou H. The Effect of Blood Coagulation Factor XIII on Fibrin Clot Structure and Fibrinolysis. *Journal of Thrombosis and Haemostasis*. 2013.
9 Jackson G, Ashpole K, Yentis S. The TEG® vs the ROTEM® thromboelastography/thromboelastometry systems. *Anaesthesia*. 2009; **64**: 212-5.
10 Chitlur M, Rivard GE, Lillicrap D, Mann K, Shima M, Young G. Recommendations for performing thromboelastography/thromboelastometry in hemophilia: communication from the SSC of the ISTH. *Journal of Thrombosis and Haemostasis*. 2014; **12**: 103-6.
11 Whitten CW, Greilich PE. Thromboelastography®: Past, Present, and Future. *Anesthesiology*. 2000; **92**: 1226.
12 Bird RB, Stewart WE, Lightfoot EN. *Transport phenomena*. John Wiley & Sons, 2007.
13 Cohen I, Gerrard JM, White JG. Ultrastructure of clots during isometric contraction. *The Journal of cell biology*. 1982; **93**: 775-87.
14 Kasahara K, Souri M, Kaneda M, Miki T, Yamamoto N, Ichinose A. Impaired clot retraction in factor XIII A subunit–deficient mice. *Blood*. 2010; **115**: 1277-9.
15 Ono A, Westein E, Hsiao S, Nesbitt WS, Hamilton JR, Schoenwaelder SM, Jackson SP. Identification of a fibrin-independent platelet contractile mechanism regulating primary hemostasis and thrombus growth. *Blood*. 2008; **112**: 90-9.
16 Devine DV, Bishop PD. Platelet-associated factor XIII in platelet activation, adhesion, and clot stabilization. *Seminars in thrombosis and hemostasis*: Copyright© 1996 by Thieme Medical Publishers, Inc., 1996, 409-13.
17 Gorbet MB, Sefton MV. Biomaterial-associated thrombosis: roles of coagulation factors, complement, platelets and leukocytes. *Biomaterials*. 2004; **25**: 5681-703.
18 Ariens RA, Lai TS, Weisel JW, Greenberg CS, Grant PJ. Role of factor XIII in fibrin clot formation and effects of genetic polymorphisms. *Blood*. 2002; **100**: 743.

Chapter 8:

Treatment of Hepatic Resection in Swine using Novel Delivery Methods for Fibrin Sealant

Nicholas C. Vanderslice*, Jennifer Calcaterra*, Ayman Ismail*, Mostafa Fatemi**, Ujwal Yanala***, Gustavo Larsen*, Luis Nuñez**, Mark A. Carlson***, William H. Velander*

* Chemical and Biomolecular Engineering, University of Nebraska

** LNK CHEMsolutions, LLC

*** Department of Surgery, University of Nebraska Medical Center

8.1 Abstract

Fibrinogen, factor XIII, and thrombin are three coagulation factors that can be used to create a liquid fibrin sealant (FS) capable of regaining hemostasis in the case of uncontrolled bleeding. Several novel prototype systems have been designed to apply FS derived from recombinant and human plasma sources. A porcine hepatic resection model was developed as a tool to study FS hemostatic devices. Several prototype applications platforms were designed to deliver FS to the wound site. These device designs include: a spray device capable of delivering a mist of FS to the wound site, a biodegradable electrospun polymer gauze treated with FS before application to the liver, and a carrier foam device capable of creating an abdominal tamponade effect while delivering FS to the site of the injury. Including control surgeries, over 200 combined swine surgeries have been performed to date using these devices. Together these devices provide a suite

of applications that have potential medical uses for applying fibrin sealant in both emergency and surgical applications.

8.2 Introduction

Liquid fibrin sealant (FS) has been commercially available since the 1970s [1] for treatment of severe hemorrhage. Containing fibrinogen (FI) [2-4], thrombin (FIIa) [5, 6], and occasionally factor XII (FXIII) [7, 8], FS forms a thick fibrin gel that is capable of adhering to a wound site and ceasing blood loss [9-12]. However, several technical and economic issues have limited the number of applications for FS. Foremost of these issues is the prohibitive cost of plasma-derived coagulation factors. The cost of these factors depends on the availability of donor blood [13], a commodity in notoriously high-demand.

The recent advent of recombinant technology provides an alternative avenue for approaching the supply of coagulation factors, but due to the high complexity of most coagulation factors, mammalian cells are required to produce most coagulation serine proteases and glycoproteins [2, 9, 14]. Concomitant to this is the large amount of materials needed to ensure that the FS is not carried away from the wound site by the blood loss. Due to both of these issues, the US defense department has sponsored various programs to develop devices that can economically be used to treat combat injuries [15, 16].

Current delivery devices rely on either a disposable dual syringe (Duploject, Baxter) (Fig. 8.1A) or aerosolization (PTI) to deliver FI and FII independently to the wound site without significantly clogging the device. We have previously published

information on a modified, preclinical dual-syringe designed to deliver FS without developing a clot in the syringe (Fig 8.1B) [9, 17] and previous dissertations [18] have described a spray device designed to deliver FS directly to the wound site (Fig. 8.1C) and a bioabsorbable propriety electrospun poly(D,L-lactide) (PLA) polymer (Fig. 8.1D) designed to be coated with FS and provide a scaffold that ensures the FS is applied directly to the wound site with limited washing away of the coagulation factors. This chapter is designed to show the progress made in designing a robust FS delivery device capable of treating severe hemorrhaging.

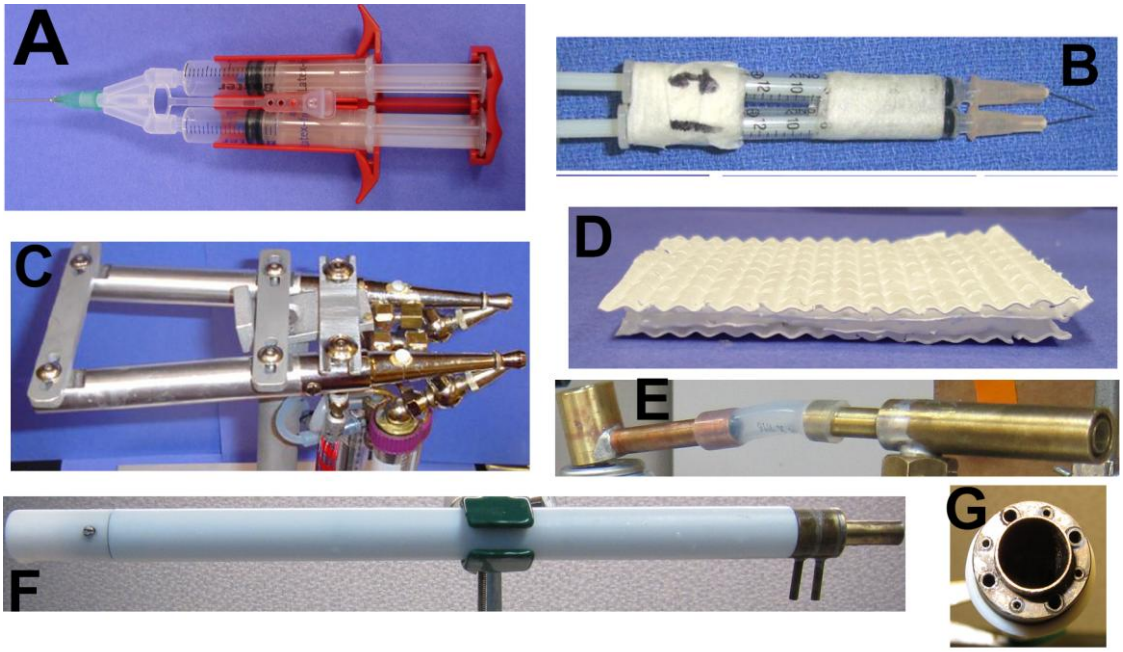

Figure 8.1. Fibrin sealant devices used for swine surgeries. Proprietary dual-chamber syringe device (Duploject, Baxter) for administration of the commercial FS [2]. (B) Improvised double syringe assembly for administration of FS [2]. (C) Dual-airbrush FS device designed to mix fibrin sealant as a mist in transport (D) Perforated, corrugated PLA bandage. (E) Device designed to coat carrier foam with FS. (E) Multi-channel device designed to coat carrier foam with FS. (G) Front of multi-channel device. Large channels are designed to carry highly viscous fibrinogen at the same rate as the low viscosity thrombin and factor XIII in the smaller channels.

8.3 Materials and Methods

Materials

Recombinant thrombin (Recothrom®) was purchased from Zymogenetics. Purified plasma-derived fibrinogen was purchased from Enzyme Research Laboratories or purified from donated blood. Purified recombinant fibrinogen (rFI), expressed in the milk of transgenic Swiss Brown cows, was obtained from Pharming Group NV (Leiden, Netherlands). Recombinant FXIII was obtained from *Pichia pastoris* using methods described in Chapter 6. Unless otherwise specified, reagents were purchased from Sigma (St. Louis, MO). Shaving cream (Barbasol) or proprietary butane propelled alginate foam (LNK Chemsolutions) was used as FS carrier foam for these studies. FS was applied at 9 mg/mL FI, 0.36 mg/mL FXIII, and 0.18 mg/mL FII. These levels were previously determined to be optimal for maximum clot strength and minimum clot formation time [9, 18].

Swine Studies

Surgeries were conducted on crossbred commercial (domestic) swine from UNL Agricultural Research and Development Center (Mead). The Omaha Veteran's Affairs Institutional Animal Care and Use Committee approved all procedures. All animals were treated according to the *Guide for the Care and Use of Laboratory Animals* (National Institute of Health publication 86-23, revised 1996).

The abdominal cavity of the anesthetized swine was opened prior to hepatic resection. A splenectomy was performed on the animal to allow for exsanguination similar to humans to occur after hepatic resection. The portal and hepatic veins of the left

lateral lobe of the animals were transected and allowed to bleed for 30 seconds before administration of FS-coated carrier foam. Hemostats were used to seal the abdominal cavity and pressure was allowed to build inside the cavity. Animals were observed for 1 hour or 3 hours unless exsanguination occurred prior to this time. Animals surviving the observation period were euthanized and a post-mortem analysis was conducted on the liver for presence of clot at the site of the injury and to ensure transection of the portal and hepatic veins. The atriums of the heart were also opened to detect the presence of clot or foam inside.

Liquid Fibrin Sealant Coated Carrier Foam Device

An annulus device was designed to deliver FS coated carrier foam to the abdominal cavity of the swine (Fig. 8.1E). This device contained a large inner tube for delivery of carrier foam, and was surrounded by an isolated outer ring that delivers the FS around the foam. The device used the 28 mL delivery system described in a previous dissertation [18]. This system was designed to simultaneously deliver a 14 mL mixture of fibrinogen and Ringer's solution in addition to 14 mL mixture of FII, FXIII, calcium, and Ringer's Solution.

Multi-Channel Liquid Fibrin Sealant Coated Carrier Foam Device

A multi-channel device was designed to delivery FS-coated carrier foam directly to the wound site using longer channels that mixed the FS components directly at the site of coating (Figure 8.1 F and 8.1G). This device contains 8 staggered channels designed to mix of the fibrinogen with FXIII and FII on the carrier foam inside a beveled tip of the device. This bevel applies minimal compaction to the foam while preventing the FS from being sprayed into the wound site. Large channels of the device are designed to carry

highly viscous fibrinogen at the same rates as lower viscosity FXIII and FII in the smaller tubes. A second set of reservoirs for FS was also constructed to allow the use two 45 mL tubes instead of the previous 15 mL tubes.

8.4 Results and Discussion

Liquid Fibrin Sealant Coated Carrier Foam Device

The FS-coated carrier device proved to be an adequate device for applying the materials to the wound site. However, several technical problems prevented significant study of this device. The foremost issue was the mixing of the FS inside of the device, resulting in clot formation inside the nozzle that prevented the material from coating the carrier foam. FS also tended to unequally coat the bottom side of the foam due to gravitational effects. Additionally, while the short nozzle proved effective for coating the foam *in vitro,* the device ultimately proved difficult to position in the surgical theatre and unable to penetrate deep enough into the abdominal cavity to reliably deliver the FS-coated foam.

Multi-Channel Liquid Fibrin Sealant Coated Carrier Foam Device

The multi-channel device fixed many of the issues that plagued the initial device. The longer nozzle allowed for easier manipulation and application of the foam directly to a desired location in the abdominal cavity (Fig. 8.2A). The device also has minimal clotting issues as long as the delivery pressures of both the carrier foam and FS remain approximately the same. In addition, a more consistent cyclical coating was applied due to the multiple channels.

While the carrier foam is still in the process of being optimally designed by LNK Chemsolutions, two morphologies of FS coated alginate foam have been observed. The first formulation conformed to the shape of the abdominal cavity and organs of the swine (Fig. 8.2 B). This foam also demonstrated a decrease from 4 L of foam injected into the cavity to less than 1 L of foam removed from the cavity 60 minutes after injection. This dissociation or compaction of foam proved insufficient for maintaining a tamponade effect at the injury site. A second formulation containing an increased percentage of alginate was formulated and provided a "tofu-like" morphology that maintained the tamponade effect for three hours (Fig. 8.2C)

The application of FS coated carrier foam in preclinical trials did not present with unqualified success. The current version of the device has had 8 preclinical trials, 50% which survived for at least 1 hour, however, 37.5% of the swine presented with either a foam or clot obstruction in the heart (Fig. 8.3), and one swine did not respond to treatment. Compared to a 60% survival rate in control surgeries, it is clear that more work must be done to ensure that the treatment is not riskier than the injury alone. However, post-mortem analysis of the livers of some surviving pigs (Fig. 8.4) indicates the goal of forming a clot around the wound site while applying a tamponade effect to prevent further bleeding is obtainable.

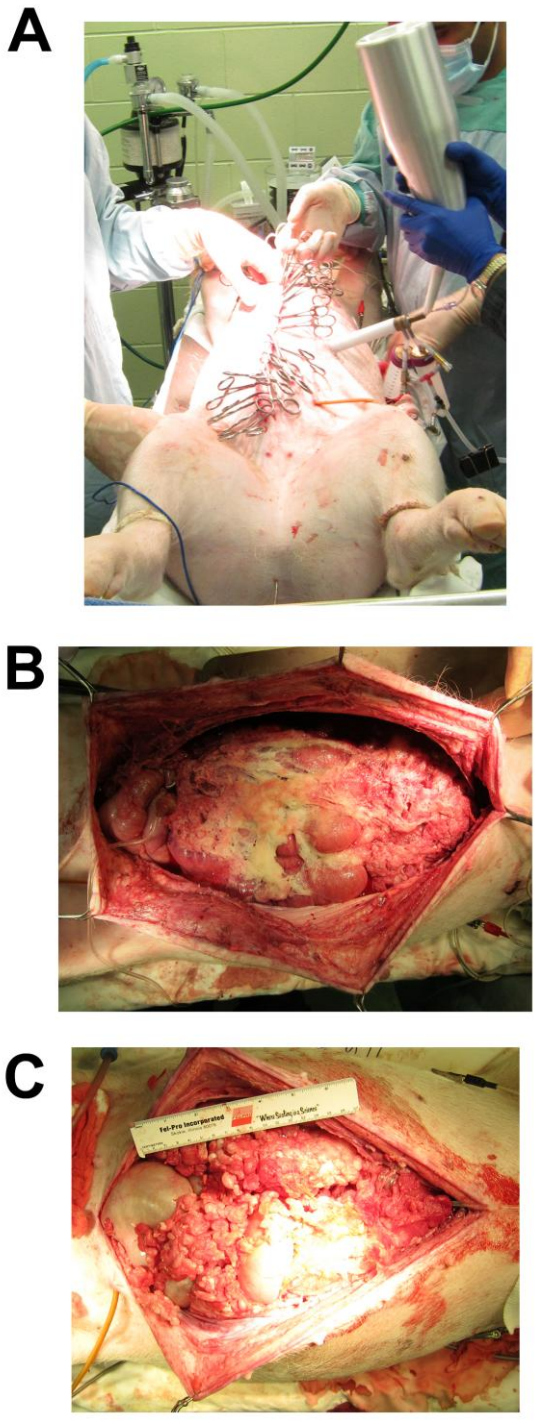

Figure 8.2. Delivery of fibrin sealant coated carrier foam to a swine abdominal cavity. Injection of the foam 30 seconds after liver resection. B) Swine abdominal cavity one hour after administration of first prototype carrier foam. C) Swine abdominal cavity one hour after administration of second prototype carrier foam.

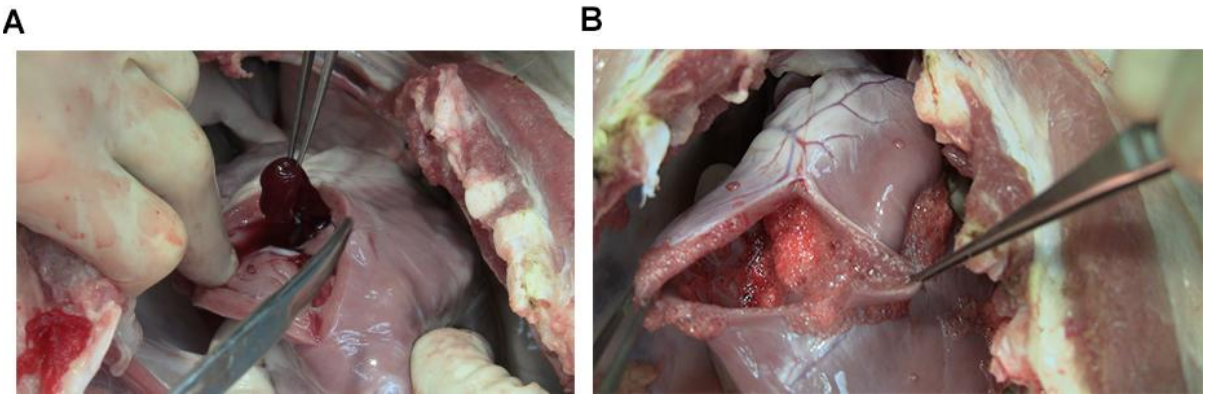

Figure 8.3. Formation of blockages in the heart of swine. A) Blockage formed by clotting factors and endogenous blood. B) Blockage formed by FS coated carrier foam.

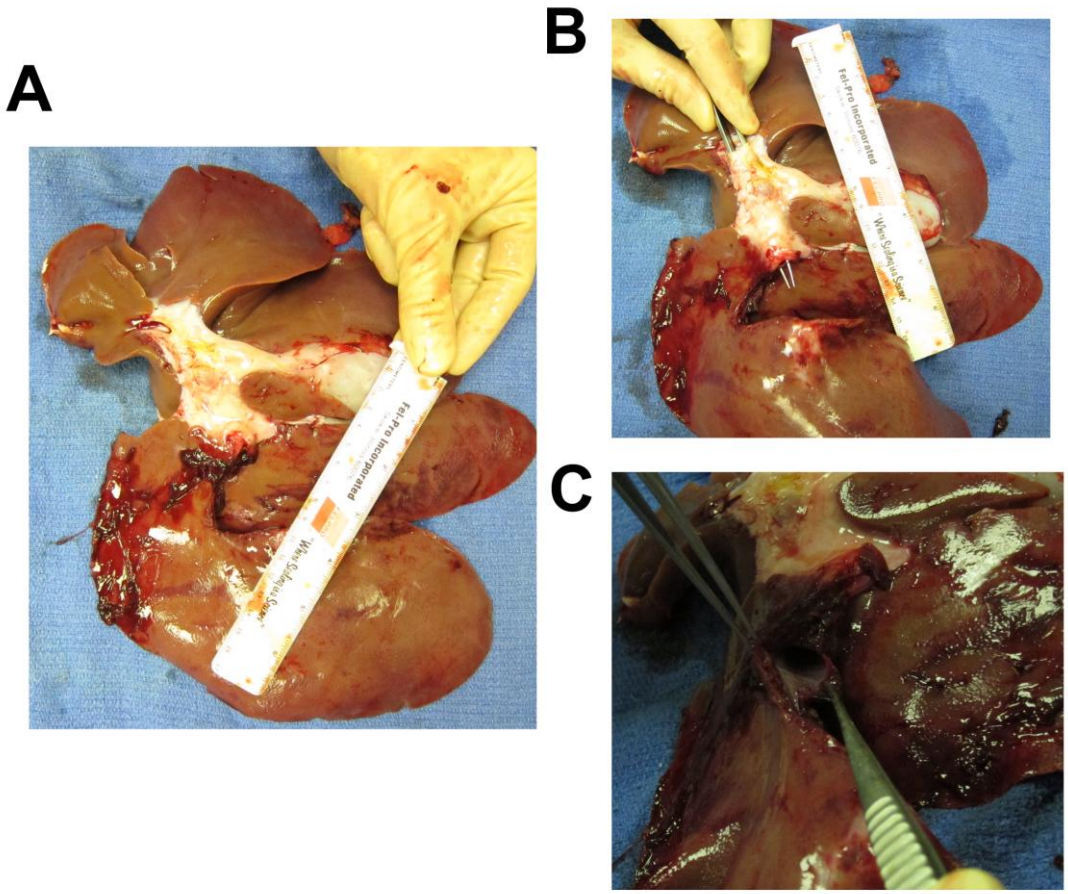

Figure 8.4. Post-mortem analysis of hepatic resection. FS coated carrier foam was delivered to the swine abdominal cavity after hepatic resection. The swine survived for the one-hour observation period. A)

Post-mortem removal of the liver revealed the presence of clot at the site of the hepatic resection. B) After removal of the clot at the site of the liver, the portal vein branch to the left lateral lobe and C) hepatic vein were confirmed to be transected.

8.5 Acknowledgements

I would like to thank Jennifer Calcaterra and Ayman Ismail for their assistance in these surgeries. I am also grateful to Dr. Mark Carlson, Dr. John Cavanaugh, and Dr. Ujwal Yanala, Dean Heimann, and Chris Hansen for assisting and carrying out these surgical procedures. Additionally, I would like to thank Mostafa Fatemi, Dr. Gustavo Larsen, Dr. Ruben Spretz, and Dr. Sandra Noriega for providing many different polymer gauzes and carrier foams. Finally, I would like to thank Leonard Akert for designing and producing these devices, often at less than ideal notice, and for always coming up with solutions to our multitude of problems. This work was supported by a grant from the Department of Defense titled "Production and Purification of Fibrinogen Components for the Production of a Fibrin Sealant Hemostatic Dressing."

8.6 References

1 Radosevich M, Goubran H, Burnouf T. Fibrin sealant: scientific rationale, production methods, properties, and current clinical use. *Vox sanguinis*. 1997; **72**: 133-43.

2 Calcaterra J, Van Cott KE, Butler SP, Gil GC, Germano M, van Veen HA, Nelson K, Forsberg EJ, Carlson MA, Velander WH. Recombinant Human Fibrinogen That Produces Thick Fibrin Fibers with Increased Wound Adhesion and Clot Density. *Biomacromolecules*. 2013; **14**: 169-78.

3 Doolittle RF. Fibrinogen and fibrin. *eLS*. 2001.

4 Sierra DH. Fibrin sealant adhesive systems: a review of their chemistry, material properties and clinical applications. *Journal of Biomaterials Applications*. 1993; **7**: 309-52.

5 Greenberg CS, Miraglia CC, Rickles FR, Shuman MA. Cleavage of blood coagulation factor XIII and fibrinogen by thrombin during in vitro clotting. *Journal of Clinical Investigation*. 1985; **75**: 1463.
6 Ratner M. Recombinant thrombin approved. *Nature Biotechnology*. 2008; **26**: 250-.
7 Ariens RA, Lai TS, Weisel JW, Greenberg CS, Grant PJ. Role of factor XIII in fibrin clot formation and effects of genetic polymorphisms. *Blood*. 2002; **100**: 743.
8 Marx G, Mou X. Characterizing fibrin glue performance as modulated by heparin, aprotinin, and factor XIII. *Journal of Laboratory and Clinical Medicine*. 2002; **140**: 152-60.
9 Carlson MA, Calcaterra J, Johanning JM, Pipinos II, Cordes CM, Velander WH. A totally recombinant human fibrin Sealant. *Journal of Surgical Research*. 2013.
10 Dunn CJ, Goa KL. Fibrin sealant. *Drugs*. 1999; **58**: 863-86.
11 Jackson MR. Fibrin sealants in surgical practice: an overview. *The American journal of surgery*. 2001; **182**: S1-S7.
12 Spotnitz WD. Fibrin sealant: past, present, and future: a brief review. *World journal of surgery*. 2010; **34**: 632-4.
13 Frey BM, Schlenke P. Safeguards in blood supply: a national and European challenge. *Transfusion Medicine and Hemotherapy*. 2010; **37**: 109-10.
14 Morcöl T, Akers RM, Johnson JL, Williams BL, Gwazdauskas FC, Knight JW, Lubon H, Paleyanda RK, Drohan WN, Velander WH. The Porcine Mammary Gland as a Bioreactor for Complex Proteinsa. *Annals of the New York Academy of Sciences*. 1994; **721**: 218-33.
15 Baer D, Dubick M, Wenke J, Brown K, McGhee L, Convertino V, Cancio LC, Wolf SE, Blackbourne LH. Combat casualty care research at the US Army Institute of Surgical Research. *Journal of the Royal Army Medical Corps*. 2009; **155**: 327-32.
16 Pusateri AE, Holcomb JB, Kheirabadi BS, Alam HB, Wade CE, Ryan KL. Making sense of the preclinical literature on advanced hemostatic products. *Journal of Trauma-Injury, Infection, and Critical Care*. 2006; **60**: 674-82.
17 Calcaterra J, Van Cott KE, Butler SP, Gil GC, Germano M, van Veen HA, Nelson K, Forsberg EJ, Carlson MA, Velander WH. Recombinant human fibrinogen that produces thick fibrin fibers with increased wound adhesion and clot density. *Biomacromolecules*. 2012; **14**: 169-78.
18 Calcaterra J. Recombinant factors for hemostasis. *ETD collection for University of Nebraska - Lincoln*. 2010: Paper AAI3412913.

Chapter 9:

Future Work

9.1 Preclinical Trials of r-FXIIIA1a for Topical Use alongside Commercial Coagulation Proteins

Intravenous administration of activated coagulation factors has recently become an issue of concern after factor VIIa was found to be linked to adverse thrombotic events [1]. However, r-FXIIIA1a still has numerous applications as a topical treatment in conjunction with other proteins. Treatments for burns [2], venous ulcers [3], and lacerations [4, 5] all have the potential to benefit from a topical FXIII. The lack of an activation lag for r-FXIIIA1a, as discussed in Chapter 2, allows for treatments to be effective in a small time frame. A preclinical trial designed to test r-FXIIIa alone, in conjecture with commercial r-FIIa, and with commercial fibrin sealant for treatment of the above mentioned ailments in mice would be the ideal next step for this protein.

9.2 Future Animal Models for Study of the Reservoir Phenomena of FIX

The reservoir phenomena of FIX have been indirectly characterized by the pharmacokinetic studies detailed in Chapters 4-6; however direct measurements of FIX storage in the extravascular reservoirs will be necessary in order to change the modern perception of hemophilia treatment. Preclinical trials in mice where histological data of the extravascular matrix is assayed using anti-FIX antibodies will be the next necessary step in the research. The histology will have to take into account both transport and

sequestration phenomena by taking multiple samples at set linear venous distances from the injection site. The research of Dr. Stern must also be considered during this trial, where bovine FIX was shown to have stronger affinity for the endothelium of baboon than baboon FIX [6], as the affinity of human tg-FIX for the extravascular matrix of mice may be different than the affinity of human tg-FIX for the extravascular matrix of humans.

9.3 Transgenically Modified Swine expressing VKOR and FIX

One of the few issues with current tg-FIX is that a considerable portion of the FIX is under-carboxylated [7, 8]. Under-carboxylated factor IX is both less active and cleared more rapidly from the bloodstream than factor IX [9]. Vitamin K epoxide reductase (VKOR) plays a role in carboxylation by recycling vitamin K [10-13]. By the addition of a VKOR to a site that produces FIX, a supply of active vitamin K can be maintained [14]. Studies in baby hamster kidney cells [15] and in mice [16] have previously established that the addition of VKOR to a construct is capable of enhancing the correct production of VKD proteins. The addition of the VKOR construct to our mammary gland ensures that less under-carboxylated FIX is produced, ensuring a higher-throughput of fully formed FIX. As the mammary gland is not known for producing an excess of VKOR, we have designed a this new swine construct using methods similar to Chauhan et al. [17] to express FIX and VKOR simultaneously, shown in Figure 9.1. In December 2012, two different lineages of the bigenic FIX/VKOR pigs were born, each containing one female pig; however, neither lineage survived long enough to be bred. A new construct has been built and will be used for future pigs. By purifying and analyzing the bigenic milk from

these new animals, a more consistently γ-carboxylated version of FIX will be purified, characterized, and formulated [18] for delivery.

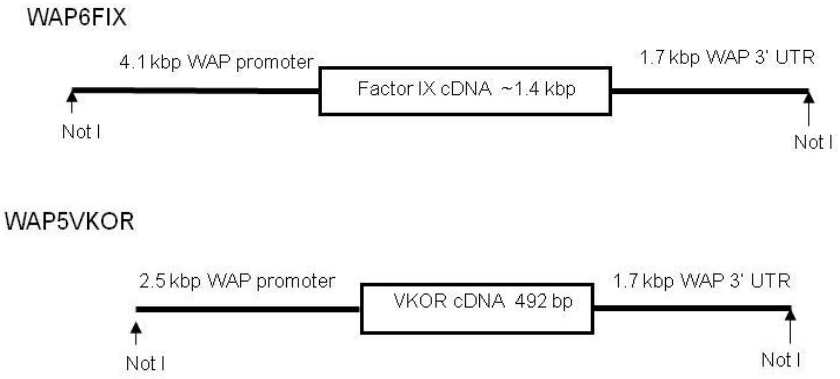

Figure 9.1. FIX and VKOR construct layout for bigenic swine [19].

9.4 Characterization of the Gla domain for pd-FIX, r-FIX, and tg-FIX

The methodology and equipment for mass spectrometry has advanced in recent years, and the recent acquisition of a new tandem mass spectrometer by the University of Nebraska Beadle Center should open up the opportunity for a collaboration between the department of chemical and biomolecular engineering and the department of biochemistry to characterize the Gla domain of factor IX. This will allow the identification of the missing γ-carboxylation sites in both tg-FIX and r-FIX; which were identified in Chapter 5 as between Gla 7-10 for tg-FIX and between 11 and 12 for r-FIX [7]. In addition, using metal-dependent Gla domain antibodies in combination with mass spectrometry and Biacore, it will be possible to isolate species of FIX missing specific Gla residues, identify the missing residue using mass spectrometry, and identify the influence of specific Gla residues collagen binding. These studies will also help fully characterize the binding cite of the 1G7 mAb described in Chapter 5, and has the

potential to further characterize antibodies such as the Toomey [20] and Bajaj [21] antibodies.

9.5 Continued Progress in the Preclinical Trials of Liquid Fibrin Sealant

Preclinical trials for our FS have surpassed over 200 swine. However, due to supply issues, most of these trials have used r-FIIa, r-FXIIIa, and pd-FI. With the recent acquisition of the tg-FI producing cattle by LFB, it is likely that a supply of tg-FI will be available for future preclinical trials. Previous research by our group has already demonstrated a drastic visible difference between FS containing pd-FI and tg-FI, and future long-term survival studies and histology will be needed in order to confirm that tg-FI promotes wound healing in a comparable manner to pd-FI *in vivo*. In addition, the use of FS with carrier foam continues to be developed in collaboration with LNK. FS will need to be re-optimized for new prototype devices, new bio-absorbable polymers, and final concentrations to maximize wound sealing properties, bio-absorption, and promotion of native cells. Preclinical studies of the addition of fibronectin to FS will also need to be resumed during the survival studies in order assess changes in healing.

9.6 References

1 O'Connell KA, Wood JJ, Wise RP, Lozier JN, Braun MM. Thromboembolic adverse events after use of recombinant human coagulation factor VIIa. *Jama*. 2006; **295**: 293-8.

2 Ogawa T, Morioka Y, Inoue T, Takano M, Tsuda S. Involvement of blood coagulation factor XIII in burn healing in the carbon tetrachloride-induced hepatic injury model in rats. *Inflammation Research*. 1995; **44**: 264-8.

3 Wozniak G, Dapper F, Alemany J. Factor XIII in ulcerative leg disease: background and preliminary clinical results. *Seminars in thrombosis and hemostasis*: Copyright© 1996 by Thieme Medical Publishers, Inc., 1996, 445-50.

4 Gerlach R, Tölle F, Raabe A, Zimmermann M, Siegemund A, Seifert V. Increased Risk for Postoperative Hemorrhage After Intracranial Surgery in Patients With Decreased Factor XIII Activity Implications of a Prospective Study. *Stroke*. 2002; **33**: 1618-23.
5 Dunn CJ, Goa KL. Fibrin sealant. *Drugs*. 1999; **58**: 863-86.
6 Stern DM, Knitter G, Kisiel W, Nawroth PP. In vivo evidence of intravascular binding sites for coagulation factor IX. *British journal of haematology*. 1987; **66**: 227-32.
7 Gillis S, Furie BC, Furie B, Patel H, Huberty MC, Switzer M, Barry Foster W, Scoble HA, Bond MD. γ-Carboxyglutamic acids 36 and 40 do not contribute to human factor IX function. *Protein science*. 1997; **6**: 185-96.
8 Makino Y, Omichi K, Kuraya N, Ogawa H, Nishimura H, Iwanaga S, Hase S. Structural analysis of N-linked sugar chains of human blood clotting factor IX. *Journal of biochemistry*. 2000; **128**: 175-80.
9 Gui T, Lin H-F, Jin D-Y, Hoffman M, Straight DL, Roberts HR, Stafford DW. Circulating and binding characteristics of wild-type factor IX and certain Gla domain mutants in vivo. *Blood*. 2002; **100**: 153-8.
10 Furie B, Bouchard BA, Furie BC. Vitamin K-dependent biosynthesis of γ-carboxyglutamic acid. *Blood*. 1999; **93**: 1798-808.
11 Hallgren KW, Qian W, Yakubenko AV, Runge KW, Berkner KL. r-VKORC1 expression in factor IX BHK cells increases the extent of factor IX carboxylation but is limited by saturation of another carboxylation component or by a shift in the rate-limiting step. *Biochemistry*. 2006; **45**: 5587-98.
12 Li T, Chang C-Y, Jin D-Y, Lin P-J, Khvorova A, Stafford DW. Identification of the gene for vitamin K epoxide reductase. *Nature*. 2004; **427**: 541-4.
13 Stenina O, Pudota BN, McNally BA, Hommema EL, Berkner KL. Tethered processivity of the vitamin K-dependent carboxylase: factor IX is efficiently modified in a mechanism which distinguishes Gla's from Glu's and which accounts for comprehensive carboxylation in vivo. *Biochemistry*. 2001; **40**: 10301-9.
14 Suttie J. Synthesis of vitamin K-dependent proteins. *The FASEB journal*. 1993; **7**: 445-52.
15 Wajih N, Hutson SM, Owen J, Wallin R. Increased production of functional recombinant human clotting factor IX by baby hamster kidney cells engineered to overexpress VKORC1, the vitamin K 2, 3-epoxide-reducing enzyme of the vitamin K cycle. *Journal of Biological Chemistry*. 2005; **280**: 31603-7.
16 Rost S, Fregin A, Ivaskevicius V, Conzelmann E, Hörtnagel K, Pelz H-J, Lappegard K, Seifried E, Scharrer I, Tuddenham EG. Mutations in VKORC1 cause warfarin resistance and multiple coagulation factor deficiency type 2. *Nature*. 2004; **427**: 537-41.
17 Chauhan M, Nadir S, Bailey T, Pryor A, Butler S, Notter D, Velander WH, Gwazdauskas F. Bovine follicular dynamics, oocyte recovery, and development of oocytes microinjected with a green fluorescent protein construct. *Journal of dairy science*. 1999; **82**: 918-26.
18 Carpenter JF, Pikal MJ, Chang BS, Randolph TW. Rational design of stable lyophilized protein formulations: some practical advice. *Pharmaceutical research*. 1997; **14**: 969-75.
19 Butler S. Personal Communication.

20 Aktimur A, Gabriel MA, Gailani D, Toomey JR. The factor IX γ-carboxyglutamic acid (Gla) domain is involved in interactions between factor IX and factor XIa. *Journal of Biological Chemistry*. 2003; **278**: 7981-7.

21 Bajaj SP, Sabharwal AK, Gorka J, Birktoft JJ. Antibody-probed conformational transitions in the protease domain of human factor IX upon calcium binding and zymogen activation: putative high-affinity Ca (2+)-binding site in the protease domain. *Proceedings of the National Academy of Sciences*. 1992; **89**: 152-6.